Memory-type Control Charts in Statistical Process Control

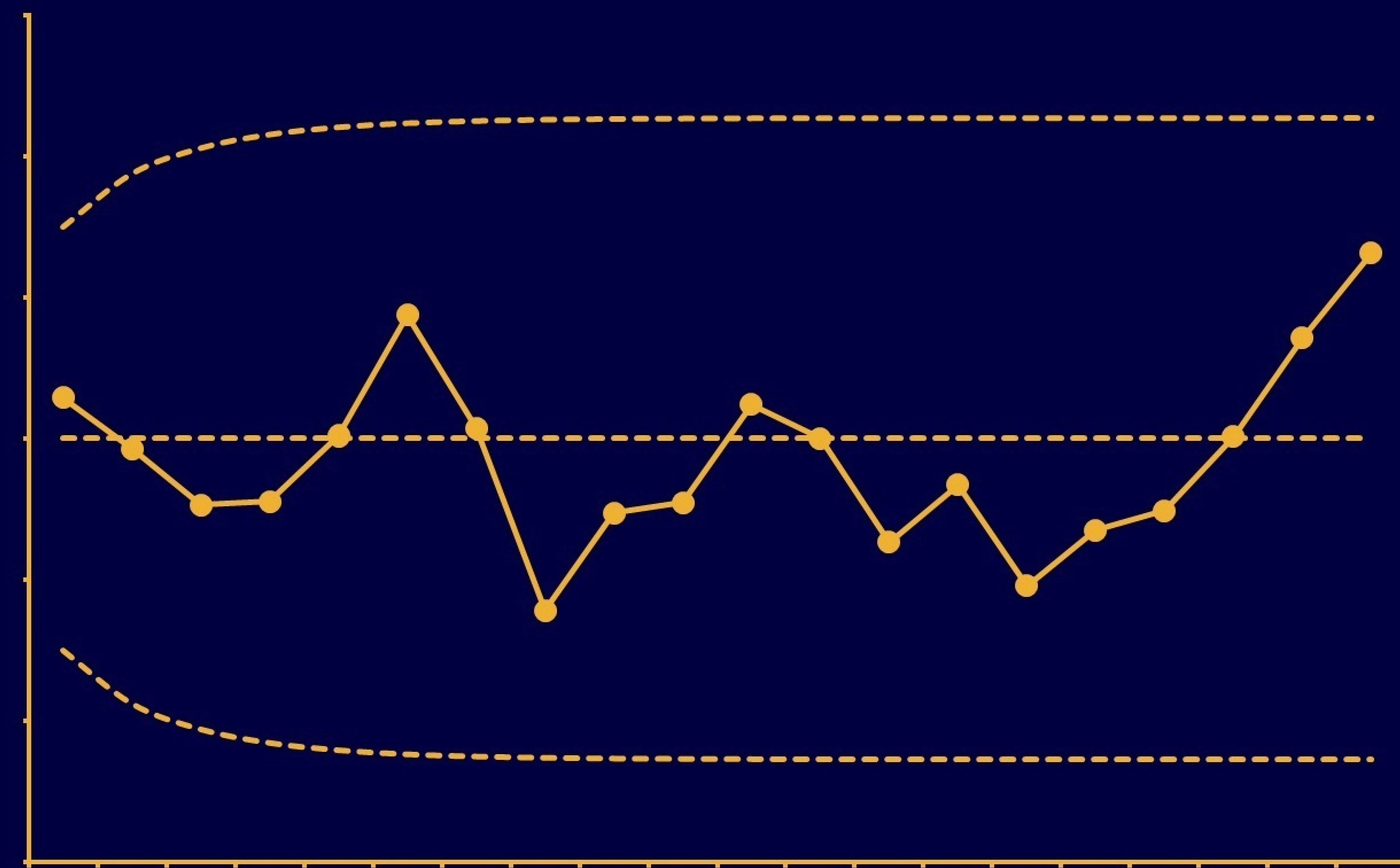

Nasir Abbas

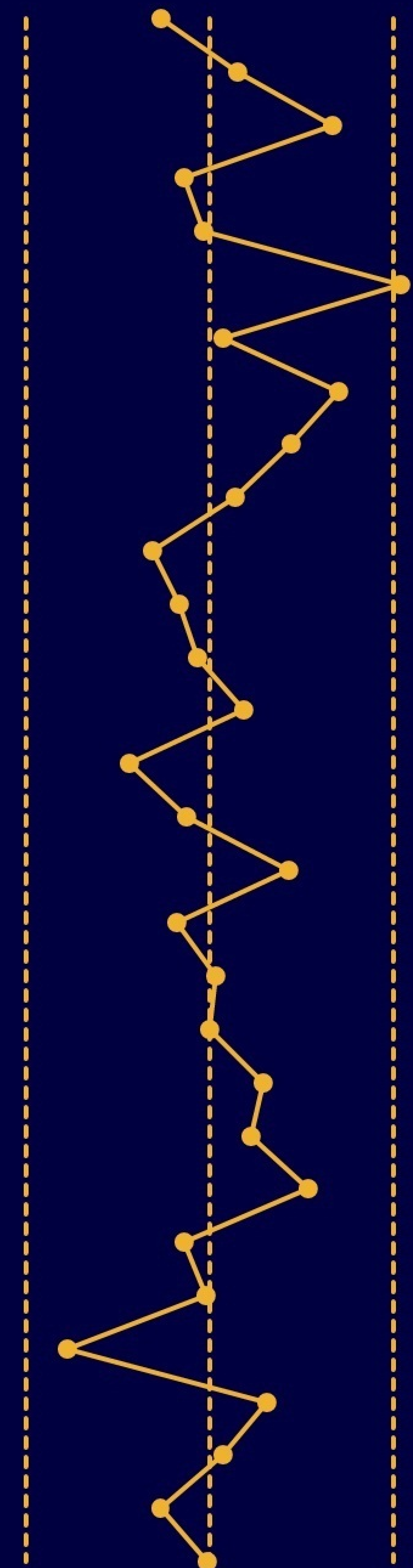

MEMORY-TYPE CONTROL CHARTS IN STATISTICAL PROCESS CONTROL

NASIR ABBAS

Memory-type Control Charts in Statistical Process Control

IBIS UvA
Instituut voor Bedrijfs- en Industriële Statistiek

Dit proefschrift is mede mogelijk gemaakt door een financiële bijdrage van het Instituut voor Bedrijfs- en Industriële Statistiek van de Universiteit van Amsterdam

Omslagontwerp: Nasir Abbas

MIX
Paper from responsible sources
FSC® C012854
www.fsc.org

ISBN: 978-94-6108-318-0

Memory-type Control Charts in Statistical Process Control

ACADEMISCH PROEFSCHRIFT

ter verkrijging van de graad van doctor
aan de Universiteit van Amsterdam
op gezag van de Rector Magnificus
prof. dr. D.C. van den Boom
ten overstaan van een door het college voor promoties ingestelde
commissie, in het openbaar te verdedigen in de Agnietenkapel
op donderdag 6 september 2012, te 10.00 uur

door

Nasir Abbas

geboren te Rawalpindi, Pakistan

Promotiecommissie:

Promotor:	Prof.dr. R.J.M.M. Does
Co-Promotor:	Dr. M. Riaz
Overige leden:	Prof.dr. P. Boswijk
	Prof.dr. C.G.H. Diks
	Prof.dr. E.R. van den Heuvel
	Prof.dr. J. de Mast
	Prof.dr. C.B. Roes
	Prof.dr. J.E. Wieringa
	Dr. M. Schoonhoven

Faculteit Economie en Bedrijfskunde

To my parents

Preface

This thesis is the result of research at the Institute for Business and Industrial Statistics of the University of Amsterdam, the Netherlands. It was really a pleasure for me to work on in the field of statistical quality control which is a very interesting field from both scientific point of view and relevance in practice. Now, I would like to thank some of the people that have supported me in writing this thesis.

I would like to thank Almighty Allah, The compassionate and the most merciful, who bestowed to me His blessings to complete this task. All respect to His Prophet (Peace be upon him) for enlightening the essence of faith in Allah, converting all his kindness and mercies upon me.

First of all I would also like to thank my promoter Prof. dr. Ronald J. M. M. Does who really enhanced my research skills and polished my ability to convert some research work into a proper written form. It was an honor for me to share the research ideas with him and take guidance in the mathematical evaluations and write up of articles and thesis.

I would like to thank my co-promoter, Dr. Muhammad Riaz. His contributions in this thesis are not negligible. He really helped me by providing me with many useful suggestions and comments. I would like to say here "Thank you Sir" for your passion, for your constructive criticism, and for being such a nice friendly supporter. I really enjoyed working with you, and I am proud to be your student.

Thanks also to all of my teachers who always guided me throughout my academic career. I would like to mention especially Dr. Muhammad Aslam, Dr. Javaid Shabir, Dr. Zawar Hussain, Dr. Zahid Asghar, Mr. Jamshaid Iqbal, Mrs. Maryam Asim at Quaid-i-Azam University Islamabad and Mr. Shafqat Hussain, Mr. Saif-ur-Rehman at F.G. Sir Syed

College, The Mall, Rawalpindi. I am thankful to Ms. Atie Buisman, Office Manager at Institute for Business and Industrial Statistics, for her cooperation in all kind of administrative matters and issues. I would also like to thank Mrs. Inez Zwetsloot for her efforts at the printing stage of the thesis.

This thesis is a combination of multiple research articles that are published or submitted in different journals. I would like to thank all the editors and anonymous referees (from those journals) for their valuable comments and criticism to improve the initial forms of the research articles.

At last but not least, thanks are due to my family for their support during all the years of my study. I especially thank my father for always believing in me and my mother for her non-ending prayers for me. Writing this thesis without my family's support was really unthinkable for me.

NASIR ABBAS

Contents

Chapter 1

Introduction

This chapter provides an introduction to statistical process control (SPC) and its main technique: the control chart. A brief description of the so called memory control charts, including cumulative sum (CUSUM) and exponentially weighted moving average (EWMA) control charts, is also given. Finally, a synopsis of the thesis containing the inspiration towards the proposals and an outline are presented.

1.1 Statistical process control

Production processes are subject to variations, e.g. in the process of filling bottles with cooking oil the amount of oil filled will not be exactly same; in the process of making tube light rods the diameter or length of any two rods will not be the same. These variations are mainly classified into two types, namely common cause variation and special cause variation. Common cause variation always exists even if the process is designed very well and maintained very carefully. This variation should be relatively small in magnitude and is, uncontrollable and due to many small unavoidable causes. A process is said to be in statistical control if only common cause variation is present. The variations outside this common cause pattern are called special cause variations. These variations are subject to some problem in the system, like poor tuning of equipment, controller fell asleep or got absent, computer stopped working, poor lot of raw material, machine break down. A process working under both types of variation is said to be out of control. The increase of variation (or the inclusion of special cause variation) in the process generally changes the process parameters like location or/and dispersion parameters. Change in the process location can lead to a greater number of nonconforming items. Similarly, a change in the process dispersion is also important to be detected as an increase in the process dispersion shows a straightforward drop in the quality of process, as a larger spread in the data leads to lower uniformity in the process. On the other hand, the detection of the decrease in the process dispersion may improve the quality of the process, if the underlying special cause can be detected as early as possible.

SPC possesses some of the most extensively used techniques to detect the presence of special cause variation in processes. The control chart is one of those techniques and it started with Shewhart control charts containing the mean ($\bar{X}$) chart for process location and the range (R), the standard deviation (S) and the variance (S^2) charts for process dispersion. The structure of these control charts is based on a statistic plotted against three additional lines: the center line (CL), the upper control limit (UCL) and the lower control limit (LCL). The two control limits (i.e. UCL and LCL) are basically the parameters of a control chart which are selected in such a way that there is a very small probability (generally referred as False Alarm Rate (FAR) in the quality control literature and denoted by α) of the in control data points falling outside these limits. Similarly, the probability of the out of control data points falling outside the control limits is called the power (used as a performance measure) of a control chart. Another performance measure for the control charts is the average run length (ARL). If we define a random variable R_L equal to the number of samples until the first out of control signal occurs then the probability distribution of this random variable R_L is known as the run length distribution. The average of this distribution is called average run length and is denoted by ARL. The in control ARL of a control chart is denoted by ARL_0, while out of control ARL is denoted by ARL_1.

A shortcoming of a Shewhart control chart is that its conclusion is merely based on the present sample which means that it pays no attention to the past data resulting into a relatively bad performance for small disturbances in the process. In contrast, the CUSUM control charts and the EWMA control charts (also referred as memory control charts) are based (in different) ways on past information along with current. Due to this feature these charts are more efficient to detect small and moderate shifts. The present study is based on providing new memory control charting techniques (by modifying the existing structures and also by designing some new structures) that perform relatively better than the existing ones, especially for small and moderate shifts in the process parameters. In the pursuing sections, we provide the detailed structures of CUSUM and EWMA charts for monitoring the process parameters.

1.2 Cumulative sum control charts

The CUSUM chart was originally introduced by Page (1954) and is suited to detect small and sustained shifts in a process. The chart measures a cumulative deviation from the mean or a target value. There exist two versions of the CUSUM chart, used to monitor the process location: the V-mask CUSUM and the tabular CUSUM. The V-mask procedure, which is not very common in use, normalizes the deviations from the mean (or target) and plots these deviations. As long as these deviations are plotted around the target value the process is said to be in control, otherwise out of control. The tabular method of evaluating a CUSUM chart works by accumulating the deviations up and down from a target value for which we use the notations C^+ and C^-, respectively. The quantities C^+ and C^- are known as upper and lower CUSUM statistics, respectively, and these are defined as:

$$C_i^+ = \max[0, (Y_i - \mu_0) - K + C_{i-1}^+], \quad C_i^- = \max[0, -(Y_i - \mu_0) - K + C_{i-1}^-] \tag{1.1}$$

where i is the sample number, Y is the study variable, μ_0 is the target mean of study variable Y, K is the reference value of CUSUM scheme, often taken equal to the half of the amount of shift which we are interested to detect (cf. Ewan and Kemp (1960)). The starting value for both plotting statistics is taken equal to zero, i.e. $C_0^+ = C_0^- = 0$. Now we plot these two statistics against the control limit H and it is concluded that the process mean has moved upward if $C_i^+ > H$ for any value of i whereas the process mean is said to be shifted downwards if $C_i^- > H$ for any value of i. The CUSUM chart is defined by two parameters i.e. K and H. These two parameters are used in the standardized manner (cf. Montgomery (2009)) given as:

$$K = k\sigma_0, \quad H = h\sigma_0 \tag{1.2}$$

where σ_0 is the in control standard deviation of the study variable Y and k and h are the two constants which have to be chosen very carefully because the ARL performance of the CUSUM chart is very sensitive to these constants.

Several CUSUM structures are also recommended for monitoring the process dispersion. Page (1963) introduced the CUSUM chart for monitoring an increase in process dispersion using sample ranges. Following him, Hawkins (1981), Tuprah and Ncube (1987), Chang and Gan (1995), Acrosta-Mejia et al. (1999) and Castagliola et al. (2009) proposed several improved versions of CUSUM charts for process dispersion. These charts are based on transforming the sample variance such that the new transformed form may be closely approximated by a normally distributed variable and hence applying the usual CUSUM structures (recommended by Page (1954)) on it.

1.3 Exponentially weighted moving average control charts

The EWMA control chart was introduced by Roberts (1959) to particularly address the shifts of small and moderate magnitude. Like the CUSUM scheme, EWMA also utilizes the past information along with the current, but the weights attached to the data are exponentially decreasing as the observations become less recent. An EWMA control chart for monitoring the location of a process is based on the statistic:

$$Z_i = \lambda Y_i + (1-\lambda)Z_{i-1} \tag{1.3}$$

where i is the sample number and λ is a constant such that $0 < \lambda \leq 1$. The quantity Z_0 is the starting value and it is taken equal to the target mean μ_0 or the average of initial data in case when the information on the target mean is not available. The control limits for the EWMA statistic given in (1.3) are given as:

$$\left.\begin{aligned} LCL_i &= \mu_0 - L\sigma_0\sqrt{\frac{\lambda}{2-\lambda}\left(1-(1-\lambda)^{2i}\right)} \\ CL &= \mu_0 \\ UCL_i &= \mu_0 + L\sigma_0\sqrt{\frac{\lambda}{2-\lambda}\left(1-(1-\lambda)^{2i}\right)} \end{aligned}\right\} \tag{1.4}$$

where L is the control limit coefficient. Like CUSUM charts, EWMA control charts also have two parameters (λ and L). λ determines the decline of weights, while L determines the width of the control limits, so jointly these two parameters determine the ARL performance of the EWMA charts. The above mentioned limits given in (1.4) are called time varying limits of the EWMA charts. For large values of i these limits converge to constant limits which are given as:

$$LCL = \mu_0 - L\sigma_0\sqrt{\frac{\lambda}{2-\lambda}}, \quad CL = \mu_0, \quad UCL = \mu_0 + L\sigma_0\sqrt{\frac{\lambda}{2-\lambda}} \tag{1.5}$$

Hence, the factor $\left(1-(1-\lambda)^{2i}\right)$ in (1.4) tends to 1 if the sample number tends to infinity.

For monitoring the process dispersion, EWMA charts are also based on normalizing the sample variance. Wortham and Ringer (1971) suggested an EWMA control chart for monitoring the process dispersion. Ng and Case (1989), Crowder and Hamilton (1992), Castagliola (2005) and Huwang et al. (2010) followed them and proposed improved versions of EWMA chart for monitoring process variance.

1.4 Outline of the thesis

After the development of Shewhart, CUSUM and EWMA charts by Shewhart (1931), Page (1954) and Roberts (1959), respectively, several modifications of these charts have been presented in order to further enhance the performance of these charts. Klein (2000), Khoo (2004), Koutras et al. (2007) and Antzoulakos and Rakitzis (2008) proposed the application of different runs rules with the Shewhart structure. Riaz (2008a) and Riaz (2008b) proposed the auxiliary based control charts for monitoring the process variability and location respectively, where both of these charts are based on regression-type estimators. Lucas (1982) presented the combined Shewhart-CUSUM quality control scheme in which Shewhart limits and CUSUM limits are used simultaneously. Lucas and Crosier (1982) recommended the use of the fast initial response (FIR) CUSUM which gives a head start to the CUSUM statistic by setting the initial values of the CUSUM statistic equal to some positive value (non-zero). This feature gives better ARL_1 performance but at the cost of a decrease in ARL_0. Yashchin (1989) presented the weighted CUSUM scheme which gives different weights to the previous information used in CUSUM statistic. Similarly, on the EWMA side, Lucas and Saccucci (1990) presented the combined Shewhart-EWMA quality control scheme which gives better ARL_1 performance for both small and large shifts. Steiner (1999) provided the

FIR EWMA which gives a head start to the initial value of the EWMA statistic (like FIR CUSUM) and hence improves the ARL_1 performance of the EWMA charts.

It is hard to find an application of the runs rules schemes with the CUSUM and EWMA charts in the literature. Chapter 2 proposes the application of some runs rules schemes with the control structure of CUSUM and EWMA charts for process location. The performance of these runs rules based CUSUM and EWMA charts is evaluated in terms of ARL. Comparisons of the proposed schemes are made with some existing representative CUSUM- and EWMA-type counterparts used for small and moderate shifts. The findings reveal that the proposed schemes are able to perform better than the other schemes under investigation. The work of Chapter 2 has been published in *Quality and Reliability Engineering International* as Riaz, Abbas and Does (2011) and Abbas, Riaz and Does (2011).

Chapter 3 introduces a new control structure named as mixed EWMA-CUSUM control chart for monitoring the process location. The core of this idea is to mix the effects of EWMA and CUSUM charts into a single structure such that the resulting mixed chart perform better than the classical ones (i.e. CUSUM by Page (1954) and EWMA by Roberts (1959)). This is done by applying the CUSUM structure over the EWMA statistic. An obvious counterpart of this mixed chart is also developed for monitoring the process dispersion which is named as CS-EWMA chart as its plotting statistic is based on cumulatively summing the exponentially weighted moving averages. Some additional material in the form of comparisons and illustrative examples are also provided. From this chapter, an article on the mixed EWMA-CUSUM chart for location is published in *Quality and Reliability Engineering International* as Abbas, Riaz and Does (2012a), while another article on CS-EWMA chart for process dispersion has been accepted for publication in *Quality and Reliability Engineering International* as Abbas, Riaz and Does (2012b).

Following the approach of Riaz (2008a) and Riaz (2008b), chapter 4 proposes several new control structures using the information from auxiliary variable(s). These charts include the CUSUM and EWMA charts (for monitoring the process location) based on the information of one or more auxiliary variables. The regression estimation technique for the mean is used in defining the control structure of the proposed charts. Comparisons with uni-variate as well as bi-variate EWMA and CUSUM charts are provided. An article on auxiliary based EWMA chart for location has been accepted for publication in *Communications in Statistics - Theory and Methods* as Abbas, Riaz and Does (2012c).

Chapter 5 proposes an alternative to the CUSUM and EWMA charts, named as the progressive mean (PM) control chart. This newly developed control chart is not only outperforming the existing memory charts, but also, its control structure is very simple as compared to the CUSUM and EWMA charts. An article on PM control chart has been published in *Quality and Reliability Engineering International* as Abbas, Zafar, Riaz and Hussain (2012). Using the idea of a progressive statistic, two new control charts are also developed (named as floating control charts) for monitoring the process dispersion. These floating charts also surpass the existing CUSUM and EWMA charts for monitoring the process standard deviation. An article on the floating charts has been submitted for publication in *International Journal of Production Research* as Abbas, Riaz and Does (2012d).

Chapter 2

Runs rules based CUSUM and EWMA

The control chart is an important statistical technique that is used to monitor the quality of a process. One of the charting procedures is the Shewhart-type control charts which are used mainly to detect large shifts. Two alternatives to the Shewhart-type control charts are the cumulative (CUSUM) control charts and the exponentially weighted moving average (EWMA) control charts which are especially designed to detect small and moderately sustained changes in quality. Enhancing the ability of design structures of control charts is always desirable and one may do it in different ways. Runs rules schemes are generally used to enhance the performance of Shewhart control charts. In this chapter we propose the use of runs rules schemes for the CUSUM and EWMA charts and evaluated their performance in terms of the ARL. Comparisons of the proposed schemes are made with some existing representative CUSUM and EWMA-type counterparts used for small and moderate shifts. The comparisons revealed that the proposed schemes perform better for small and moderate shifts while they reasonably maintain their efficiency for large shifts as well. This chapter is based on two articles for monitoring the process location i.e. Riaz, Abbas and Does (2011) and Abbas, Riaz and Does (2011).

2.1 Introduction

The CUSUM and EWMA chart structures discussed in Chapter 1 are known as the classical CUSUM and EWMA charts. The detailed study on the ARL performance of

CUSUM chart was done by Hawkins and Olwell (1998), whereas Steiner (1999) evaluated the $ARLs$ of the classical EWMA. These $ARLs$ are provided in Table 2.1 and Table 2.2, respectively.

TABLE 2.1: ARL Values for the classical CUSUM chart with $k = 0.5$

δ	0	0.25	0.5	0.75	1	1.5	2	2.5	3
$h = 4$	168	74.2	26.6	13.3	8.38	4.75	3.34	2.62	2.19
$h = 5$	465	139	38.0	17.0	10.4	5.75	4.01	3.11	2.57

TABLE 2.2: ARL values for the classical EWMA chart at $ARL_0 = 500$

$\boldsymbol{\delta}$	$\lambda = 0.1$ $L = 2.824$	$\lambda = 0.25$ $L = 3$	$\lambda = 0.5$ $L = 3.072$	$\lambda = 0.75$ $L = 3.088$
0	499.89	500.81	499.36	499.36
0.25	102.99	169.49	255.96	321.3
0.5	28.86	47.5	88.75	139.87
0.75	13.56	19.22	35.55	62.46
1	8.22	10.4	17.09	30.57
1.5	4.17	4.77	6.27	9.8
2	2.66	2.94	3.4	4.46

The results of Tables 2.1 and 2.2 are based on the test that one point falling outside the limits indicates an out of control situation (the classical scheme of signaling). This test may be further extended to a set of rules named as sensitizing rules and runs rules schemes which help to increase the sensitivity of the charts to detect out of control situations. The common set of sensitizing rules are (cf. Nelson (1984)): one or more points outside the control limits; two out of three consecutive points outside the 2 sigma warning limits but still inside the control limits; four out of five consecutive points beyond the 1 sigma limits but still inside the control limits; a run of eight consecutive points on one side of the center line but still inside the control limits; six points in a row steadily increasing or decreasing but still inside the control limits; fourteen points in a row alternating up and down but still inside the control limits. The basic principle underlying these runs rules is twofold. Firstly, specific patterns of out of control conditions might be detected earlier, such as a small but persistent trend. Secondly, the decision rules are designed to have roughly the same (marginal) false alarm probability.

To enhance the performance of control charts, many researchers have used the idea of using different sensitizing rules and runs rules schemes with the Shewhart-type control charts, e.g. see Klein (2000), Khoo (2004), Koutras et al. (2007), and Antzoulakos and Rakitzis (2008). The application of sensitizing rules causes an increase in false alarm rates, whereas the runs rules schemes take care of this issue. Klein (2000), Khoo (2004), and Antzoulakos and Rakitzis (2008) suggested different runs rules schemes, namely r out of m and modified r out of m, to be used with the Shewhart-type control charts. They studied their performance and found that these runs rules schemes perform better as compared to the usual Shewhart-type control charts.

There is a variety of literature available on CUSUM and EWMA charts. e.g. see Lucas and Crosier (1982), Yashchin (1989), and Hawkins and Olwell (1998) for CUSUM and Lucas and Saccucci (1990), Steiner (1999), and Capizzi and Masarotto (2003) for EWMA. All the existing approaches use only the usual scheme of signaling an out of control situation. It is hard to find an application of the runs rules schemes with the CUSUM and EWMA charts in the literature. However, Westgard et al. (1977) studied some control rules using combined Shewhart-CUSUM structures. They proved superiority of this combined approach on the separate Shewhart's approach but ignored any comparison with the separate CUSUM application. Also their control rules considered only one point at a time for testing an out of control situation. The false alarm rates of their control rules kept fluctuating and no attempt was made to keep them fixed at a pre-specified level which is very important for valid comparisons among different control rules/schemes.

In this chapter we analyze some of the r out of m runs rules schemes (like $2/2$, $2/3$ and modified $2/3$ schemes) with CUSUM and EWMA charts, following Klein (2000), Khoo (2004), and Antzoulakos and Rakitzis (2008), and compared their performance (in terms of the ARL) with some other schemes meant particularly for small shifts. Section 2.2 contains the detailed discussion about the proposed runs rules schemes applied on the CUSUM chart, while the discussion on the schemes applied on the EWMA chart are included in Section 2.3.

2.2 The proposed schemes for the CUSUM charts

A process is called to be out of control when a point falls outside the control limits. Specific runs rules or extra sensitizing rules can be used in addition to enhance the power of detecting out of control situations. The CUSUM charts can also take benefit out of these runs rules schemes if properly applied with the CUSUM structures. Following Klein (2000), Khoo (2004), and Antzoulakos and Rakitzis (2008), we propose here two runs rules schemes to be used with the CUSUM charts to monitor the location parameter. The proposed schemes are based on the following terms and definitions.

Action Limit (AL): This is a threshold level for the value of CUSUM chart statistic. If some value of CUSUM statistic exceeds the AL, the process is called to be out of control. The value of the AL would be greater than the classical CUSUM critical limit H for a fixed ARL_0.

Warning Limit (WL): This is a level for the value of the CUSUM chart statistic beyond which (but not crossing the AL) some pattern of consecutive points indicate an out of control situation. The value of the WL would be smaller than the classical CUSUM critical level H for a fixed ARL_0.

Using the above definitions we propose the two runs rules schemes for the CUSUM chart as:

Scheme I: A process is said to be out of control if one of the following four conditions is satisfied:

1. One point of C^+ falls above the AL.
2. One point of C^- falls above the AL.
3. Two consecutive points of C^+ fall between the WL and the AL.
4. Two consecutive points of C^- fall between the WL and the AL.

Scheme II: A process is said to be out of control if one of the following four conditions is satisfied:

1. One point of C^+ falls above the AL.
2. One point of C^- falls above the AL.
3. Two out of three consecutive points of C^+ fall between the WL and the AL.
4. Two out of three consecutive points of C^- fall between the WL and the AL.

Note that the values of the WL and the AL are proportional to the value of the ARL for a given shift; i.e. the ARL is higher if the values of the WL and the AL are higher and vice versa.

There are infinite pairs of WL and AL which fix the in control ARL_0 at a desired level. The objective is to find those pairs of AL and WL that maintain the ARL_0 value at the desired level and at the same time minimize the ARL_1 value.

The ARL computations may be carried out using different approaches, like integral equations, Markov chains, approximations and Monte Carlo simulations. Details regarding the first two may be seen in Brook and Evans (1972) and Lucas and Crosier (1982) and the references therein. An ARL approximation for the upper-sided CUSUM (ARL^+) and the lower-sided CUSUM (ARL^-) is given as (cf. Siegmund (1985)):

$$ARL^{+} = \frac{e^{-2(\delta-k)(h+1.166)} + 2(\delta-k)(h+1.166) - 1}{2(\delta-k)^2}$$

and

$$ARL^{-} = \frac{e^{-2(-\delta-k)(h+1.166)} + 2(-\delta-k)(h+1.166) - 1}{2(-\delta-k)^2}$$

The $ARLs$ for a two-sided CUSUM can be obtained by the following relation:

$$ARL = \frac{1}{{}^{1}/_{ARL^{+}} + {}^{1}/_{ARL^{-}}}$$

Monte Carlo simulation is also a standard option to obtain approximations for the ARL and we have adopted this approach in our study. For that purpose we have developed a simulation algorithm using an add-in feature of Excel software which helps calculating the $ARLs$.

2.2.1 Performance evaluation of the proposed schemes

The performance of the two proposed schemes for the CUSUM chart has been evaluated in terms of ARL under different in control and out of control situations. To meet the desired objective, we have used our simulation algorithm to find the ARL_0 and ARL_1 values for the pairs of WL and AL. We have generated for different values of δ 100,000 samples of size n from $N\left(\mu_0 + \delta\frac{\sigma_0}{\sqrt{n}}, \sigma_0^2\right)$ and we have calculated the statistics C_i^{+} and C_i^{-} for all samples. Here μ_0 and σ_0 refer to the mean and the standard deviation of the process under study and δ is the amount of shift in μ_0. Here σ is assumed to be in control i.e. $\sigma = \sigma_0$. The value of δ indicates the state of control for our process mean, i.e. $\delta = 0$ implies that the process mean μ is in control (i.e. $\mu = \mu_0$) and $\delta \neq 0$ that the process mean μ is out of control (i.e. $\mu = \mu_1$). Without loss of generality we have taken $\mu_0 = 0$ and $\sigma_0 = 1$ in our simulations. After obtaining 100,000 samples we have applied all four conditions of the two proposed runs rules schemes (i.e. Schemes I & II). In this way the run lengths are found for the two proposed schemes. This procedure is repeated 5,000 times and each time the run lengths are computed for both schemes. By taking the average of these run lengths we obtain the $ARLs$ for the two schemes.

To evaluate the performance of the two proposed schemes I and II, we will report the results for the values of the ARL_0 equal to 168, 200 and 500. Other values of the ARL_0 can be easily obtained. The choices made will show the performance of the two schemes and enable us to make comparisons with the results of other schemes and approaches from the literature. By fixing the ARL_0 at a desired level for the proposed schemes I and II, we are able to obtain pairs of WL and AL using our algorithm. Then for these pairs of WL and AL, we have obtained the ARL_1 at different values of δ for both the schemes. The results of the WL and the AL along with their corresponding ARL_1 values for the above mentioned pre-specified ARL_0s are provided in Tables 2.3 – 2.8 for both schemes. In Tables 2.3 – 2.8 the first two columns contain the WL and AL pairs which fix the ARL_0 value at a specified desired level and the remaining columns give the corresponding ARL_1 values.

Some researchers (e.g. Antzoulakos and Rakitzis (2008)) suggest also to report the standard deviations of the run lengths along with the ARL values to describe more about the run length behavior. Moreover, Palm (1990) and Shmueli and Cohen (2003) highlighted the importance of percentile points of the run length distribution and suggested to report them for the interest of practitioners. Therefore the standard deviations (denoted by $SDRL$) and the percentile points (denoted by P_i) of the run length distribution are also computed for proposed schemes I and II. The results of $SDRL$ and P_i (for $i = 10, 25, 50, 75, 90$) are provided in Riaz, Abbas and Does (2011) as Tables VIII – XI for the two proposed schemes at $ARL_0 = 168$. For the other values of ARL_0 similar tables can be easily obtained.

TABLE 2.3: WL, AL and ARL_1 values for the proposed scheme I at $ARL_0 = 168$

Limits		δ					
WL	AL	0.25	0.5	0.75	1	1.5	2
3.42	4.8	71.872	25.564	13.539	8.66	5.078	3.679
3.44	4.6	72.258	25.653	13.5	8.568	5.013	3.607
3.48	4.4	71.936	25.593	13.496	8.516	4.936	3.525
3.53	4.2	71.399	25.3	13.332	8.404	4.828	3.423

TABLE 2.4: WL, AL and ARL_1 values for the proposed scheme II at $ARL_0 = 168$

Limits		δ					
WL	AL	0.25	0.5	0.75	1	1.5	2
3.5	4.44	71.489	25.379	13.398	8.462	4.941	3.541
3.6	4.19	72.938	25.368	13.352	8.383	4.83	3.424
3.7	4.08	73.11	25.369	13.306	8.344	4.777	3.376
3.8	4.03	73.589	25.403	13.277	8.316	4.75	3.347

TABLE 2.5: WL, AL and ARL_1 values for the proposed scheme I at $ARL_0 = 200$

Limits		δ					
WL	AL	0.25	0.5	0.75	1	1.5	2
3.9	4.24	82.952	28.697	13.801	8.904	4.909	3.492
3.8	4.29	84.537	28.736	14.065	8.661	5.002	3.523
3.7	4.4	82.115	28.496	13.822	8.812	4.993	3.561
3.6	4.77	84.15	28.716	13.961	8.981	5.228	3.725
3.57	∞	79.474	28.94	14.262	9.213	5.51	4.076

TABLE 2.6: WL, AL and ARL_1 values for the proposed scheme II at $ARL_0 = 200$

Limits		δ					
WL	AL	0.25	0.5	0.75	1	1.5	2
3.9	4.23	82.975	28.206	13.77	8.869	4.978	3.435
3.8	4.28	81.403	28.356	13.903	8.699	4.966	3.503
3.7	4.6	82.732	28.824	14.078	8.874	5.14	3.687
3.64	∞	81.518	29.138	14.266	9.114	5.457	4.12

TABLE 2.7: WL, AL and ARL_1 values for the proposed scheme I at $ARL_0 = 500$

Limits		δ					
WL	AL	**0.25**	**0.5**	**0.75**	**1**	**1.5**	**2**
4.8	5.12	141.111	38.599	17.392	10.518	5.905	4.057
4.7	5.2	150.372	38.594	17.529	10.599	5.898	4.14
4.6	5.39	145.189	38.195	17.468	10.558	6.007	4.237
4.49	∞	146.564	38.492	17.725	10.857	6.333	4.689

TABLE 2.8: WL, AL and ARL_1 values for the proposed scheme II at $ARL_0 = 500$

Limits		δ					
WL	AL	**0.25**	**0.5**	**0.75**	**1**	**1.5**	**2**
4.8	5.11	139.705	38.856	17.459	10.506	5.822	4.078
4.7	5.19	142.159	37.975	17.267	10.583	5.872	4.104
4.6	5.5	145.787	38.334	17.394	10.734	6.053	4.273
4.54	∞	149.035	39.904	17.568	10.966	6.451	4.873

The standard errors of the results reported in Tables 2.3 – 2.8 are expected to remain around 1% (in relative terms) as we have checked by repeating our simulation results. We have also replicated the results Table 2.1 for $h = 4$ of the classical CUSUM scheme using our simulation routine and obtained almost the same results which ensures the validity of the algorithm developed in Excel and the simulation results obtained from it.

We have observed for the two proposed schemes I and II that:

i) many pairs of WL and AL may be found which fix the ARL_0 at a desired level but the optimum choice helps minimizing the ARL_1 value (cf. Table 2.3 – 2.8);

ii) the two proposed schemes perform very good at detecting small and moderate shifts while maintaining their ability to address the large shifts as well (cf. Tables 2.3 – 2.8);

iii) the two proposed schemes I and II are almost equally efficient for the shifts of small, moderate and large magnitude and hence may be used as a replacement of each other at least for normally distributed processes;

iv) with an increase in the value of δ the ARL_1 decreases rapidly for both the schemes, at a fixed value of ARL_0;

v) with a decrease in the value of ARL_0 the ARL_1 decreases quickly for both the schemes for a given value of δ (cf. Tables 2.3 – 2.8);

vi) the proposed schemes I and II may be extended to more generalized schemes (as given in Klein (2000), Khoo (2004), and Antzoulakos and Rakitzis (2008));

vii) the $SDRL$ decreases if the value of δ increases for both the schemes I and II (cf. Riaz, Abbas and Does (2011));

viii) the run length distributions of both the schemes are positively skewed (cf. Riaz, Abbas and Does (2011)).

2.2.2 Comparisons

In this section we compare the performance of the proposed schemes I and II with some existing schemes for detecting small, moderate and large shifts. The ARL is used as a performance measure for all the schemes under discussion. The existing schemes we have considered for comparison purpose include the classical CUSUM scheme of Page (1954), the weighted CUSUM scheme of Yashchin (1989), the EWMA scheme given in Steiner (1999) and the fast initial response (FIR) CUSUM scheme of Lucas and Crosier (1982). The ARL_1 results for the above mentioned schemes are provided in the Table 2.1 – 2.2 and Tables 2.9 – 2.10 at some selective values of ARL_0 which will be used for the comparisons.

Now we present a comparative analysis of the proposed schemes with the existing schemes one by one.

Proposed versus the classical CUSUM: The classical CUSUM scheme of Page (1954) accumulates the up and down deviations from the target and is quite efficient at detecting small shifts. Table 2.1 provides the ARL performance of the classical CUSUM scheme. Tables 2.3 – 2.4 provide the ARL performances of the two proposed schemes. The results of these tables advocate that the proposed schemes are better compared with the classical CUSUM scheme for small shifts while for moderate and large shifts their performances almost coincide.

Proposed versus the weighted CUSUM: Yashchin (1989) presented a class of weighted control schemes that generalize the basic CUSUM technique by assigning different weights to the past information used in the classical CUSUM statistic. The ARL performance of the weighted CUSUM scheme is given in Table 2.9 where γ represents the weight and the other terms as defined earlier in this article. Tables 2.7 and 2.8 provide the ARL performance of the proposed schemes at $ARL_0 = 500$ so these tables can be used to compare the proposed schemes with the weighted CUSUM scheme.

TABLE 2.9: ARL values for the symmetric two-sided weighted CUSUM scheme at $ARL_0 = 500$

$k = 0.5$		δ			
γ	h	0.5	1	1.5	2
0.7	3.16	86.30	15.90	6.08	3.52
0.8	3.46	70.20	13.30	5.66	3.50
0.9	3.97	54.40	11.40	5.50	3.60
1.0	5.09	39.00	10.50	5.81	4.02

By comparing the results of Tables 2.7, 2.8 and 2.9 we can see that the proposed schemes perform better than the weighted CUSUM for small and moderate shifts. Particularly, when δ

is small the performance of our proposed schemes is significantly better than that of the weighted CUSUM scheme. However for $\gamma = 1$ the weighted CUSUM scheme is the same as the classical CUSUM so the comments of the proposed versus the classical CUSUM scheme hold here as well.

Proposed versus the classical EWMA: Steiner (1999) gave a simple method for studying the run length distribution of the classical EWMA chart. Table 2.2 presents some selective $ARLs$ of the EWMA chart where λ is the weighting constant and L is the control limits coefficient. As the proposed schemes have $ARL_0 = 500$ in Tables 2.7 and 2.8 we use these tables for a comparison with the EWMA chart. From the Tables 2.2, 2.7 and 2.8 we see that for $\delta = 0.25$ the classical EWMA chart has an ARL_1 value of 171.09 whereas the proposed schemes are minimizing the same ARL_1 value around 140. This shows that the proposed schemes perform better than the classical EWMA scheme for $\delta = 0.25$. The same superiority also holds for all $0.25 \leq \delta \leq 1$. However, for $\delta > 1$ the proposed schemes and the classical EWMA scheme have almost the same behavior as can be easily seen from the corresponding tables.

Proposed versus the FIR CUSUM: Lucas and Crosier (1982) presented the Fast Initial Response (FIR) CUSUM which gives a head start value, say C_0, to the classical CUSUM statistic. A standard CUSUM has $C_0^+ = C_0^- = 0$ while an FIR CUSUM sets C_0^+ and C_0^- to some nonzero value. Table 2.10 presents the $ARLs$ for the FIR CUSUM at $h = 4$ and $C_0 = 1$ for discussion and comparison purposes. The FIR CUSUM scheme decreases the ARL_1 values as compared to those of the classical CUSUM scheme at the cost of reduction in ARL_0 value from 168 to 163 (see Table 2.1 vs. Table 2.10) which is generally undesirable in sensitive processes (e.g. those directly related to intensive care units which are highly time sensitive, cf. Bonetti et al. (2000)). The ARL_1 results given in Tables 2.3 and 2.4 of the proposed schemes are also obtained for $ARL_0 = 168$ and hence can be used for comparison purposes here. Looking at the ARL_1 results of Tables 2.3 and 2.4 we can see that almost the same amount of reduction in ARL_1 may be achieved, as obtained by FIR CUSUM, using the proposed schemes without paying any cost in terms of a decrease in ARL_0 value and the need of a head start value.

TABLE 2.10: $ARLs$ for FIR CUSUM scheme with $C_0 = h/4$ and $k = 0.5$

$\boldsymbol{\delta}$	0	0.25	0.5	0.75	1	1.5	2
$\boldsymbol{h = 4, C_0 = 1}$	163	71.1	24.4	11.6	7.04	3.85	2.7

In brief the proposed schemes have shown better performance for the smaller values of δ (i.e. small shifts), which is the main concern of CUSUM charts, while for larger values of δ the proposed schemes can perform equally well as the other schemes. The better performance can be further enhanced with the help of other runs rules schemes of Khoo (2004) and Antzoulakos and Rakitzis (2008).

2.2.3 Illustrative example

To illustrate the application of the proposed CUSUM schemes we use the same method as in Khoo (2004). Two datasets are simulated consisting of some in control and some out of control sample points. For dataset 2.1 we have generated 50 observations in total, of which the first 20 observations are from $N(0,1)$ (showing the in control situation) and the remaining 30 observations are generated from $N(0.25,1)$ (showing a small shift in the mean level) while for dataset 2.2 we have generated 30 observations in total, of which the first 20 observations are same as for dataset 2.1 and the remaining 10 observations are generated from $N(1,1)$ (showing a moderate shift in the mean level).

The two proposed CUSUM schemes of this study (i.e. schemes I and II) are applied to the above mentioned two datasets. Additionally, the classical CUSUM scheme is also applied to these two datasets for illustration and comparison purposes. The CUSUM statistics are computed for the two datasets and are plotted against the respective control limits used with the three CUSUM schemes by fixing the ARL_0 at 500. For the classical CUSUM scheme, $h = 5.07$ is used as the control limit to have $ARL_0 = 500$. For the proposed scheme I, $WL = 4.8$ and $AL = 5.12$ are used, while for the proposed scheme II $WL = 4.8$ and $AL = 5.11$ are used to have the ARL_0 value equal to 500 for both schemes. The graphical displays of the three CUSUM schemes for the two datasets are given in the following two figures.

Figure 2.1 exhibits the behavior of dataset 2.1, where a small mean shift was introduced. Figure 2.2 illustrates the behavior of dataset 2.2, where a moderate mean shift was introduced.

Figure 2.1: CUSUM chart of the classical scheme and the proposed scheme I and II for dataset 2.1

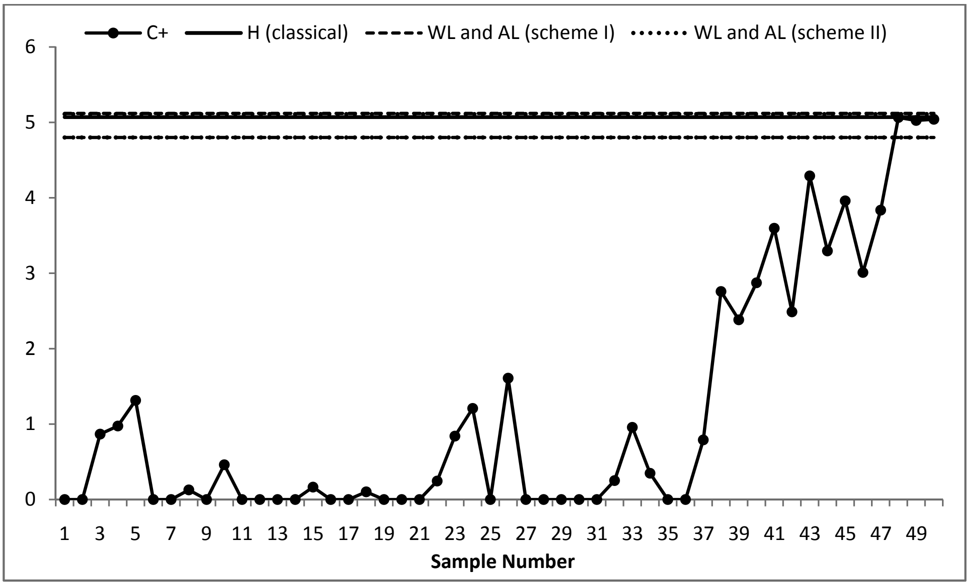

Figure 2.2: CUSUM chart of the classical scheme and the proposed scheme I and II for dataset 2.2

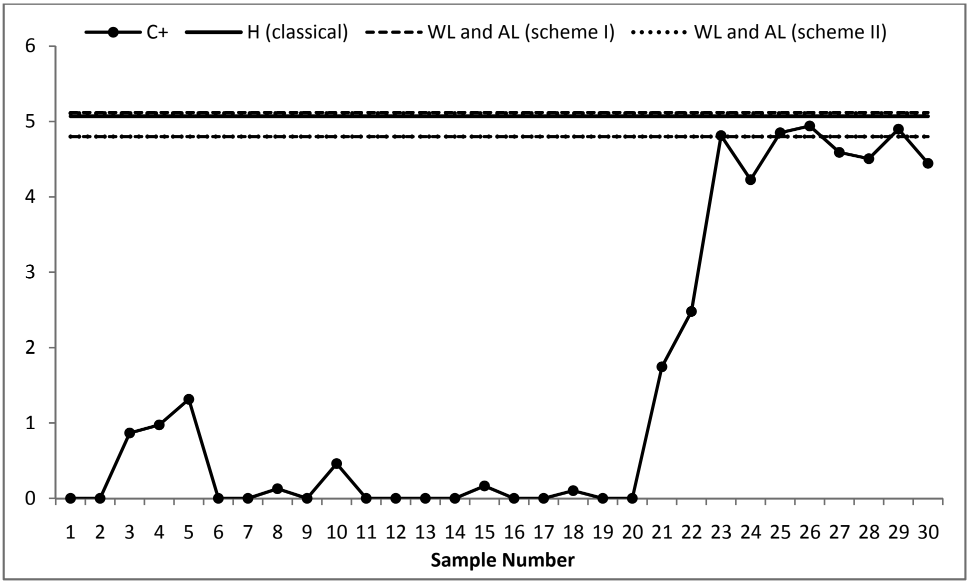

In Figure 2.1 we see that an out of control signal is received at sample points # 49 and 50 by the proposed scheme I (i.e. two out of control signals) and at sample points # 49 and 50 by the proposed scheme II (i.e. two out of control signals). Similarly, in Figure 2.2 the out of control signals are received at sample point # 26 by proposed scheme I (i.e. one out of control signal) and at sample points # 25, 26 and 27 by the proposed scheme II (i.e. two out of control signal). For both datasets, the classical CUSUM scheme failed to detect any shift in the process mean.

It is evident from the above figures that the proposed schemes have detected out of control signals, which are not spotted by the classical CUSUM scheme for the dataset 2.1, where a small mean shift was present, while the situation is almost identical for dataset 2.2, where a moderate shift we introduced. It is to be noted that these signaling performances of the proposed schemes versus the classical CUSUM scheme are in accordance with the findings of subsection 2.2.2, where we found that the proposed schemes are more efficient than the classical CUSUM scheme for small shifts, while almost equally good for other shifts.

2.3 The proposed schemes for the EWMA charts

Shewhart control charts are good in detecting large disturbances in the process, but it takes too long for Shewhart-type charts to detect a small or moderate shift. To overcome this problem some sensitizing rules are designed but their implementation inflates the pre-specified false alarm rate. This issue may be resolved by the introduction of the runs rules schemes as we have mentioned in Section 2.2. Klein (2000), Khoo (2004) and Antzoulakos and Rakitzis (2008) presented runs rules schemes applied on the Shewhart control charts to enhance their performance for small and moderate shifts, keeping the false alarm rate at the pre-specified level. The application of these runs rules schemes is not commonly used with the CUSUM and EWMA control charts. Taking inspiration from the application of runs rules on CUSUM charts, we propose two runs rules schemes in this section for the design structure of the EWMA control chart named as “simple $2/2$ EWMA scheme” and “modified $2/3$ EWMA scheme”. The procedural and conceptual framework of these two proposed schemes is defined as:

Simple $2/2$ EWMA scheme: According to the simple $2/2$ EWMA scheme a process is said to be out of control if two consecutive points are plotted either below a lower signaling limit (LSL) or above an upper signaling limit (USL).

Modified $2/3$ EWMA scheme: According to the modified $2/3$ EWMA scheme a process is said to be out of control if one of the following two conditions is satisfied.

i. At least two out of three consecutive points fall below an LSL and the point above the LSL (if any) falls between the CL and the LSL.

ii. At least two out of three consecutive points fall above a USL and the point below the USL (if any) falls between CL and the USL.

The signaling limits LSL and USL mentioned above in the definitions of our two proposals are especially set limits chosen for the two schemes separately, depending upon the desired ARL_0, while CL is the same as defined in (1.4). The control structure for the proposed schemes is given as:

$$\left.\begin{aligned} LSL_i &= \mu_0 - L_s\sigma_0\sqrt{\frac{\lambda}{2-\lambda}(1-(1-\lambda)^{2i})} \\ CL &= \mu_0 \\ USL_i &= \mu_0 + L_s\sigma_0\sqrt{\frac{\lambda}{2-\lambda}(1-(1-\lambda)^{2i})} \end{aligned}\right\} \tag{2.1}$$

where L_s is the signaling limit coefficient of the proposed schemes and the other terms are the same as defined in Section 1.3. It has to be mentioned that the above mentioned signaling limits coefficient L_s is set according to the pre-specified value of ARL_0. Moreover, a signaling limit on either side may be split into two lines (as is done in Section 2.2) to reach at some optimum pair. We opted the choice where the outer split of the line is taken at infinity. However, one may take some different appropriately chosen outer splits other than infinity.

The parameters of these two proposed schemes are the central line and two signaling limits as given in (2.1) (i.e. CL, LSL and USL). The upper and lower signaling limits are symmetric around the CL and will vary according to the pre-specified ARL_0. Using the positive relation between ARL and width of the signaling limits (depending upon L_s), we fix ARL_0 at the desired level and find the corresponding pair of symmetric signaling limits. Based on these especially set signaling limits we carry out our ARL_1 study at the desired ARL_0 values.

The calculation of ARL may be carried out using different approaches such as integral equations, Markov chains, approximations and Monte Carlo simulations. We have chosen to use Monte Carlo simulations to obtain ARL values. The simulation algorithms for the calculation of ARL values of the proposed schemes are developed in Excel using an Add-In feature $MCSim$.

2.3.1 Performance evaluation of the proposed schemes

To investigate the performance of our proposed EWMA schemes we have considered different in control and out of control situations. A suitable number of samples (say 100,000) of a fixed size n are generated from $N\left(\mu_0 + \delta\frac{\sigma_0}{\sqrt{n}}, \sigma_0^2\right)$. The EWMA statistics for these samples are then calculated and the conditions of the two proposed EWMA schemes (as listed in Section 2.3) are applied on them using the signaling limits given in (2.1) through our simulation algorithm. By executing this process repeatedly we obtain different run length values which ultimately help computing ARL values and other properties as well. It is to be noted that the value of L_s is worked out such that the desired ARL_0 value is achieved. For $\delta = 0$, the ARL_0 values are evaluated with the help of their corresponding L_s and then, for $\delta \neq 0$, the ARL_1 values are computed by introducing different shifts in the process.

To evaluate the performance of the two proposals we fix the pre-specified ARL_0 values, in this section, at 168, 200 and 500. These choices will suffice to exhibit the behavior of our proposed schemes and will enable us to make valid comparisons with their already existing counterparts. On similar lines other choices of ARL_0 can also be obtained. By fixing the ARL_0 values at the above mentioned levels (using their corresponding L_s) we have obtained the ARL_1 at different values of δ. These ARL_1 values are provided in Tables 2.11 – 2.16 for the aforementioned desired ARL_0 preferences (along with their corresponding L_s values) at different choices of λ.

TABLE 2.11: ARL values for the simple $2/2$ EWMA scheme at $ARL_0 = 168$

δ	$\lambda = 0.1$ $L_s = 2.145$	$\lambda = 0.25$ $L_s = 2.184$	$\lambda = 0.5$ $L_s = 2.034$	$\lambda = 0.75$ $L_s = 1.83$
0	169.8676	169.4769	169.6763	169.7112
0.25	54.5771	73.4836	94.8246	110.7766
0.5	19.8026	26.6284	37.9883	49.063
0.75	10.5927	12.9547	17.408	23.2892
1	6.9435	7.9456	9.8833	13.0739
1.5	4.1117	4.3476	4.7293	5.5777
2	2.9796	3.0954	3.1231	3.3368

TABLE 2.12: ARL values for the modified $2/3$ EWMA scheme at $ARL_0 = 168$

δ	$\lambda = 0.1$ $L_s = 1.807$	$\lambda = 0.25$ $L_s = 1.936$	$\lambda = 0.5$ $L_s = 1.85$	$\lambda = 0.75$ $L_s = 1.67$
0	167.3173	169.9927	168.5416	170.9464
0.25	34.367	43.3236	55.4569	62.6484
0.5	14.0389	17.8611	23.0836	27.6195
0.75	8.1338	9.4968	11.9229	14.2207
1	5.7064	6.4798	7.6037	8.5804
1.5	3.7755	3.9823	4.2103	4.5232
2	3.2047	3.2708	3.3136	3.4072

TABLE 2.13: ARL values for the simple $2/2$ EWMA scheme at $ARL_0 = 200$

δ	$\lambda = 0.1$ $L_s = 2.211$	$\lambda = 0.25$ $L_s = 2.24$	$\lambda = 0.5$ $L_s = 2.09$	$\lambda = 0.75$ $L_s = 1.875$
0	200.5694	199.8855	200.8923	201.1229
0.25	60.9801	80.7515	107.709	126.1691
0.5	20.9561	28.6011	42.0774	55.7335
0.75	11.2452	13.7306	19.0848	25.862
1	7.1859	8.1962	10.6258	13.9457
1.5	4.198	4.4825	4.9002	5.7061
2	3.0577	3.1331	3.1899	3.4272

The standard deviation of the run lengths (denoted by $SDRL$) and the i^{th} percentiles denoted by P_i ($i = 10, 25, 50, 75$ and 90) are also provided at $ARL_0 = 500$ in Abbas, Riaz and Does (2011). Similar results can be easily obtained for other values of ARL_0. These measures along with ARL may help studying the behavior of the run length distribution.

TABLE 2.14: ARL values for the modified $2/3$ EWMA scheme at $ARL_0 = 200$

δ	$\lambda = 0.1$ $L_s = 1.895$	$\lambda = 0.25$ $L_s = 2.008$	$\lambda = 0.5$ $L_s = 1.902$	$\lambda = 0.75$ $L_s = 1.715$
0	201.9206	200.5236	200.5969	200.886
0.25	39.1578	50.0565	63.1482	70.9068
0.5	15.4204	19.5705	25.1144	30.4725
0.75	8.6061	10.1922	12.8642	15.3578
1	5.981	6.7621	7.7437	9.1272
1.5	3.8655	4.1115	4.3324	4.6841
2	3.2523	3.3186	3.3386	3.4238

TABLE 2.15: ARL values for the simple $2/2$ EWMA scheme at $ARL_0 = 500$

δ	$\lambda = 0.1$ $L_s = 2.556$	$\lambda = 0.25$ $L_s = 2.554$	$\lambda = 0.5$ $L_s = 2.36$	$\lambda = 0.75$ $L_s = 2.115$
0	501.7558	505.5284	501.2598	502.0725
0.25	103.3109	169.1349	235.1138	280.6187
0.5	29.5748	47.0105	78.0771	108.8792
0.75	14.3216	19.2776	30.8742	45.3405
1	8.9561	10.5964	15.1992	22.1033
1.5	4.9197	5.2578	6.1014	7.7862
2	3.4498	3.5527	3.6815	4.0883

TABLE 2.16: ARL values for the modified $2/3$ EWMA scheme at $ARL_0 = 500$

δ	$\lambda = 0.1$ $L_s = 2.3$	$\lambda = 0.25$ $L_s = 2.345$	$\lambda = 0.5$ $L_s = 2.202$	$\lambda = 0.75$ $L_s = 1.982$
0	502.883	499.6153	505.3564	501.9698
0.25	66.6864	97.0108	133.7117	155.7078
0.5	21.4251	31.2023	46.3541	57.7739
0.75	11.7427	14.4295	20.6223	26.0312
1	7.5539	8.6761	11.0991	13.8363
1.5	4.4676	4.7066	5.1336	5.7812
2	3.4534	3.549	3.6276	3.7787

The relative standard errors of the results reported in Tables 2.11 – 2.16 are also calculated and are found to be around 1%. We have also replicated the results of the classical EWMA chart and found almost the same results as Steiner (1999) which ensures the validity of our simulation algorithm.

Mainly, the findings for the two proposed schemes are:

i. the two proposed schemes are performing very well at detecting small and moderate shifts while their performance for large shifts is not bad either (cf. Tables 2.11– 2.16);
ii. with an increase in the value of δ the ARL_1 decreases rapidly for both schemes, at a given ARL_0 (cf. Tables 2.11– 2.16);
iii. with a decrease in the value of ARL_0 the ARL_1 decreases quickly for both schemes for a given value of δ (cf. Tables 2.11– 2.16);
iv. the modified $2/3$ scheme is performing significantly better than the simple $2/2$ scheme for all choices of λ (cf. Tables 2.11– 2.16);
v. performance of the two proposed schemes is generally better for smaller choices of λ (cf. Tables 2.11– 2.16);
vi. the modified $2/3$ scheme has the ability to perform well even for moderately large values of λ;
vii. the application of both the schemes is quite simple and easily executable;
viii. the performance of the EWMA type charts can further be enhanced by extending the proposed schemes with the help of other runs rules schemes;
ix. the $SDRL$ decreases for both schemes as the value of δ increases (cf. Abbas, Riaz and Does (2011));
x. the run length distribution of both schemes is positively skewed (cf. Abbas, Riaz and Does (2011)).

2.3.2 Comparisons

In this section we provide a detailed comparison of the proposed schemes with their already existing counterparts meant for detecting small shifts, i.e. EWMA- and CUSUM-type charts. The performance of all the control charting schemes is compared in terms of ARL. The control schemes used for the comparison purposes include the classical EWMA, the classical CUSUM, the FIR CUSUM, the FIR EWMA, the weighted CUSUM, the double CUSUM, the distribution-free CUSUM and the runs rules schemes based CUSUM.

Proposed versus the classical EWMA: The classical EWMA is defined by Roberts (1959). ARL values for the classical EWMA are given in Table 2.2. The classical EWMA refers to one out of one $(1/1)$ scheme. The comparison of the three schemes (i.e. the classical EWMA and the two proposed schemes) shows that both proposed EWMA schemes of Section 2.3 are performing better than the classical scheme in terms of ARL (cf. Tables 2.15 & 2.16 vs. Table 2.2). Moreover the modified $2/3$ scheme is outperforming the simple $2/2$ scheme with a great margin for the small shifts (i.e. $0.25 \leq \delta \leq 1.5$). The performance of the two proposed schemes almost coincide for larger values of δ.

Proposed versus the classical CUSUM: The classical CUSUM is defined by Page (1954). The ARL values of the classical CUSUM are given in Table 2.1 at ARL_0 168 and 465. The comparison of the classical CUSUM with the proposed schemes reveals that both schemes are outperforming the classical CUSUM scheme at all the values of δ (cf. Tables 2.11 & 2.12 vs. Table 2.1). Particularly, comparing the three schemes at $\delta = 0.25$, we observe that the modified $2/3$ scheme is performing the best with $ARL_1 = 34.4$ followed by the simple $2/2$ scheme with $ARL_1 = 54.6$, whereas the classical CUSUM has $ARL_1 = 74.2$ which mean that the modified $2/3$ scheme is giving almost half ARL_1 than the classical CUSUM scheme with ARL_0 fixed at 168.

Proposed versus the FIR CUSUM: The FIR CUSUM presented by Lucan and Crosier (1982) gives a head start to the CUSUM statistic rather than setting it equal to zero. The $ARLs$ of FIR CUSUM with two different values for the head start (C_0) are given in Table 2.10. Comparing the performance of FIR CUSUM with the proposed schemes we can see that the modified $2/3$ scheme is performing better than the FIR CUSUM even though that there is a problem with the FIR CUSUM because its ARL_0 value is less than 168 (the desired level). Moreover, we see that if the value of C_o increases than the value of ARL_0 decreases, which is not recommended in case of sensitive processes (cf. Bonetti et al. (2000)). The proposed schemes are not only fixing the ARL_0 at the pre-specified level (so that valid comparison can be made) but also performing better in terms of ARL_1s, i.e. the proposed schemes are minimizing the ARL_1 (with a fixed ARL_0) without a decrease in ARL_0 and without the need of any head start value (cf. Tables 2.11 & 2.12 vs. Table 2.10).

Proposed versus the FIR EWMA: Lucas and Saccucci (1990) proposed the application of the FIR feature with the EWMA control chart (especially with small values of λ). The ARL values of the EWMA control chart with FIR feature are provided in Table 2.17.

TABLE 2.17: ARL values for the FIR EWMA scheme

δ	% Head Start	$\lambda = 0.1$ $L = 2.814$	$\lambda = 0.25$ $L = 2.998$	$\lambda = 0.5$ $L = 3.071$	$\lambda = 0.75$ $L = 3.087$
0	25	487	491	497	498
	50	468	483	487	496
0.5	25	28.3	46.5	87.8	140
	50	24.2	43.6	86.1	139
1	25	8.75	10.1	16.9	30.2
	50	6.87	8.79	15.9	29.7
2	25	3.57	3.11	3.29	4.33
	50	2.72	2.5	2.87	4.09

Comparing the FIR EWMA with the proposed schemes we observe that the proposed schemes are not only having smaller ARL_1s but they also fix the ARL_0 value at desired level which is not the case with the FIR EWMA (cf. Tables 2.15 & 2.16 vs. Table 2.17). The other comments made in favor of the proposed schemes versus the FIR CUSUM are also valid here with the same spirit and strength.

Proposed versus the weighted CUSUM: Yashchin (1989) proposed a class of weighted CUSUM charts which generalize the classical CUSUM charts by giving weights to the past information and can be viewed as the EWMA version of the CUSUM charts. The $ARLs$ for the weighted CUSUM are given in Table 2.9 where the weights given to the past information are represented by γ. Comparing the weighted CUSUM with the proposed schemes we notice that the proposed schemes are performing better than the weighted CUSUM for all the values of δ, which shows the uniform superiority of the proposed schemes over the weighted CUSUM (cf. Tables 2.15 & 2.16 vs. Table 2.9).

Proposed versus the double CUSUM: Waldmann (1995) has shown that the simultaneous use of two classical CUSUMs improves the ARL performance of the CUSUM chart. This simultaneous use of the two CUSUM charts is being given the name of double CUSUM. The ARL performance of the double CUSUM is given in Table 2.18 in which parameters of the 1st CUSUM are K and H and parameters of the 2nd CUSUM are K' and H'.

TABLE 2.18: $ARLs$ for the double CUSUM with $K = 3.3$, $H' = 6.8$ and $K' = 3.3$ at $ARL_0 = 500$

δ	0	0.5	1	1.5	2
$H = 2.6$	507	27.1	9.85	5.55	3.57

Comparison of the double CUSUM with the proposed schemes shows that the double CUSUM performs better than the simple $2/2$ scheme for $\delta = 0.5$ but the modified $2/3$ scheme performs better than both the simple $2/2$ scheme and the double CUSUM. For all other values of δ, the modified $2/3$ scheme is performing the best followed by the simple $2/2$ scheme (cf. Tables 2.15 & 2.16 vs. Table 2.18).

Proposed versus the distribution-free CUSUM: Chatterjee and Qiu (2009) proposed a class of distribution-free CUSUM charts. The three non-parametric control charts named as B1, B2 and B3 depend upon the variable T_i which is defined as:

$$T_i = \begin{Bmatrix} 0, & \text{if } C_i = 0 \\ j, & \text{if } C_i \neq 0, C_{i-1} \neq 0, \dots\dots, C_{i-j+1} \neq 0; j = 1,2,\dots\dots, n \end{Bmatrix}$$

where T_i is the number of samples since the last time the statistic C_i was zero. The ARL performance of these non-parametric charts is given in Table 2.19.

TABLE 2.19: ARL values for different distribution-free CUSUM schemes with nominal $ARL_0 = 200$

j_{max}	Chart	δ		
		0	0.5	1
5	B1	178.43	25.31	12.54
	B2	173.78	18.37	7.94
	B3	201.86	27.38	9.14
30	B1	202.92	18.89	6.60
	B2	194.44	18.68	6.43
	B3	197.79	19.20	6.45
40	B1	195.04	22.40	5.66
	B2	198.98	20.52	5.70
	B3	201.87	21.36	5.77
50	B1	190.88	16.96	6.59
	B2	199.35	18.73	6.84
	B3	202.79	17.51	6.50

For $\delta = 0.5$ the best ARL performance is at $j_{max} = 50$ by chart B1. In this case the $ARL_1 = 17.0$ whereas the ARL_1 for the simple $2/2$ and modified $2/3$ schemes is 21.0 and 15.4, respectively, which shows superiority of the modified $2/3$ scheme. For $\delta = 1$ the distribution-free charts perform slightly better for $j_{max} = 40$ but for all other values of j_{max}, the modified $2/3$ scheme is again performing better. This proves the dominance of the modified $2/3$ scheme as compared to the distribution-free CUSUM charts in general (cf. Tables 2.13 & 2.14 vs. Table 2.19).

Proposed versus the runs rules based CUSUM: In Section 2.2 we proposed two runs rules schemes, namely CUSUM scheme I and CUSUM scheme II, on the CUSUM charts and computed the ARL values for the two schemes which are given in Tables 2.5 and 2.6 for $ARL_0 = 200$. Comparing the proposed EWMA schemes with these runs rules based CUSUM schemes I and II we see that the two proposed EWMA schemes are performing better than the CUSUM schemes of Section 2.1 (cf. Tables 2.13 & 2.14 vs. Tables 2.5 & 2.6).

Moreover, for an overall comparison of the proposed schemes with their existing counterparts mentioned and compared above we have made some graphs showing ARL curves of different schemes.

It is evident from the Figures 2.3 – 2.5 that the ARL curves of the two proposed EWMA schemes exhibit dominance in general as compared to all the other schemes covered in this chapter.

Figure 2.3: ARL curves for the simple $2/2$ and modified $2/3$ EWMA schemes, the classical CUSUM and the FIR CUSUM at $ARL_0 = 168$

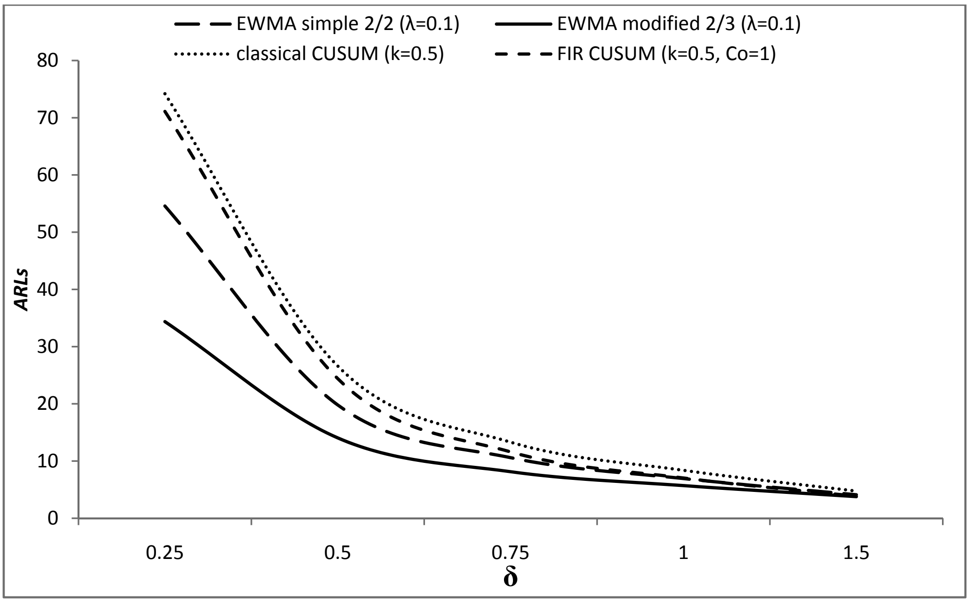

Figure 2.4: ARL curves for the simple $2/2$ and modified $2/3$ EWMA schemes, the runs rules scheme I for CUSUM and the the runs rules scheme II for CUSUM at $ARL_0 = 200$

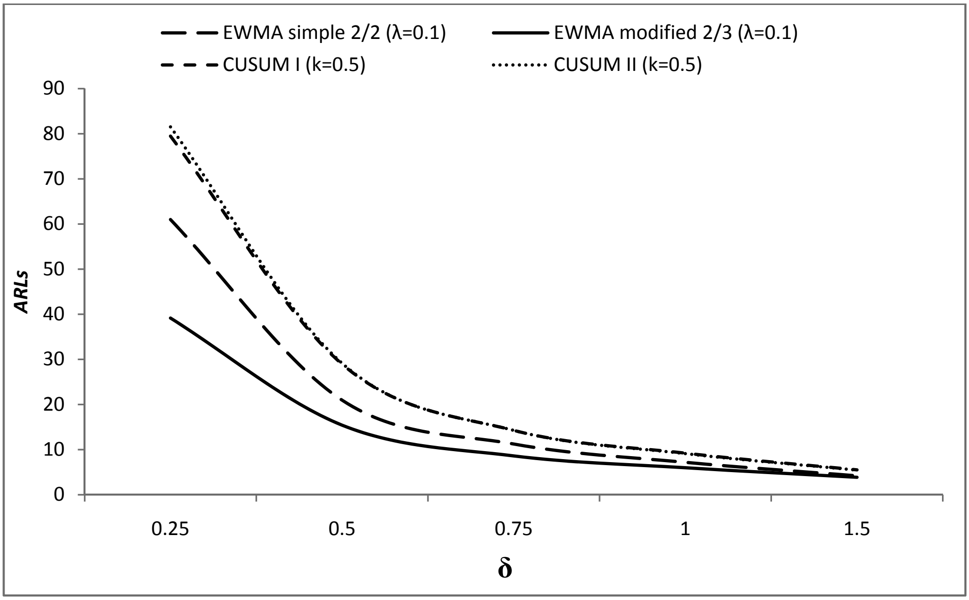

Figure 2.5: ARL curves for the simple $2/2$ and modified $2/3$ EWMA schemes, the classical EWMA, the FIR EWMA, the weighted CUSUM and the double CUSUM at $ARL_0 = 500$

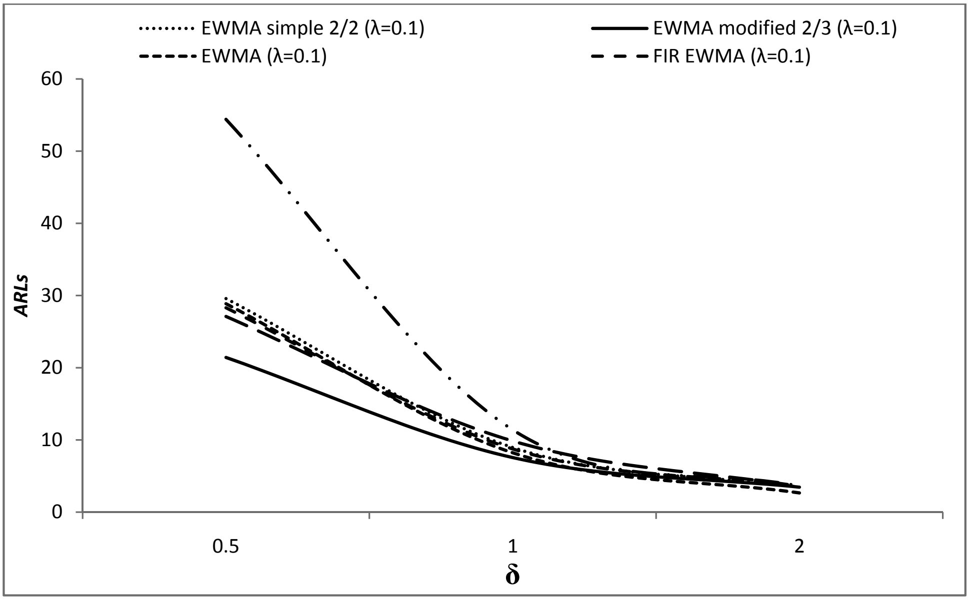

Particularly, the ARL curve of the modified $2/3$ EWMA scheme is on the lower side compared to all other schemes. This shows the best ARL performance of the modified $2/3$ EWMA scheme compared to all others. For the small shifts, the gap between the ARL curves of the proposed schemes with those of the other schemes is large, whereas this gap reduces as the size of the shift increases. This implies that the proposals of the study (particularly modified $2/3$ EWMA scheme) are generally more beneficial for small shifts.

2.3.3 Illustrative example

This section presents an illustrative example to show how the proposed schemes can be applied in real situations. For this purpose we have used dataset 2.1 and dataset 2.2 from subsection 2.2.3. The EWMA statistics are calculated with $\lambda = 0.1$ and the three schemes (i.e. the two proposed schemes and the classical scheme with $ARL_0 = 500$) are applied to the datasets. The graphical display of the control chart with all the three schemes applied to the datasets 2.1 and 2.2 are given in Figures 2.6 and 2.7 respectively.

From Figure 2.6 we can see that the first 20 points are plotted around the central line whereas an upward shift in the points can be seen afterwards. The classical scheme is not signaling any shift whereas the simple $2/2$ scheme is signaling at points # 49 and 50. The modified $2/3$ scheme is giving 3 out of control signals and these are at points # 45, 49 and 50. This clearly indicated that the modified $2/3$ scheme is not only signaling earlier than the classical scheme but also is giving more number of signals. The situation is not much different in Figure 2.7 where the classical and the simple $2/2$ schemes failed to detect any shift while the modified $2/3$ scheme gives out of control signals at points # 25, 26 and 27.

Figure 2.6: EWMA chart of the classical scheme and the the simple 2/2 and modified 2/3 schemes for the dataset 2.1

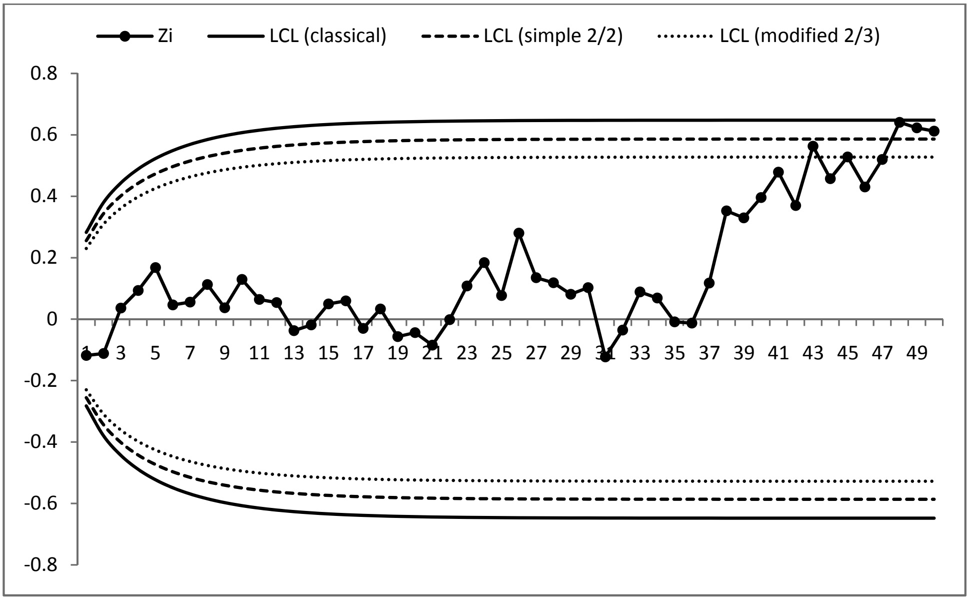

Figure 2.7: EWMA chart of the classical scheme and the the simple 2/2 and modified 2/3 schemes for the dataset 2.2

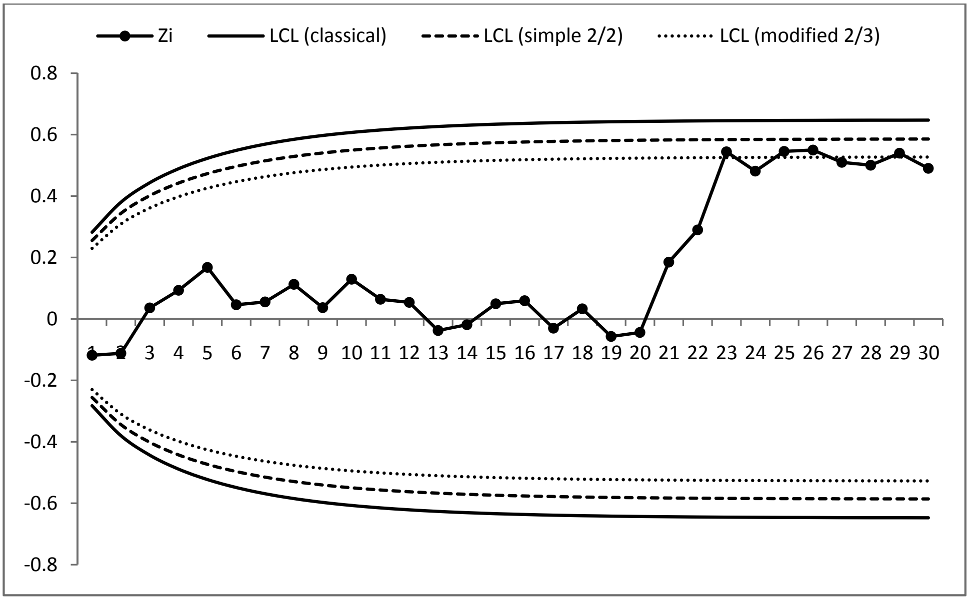

The above example indicates that the modified 2/3 EWMA scheme is giving the advantage in terms of run length as well the number of signals for both small and moderate shifts. The outcomes of these two illustrative examples are completely in accordance with the findings of subsection 3.3.1.

2.4 Concluding remarks

For small shifts CUSUM charts and EWMA charts are considered most effective. The efficiency of these charts can also be increased by using different sensitizing rules and runs rules schemes with their usual design structure. We have proposed two runs rules schemes each for CUSUM and EWMA charts for the location parameter. By investigating the performance of the these proposed schemes and by comparing them with some existing schemes we found that the proposed schemes have the ability to perform better for small and moderate shifts while reasonably maintaining their efficiency for large shifts as well.

To make the CUSUM and EWMA charts even more efficient, some other sensitizing rules/runs rules schemes can be used with their respective structures on the similar lines as followed in this chapter. The proposals and the recommendations of this chapter can also be extended for the attribute control charts based on CUSUM and EWMA patterns.

Chapter 3

Mixed EWMA-CUSUM charts

Shewhart-type control charts are sensitive for large disturbances in the process, while CUSUM- and EWMA-type control charts are intended to spot small and moderate disturbances. In this chapter we propose a mixed EWMA-CUSUM control chart for detecting a shift in the process mean and evaluating its $ARLs$. Comparisons of the proposed control chart are made with some representative control charts including the classical CUSUM, classical EWMA, Fast Initial Response (FIR) CUSUM, FIR EWMA, adaptive CUSUM with EWMA based shift estimator, weighted CUSUM and runs rules based CUSUM and EWMA. The comparisons reveal that the mixing of the two charts makes the proposed scheme even more sensitive to small shifts in the process mean than the other schemes designed for detecting small shifts.

Following the mixed EWMA-CUSUM chart for location, we also propose a new control chart for monitoring the process dispersion. This chart is named the CS-EWMA chart as its plotting statistic is based on a cumulative sum of the exponentially weighted moving averages. Comparisons with other memory charts used to monitor the process dispersion are done by means of the ARL. An illustration of the proposed technique is done by applying the CS-EWMA chart on a simulated dataset.

This chapter is based on two papers; one for monitoring the location parameter (cf. Abbas, Riaz and Does (2012a)) and the other for monitoring the dispersion parameter (cf. Abbas, Riaz and Does (2012b)).

3.1 Mixed EWMA-CUSUM chart for location

After the development of CUSUM and EWMA charts, several modifications of these charts have been presented in order to further enhance the performance of these charts. Lucas (1982) presented the combined Shewhart-CUSUM quality control scheme in which Shewhart limits and CUSUM limits are used simultaneously. Lucas and Crosier (1982) recommended the use of the FIR CUSUM which gives a head start to the CUSUM statistic by setting the initial values of the CUSUM statistic equal to some positive value (non-zero). This feature gives better ARL_1 performance but at the cost of a decrease in ARL_0. Yashchin (1989) presented the weighted CUSUM scheme which gives different weights to the previous information used in CUSUM statistic. Section 2.2 introduced the runs rules schemes to the CUSUM charts and shown that the runs rules based CUSUM performs better than the classical CUSUM for small shifts. Similarly, on the EWMA side, Lucas and Saccucci (1990) presented the combined Shewhart-EWMA quality control scheme which gives better ARL_1 performance for both small and large shifts. Steiner (1999) provided the FIR EWMA which gives a head start to the initial value of the EWMA statistic (like FIR CUSUM) and hence improves the ARL_1 performance of the EWMA charts. Section 2.3 discussed the runs rules schemes to the EWMA charts and showed that the runs rules based EWMA performs better than the classical EWMA for small shifts. In the next subsection we present a mixed EWMA-CUSUM quality control scheme for monitoring the mean of a normally distributed process. The inspiration is to get an improved ARL performance by combining the features of EWMA and CUSUM charts in a single control structure.

3.1.1 Design structure of the proposed chart

In this subsection we propose an assortment of the classical EWMA and CUSUM schemes by combining the features of their design structures. The said proposal mainly depends on two statistics named as M_i^+ and M_i^- which are defined as:

$$\left.\begin{aligned} M_i^+ &= \max\left[0, (Q_i - \mu_0) - K_q' + M_{i-1}^+\right] \\ M_i^- &= \max\left[0, -(Q_i - \mu_0) - K_q' + M_{i-1}^-\right] \end{aligned}\right\} \tag{3.1}$$

where K_q' is a time varying reference value for the proposed charting structure, the quantities M_i^+ and M_i^- are known as the upper and lower CUSUM statistics which are initially set to zero (i.e. $M_i^+ = M_i^- = 0$) and are based on the EWMA statistic Q_i which is defined as:

$$Q_i = \lambda_q Y_i + (1 - \lambda_q) Q_{i-1} \tag{3.2}$$

In (3.2), λ_q is the constant like λ in (1.3) such that $0 < \lambda_q \leq 1$ and the initial value of the Q_i statistic is set equal to the target mean i.e. $Q_0 = \mu_0$. Now the mean and variance of statistic Q_i is given as:

$$\text{Mean}(Q_i) = \mu_0, \qquad \text{Var}(Q_i) = \sigma_Y^2 \left[\frac{\lambda_q}{2-\lambda_q}\left(1 - (1 - \lambda_q)^{2i}\right)\right] \tag{3.3}$$

and this will be used later in the calculation of the parameters of the proposed chart.

In (3.1) and (3.2) we are considering the case of individual observations $(n = 1)$ which may be extended easily for the subgroups. Now the statistics M_i^+ and M_i^- are plotted against the control limit, say H_q'. As long as the values of M_i^+ and M_i^- are plotted inside the control limit, the process is said to be in control, otherwise out of control. It is to be noted here that if the statistic M_i^+ is plotted above H_q' the process mean is said to be shifted above the target value and if the statistic M_i^- is plotted above H_q' the process is said to be shifted below the target value. The control limit H_q' is selected according to a prefixed ARL_0. A large value of the prefixed ARL_0, will give a larger value of H_q' and vice versa. The two quantities K_q' and H_q' are defined as:

$$\left.\begin{aligned} K_q' &= k_q \times \sqrt{Var(Q_i)} = k_q \times \sigma_Y \sqrt{\tfrac{\lambda_q}{2-\lambda_q}\left(1-\left(1-\lambda_q\right)^{2i}\right)} \\ H_q' &= h_q \times \sqrt{Var(Q_i)} = h_q \times \sigma_Y \sqrt{\tfrac{\lambda_q}{2-\lambda_q}\left(1-\left(1-\lambda_q\right)^{2i}\right)} \end{aligned}\right\} \quad (3.4)$$

where k_q and h_q are the constants like k and h, respectively, in the classical set up for the CUSUM (cf. Section 1.2). The time varying values K_q and H_q are due to the variance of the EWMA statistic in expression (3.3). For a fixed value of k_q, we can select the value of h_q from the tables (that are given later in this subsection) that fix the ARL_0 at our desired level. In general K_q' is chosen equal to half of the shift (in units of the standard deviation of Q_i). Hence, we choose $k_q = 0.5$ as it makes the CUSUM structure more sensitive to the small and moderate shifts (cf. Montgomery (2009)), to which memory charts actually target.

To evaluate the ARL performance of a control scheme, we have used the Monte Carlo simulation approach in this chapter. An algorithm in R language (provided in Appendix 3.1) is developed to calculate the run lengths. The algorithm is run 50,000 times to calculate the average of those 50,000 run lengths. A detailed study on the ARL performance of the proposed EWMA-CUSUM control chart to monitor the mean of a normally distributed process is provided in Tables 3.1 – 3.3 for some selective choices of δ, λ_q and h_q. For this purpose $ARL_0's$ are fixed at 168, 400 and 500 which are the commonly used choices. For other values of $ARL_0's$ one may easily obtain the results on similar lines.

The relative standard errors for the results provided in Tables 3.1 – 3.3 are also calculated and found to be less than 1.2%. Moreover, we have also replicated the ARL results of the classical CUSUM and the classical EWMA using our simulation algorithm and found almost similar results as by Hawkins and Olwell (1998) and Lucas and Saccucci (1990), respectively, ensuring the validity of the simulation algorithm used.

TABLE 3.1: ARL values for the proposed EWMA-CUSUM scheme with $k_q = 0.5$ at $ARL_0 = 168$

δ	$\lambda_q = 0.1$ $h_q = 21.3$	$\lambda_q = 0.25$ $h_q = 13.29$	$\lambda_q = 0.5$ $h_q = 8.12$	$\lambda_q = 0.75$ $h_q = 5.48$
0	168.0441	168.0652	169.8763	171.0422
0.25	52.6449	54.1752	59.7829	68.15245
0.5	24.85945	22.40665	22.54895	24.12865
0.75	17.0208	14.0235	12.85555	12.60565
1	13.3323	10.4832	8.9565	8.2741
1.5	9.743	7.3272	5.78565	4.99665
2	7.90705	5.8231	4.4341	3.7365

TABLE 3.2: ARL values for the proposed EWMA-CUSUM scheme with $k_q = 0.5$ at $ARL_0 = 400$

δ	$\lambda_q = 0.1$ $h_q = 33.54$	$\lambda_q = 0.25$ $h_q = 18.7$	$\lambda_q = 0.5$ $h_q = 10.52$	$\lambda_q = 0.75$ $h_q = 6.94$
0	402.0894	397.404	398.6486	400.8962
0.25	73.31955	78.02035	90.45915	108.0086
0.5	33.06085	29.0845	28.94885	31.44015
0.75	22.39445	17.79425	15.75695	15.66785
1	17.63975	13.2232	10.94695	10.17115
1.5	12.88105	9.113	6.9587	6.03875
2	10.45315	7.2235	5.2808	4.4203

TABLE 3.3: ARL values for the proposed EWMA-CUSUM scheme with $k_q = 0.5$ at $ARL_0 = 500$

δ	$\lambda_q = 0.1$ $h_q = 37.42$	$\lambda_q = 0.25$ $h_q = 20.18$	$\lambda_q = 0.5$ $h_q = 11.2$	$\lambda_q = 0.75$ $h_q = 7.32$
0	498.3882	502.018	507.9555	507.5152
0.25	80.13585	83.7529	100.2635	121.9883
0.5	35.524	30.88825	30.7466	33.5054
0.75	24.0522	18.8755	16.6399	16.5139
1	18.8637	13.8816	11.45835	10.6107
1.5	13.79075	9.6036	7.29565	6.3101
2	11.19775	7.59055	5.52345	4.589

The main findings about our proposed EWMA-CUSUM quality control scheme for monitoring the mean of a normally distributed process are given as:

i. mixing of the EWMA and CUSUM schemes really boosts the ARL performance of the resulting combination of the two charts especially for small and moderate shifts in the process (cf. Tables 3.1 – 3.3);

ii. for detecting small shifts in the process, the performance of the proposed scheme is better with smaller values of λ_q and vice versa (cf. Tables 3.1 – 3.3);

iii. the proposed scheme is ARL unbiased, i.e. for a fixed value of ARL_0, the ARL_1 decreases with a decrease in the value of δ and vice versa (cf. Tables 3.1 – 3.3);

iv. for a fixed value of δ, the ARL_1 of the proposed scheme decreases with a decrease in ARL_0 (cf. Tables 3.1 – 3.3);

v. for a fixed value of ARL_0, the control limit coefficient h_q decreases with the increase in λ_q (cf. Tables 3.1 – 3.3).

3.1.2 Comparisons

In this subsection we present a comprehensive comparison of the proposed mixed EWMA-CUSUM scheme with some existing representative EWMA and CUSUM control charts available in the literature. The performance of the control chart is compared in terms of ARL. The set of the schemes considered for the comparison consist of the classical CUSUM, the classical EWMA, the FIR CUSUM, the FIR EWMA, the adaptive CUSUM with EWMA based shift estimator, the weighted CUSUM and the runs rules based CUSUM and EWMA.

Proposed versus the classical CUSUM: The ARL values for the classical CUSUM control scheme proposed by Page (1954) are given in Table 2.1. Comparison of the classical

CUSUM with the proposed schemes reveal that the proposed scheme is performing really good for all the values of λ_q, particularly for small values of λ_q. We can see that, for all values of λ_q, the proposed scheme has better ARL performance as compared to the classical CUSUM (cf. Table 2.1 vs. Table 3.1).

Proposed versus the classical EWMA: The ARL values for the classical EWMA with time varying limits, given by Steiner (1999), are provided in Table 2.2. Comparing the classical EWMA ($\lambda = 0.25$) with the proposed scheme we observe that the proposed scheme has better $ARL_1's$ performance with its respective values of λ_q (cf. Table 2.2 vs. Table 3.3).

Proposed versus the FIR CUSUM: The FIR CUSUM presented by Lucas and Crosier (1982) provides a head start to the CUSUM statistic. The $ARLs$ of the CUSUM with FIR feature are given in Table 2.10 in which head start is represented by C_0. The FIR feature decreases the ARL_0 of the CUSUM chart and more importantly this decreased ARL_0 becomes very small for the larger values of C_0 (for $C_0 = 1$, $ARL_0 = 163$) which is not recommended in case of sensitive processes like in health care (cf. Bonetti et al. (2000)). Comparing the proposed scheme with the FIR CUSUM we see that for smaller values of λ_q the proposed scheme has a better ARL performance than the FIR CUSUM, even if the FIR CUSUM does not have the fixed ARL_0 at 168 but has smaller ARL_0 value, i.e. 163 (cf. Table 2.10 vs. Table 3.1).

Proposed versus the FIR EWMA: FIR EWMA presented by Steiner (1999) is similar to the FIR CUSUM as it also gives a head start to the EWMA statistic. The control limits for the FIR based EWMA chart are given as:

$$\mu_0 \pm L\sigma_X\left(1-(1-f)^{1+a(t-1)}\right)\sqrt{\frac{\lambda}{2-\lambda}(1-(1-\lambda)^{2i})}$$

where $a = (-2/log(1-f) - 1)/19$. The $ARLs$ for the FIR EWMA with $\lambda = 0.1$ and the proposed chart with $\lambda_q = 0.1$ are given in Table 3.4. Comparing the proposed scheme with the FIR EWMA we see that the proposed scheme is performing better than the FIR EWMA for smaller shifts i.e. $\delta < 0.5$. For moderate and larger shifts, FIR EWMA seems superior as compared to the proposed chart.

TABLE 3.4: ARL values for the FIR EWMA scheme and the proposed chart

δ	FIR EWMA		EWMA-CUSUM	
	$\lambda = 0.1, L = 3$ $f = 0.4$	$\lambda = 0.1, L = 3$ $f = 0.5$	$\lambda_q = 0.1, a^* = 0.5$ $b^* = 37.94$	$\lambda_q = 0.1, a^* = 0.5$ $b^* = 40.8$
0	515.6	613.8	516.48	613.62
0.25	83.1	99.2	81.03	85.79
0.5	18.5	22.1	35.76	37.55
0.75	7.3	8.8	24.2	25.41
1	3.8	4.6	19.01	19.94
1.5	1.7	2.1	13.9	14.55
2	1.3	1.4	11.29	11.8
3	1	1	8.48	8.88
4	1	1	6.96	7.29

Proposed versus the adaptive CUSUM with EWMA based shift estimator: Jiang et al. (2008) proposed the use of adaptive CUSUM with EWMA-based shift estimator. They used the concept of adaptively updating the reference value of the CUSUM chart using the EWMA estimator and then using a suitable weighting function. The ARL values for the adaptive CUSUM are given in Table 3.5 in which δ^+_{min}, λ, γ and h are the parameters of the chart. Comparing the performance of the proposed scheme we notice that the proposed scheme is outperforming the adaptive CUSUM for small values of δ. For moderate and large values of δ, both the proposed scheme and adaptive CUSUM have almost the same ARL performance (cf. Table 3.5 vs. Table 3.2).

TABLE 3.5: ARL values for adaptive CUSUM with $\delta_{min}^{+} = 0.5$ and $\lambda = 0.3$ at $ARL_0 = 400$

δ	$\gamma = 1.5$ $h = 5.05$	$\gamma = 2$ $h = 4.73$	$\gamma = 2.5$ $h = 4.505$	$\gamma = 3$ $h = 4.394$	$\gamma = 4$ $h = 4.337$	$\gamma = \infty$ $h = 4.334$
0	399.7	400.85	400.19	399.29	399.39	399.97
0.25	92.82	91.65	88.96	87.02	85.81	85.8
0.5	30.52	30.1	29.32	28.79	28.46	28.45
0.75	14.7	14.5	14.2	14	13.89	13.88
1	9.07	8.96	8.81	8.72	8.67	8.66
1.5	4.89	4.87	4.84	4.83	4.83	4.82
2	3.23	3.25	3.28	3.31	3.35	3.34

There is also an adaptive EWMA chart (cf. Capizzi and Masarotto (2003)), but its performance is inferior to the adaptive CUSUM, so the results of our proposal are superior to the adaptive EWMA as well.

Proposed versus the weighted CUSUM: Weighted CUSUM presented by Yashchin (1989) gives weights to the past information in the CUSUM statistic. The $ARLs$ for the weighted CUSUM are given in Table 2.9 in which the weights given to the past information are represented by γ. The comparison of the proposed scheme with the weighted CUSUM shows that the proposed scheme is performing better than the weighted CUSUM for the small and moderate shifts (like $\delta < 1.5$). For larger values of δ, the weighted CUSUM almost coincide with the proposed scheme (cf. Table 2.9 vs. Table 3.3).

Proposed versus the runs rules based CUSUM: Section 2.2 introduced the use of the runs rules schemes with the design structure of the CUSUM charts. The $ARLs$ for the two runs rules based CUSUMs are given in Tables 2.3 and 2.4 in which WL and AL are representing the warning limits and action limits, respectively. The comparison of the proposed scheme with both the runs rules based CUSUM schemes shows that the proposed scheme has the ability to perform better than the runs rules based CUSUM for all the choices of λ_q (cf. Tables 2.3 and 2.4 vs. Table 3.1).

Proposed versus the runs rules based EWMA: Section 2.3 introduced the use of the runs rules schemes EWMA structure. The $ARLs$ for the two runs rules based EWMAs are given in Tables 2.15 and 2.16. The comparison of the proposed schemes with both the runs rules based EWMA schemes shows that the proposed scheme is performing better as long as $\lambda > 0.1$ for the runs rules based EWMA schemes. For $\lambda = 0.1$, modified $2/3$ EWMA scheme becomes a bit superior to the proposed chart (cf. Tables 2.15 and 2.16 vs. Table 3.3).

Overall View: In order to provide an overall comparative view of the proposed scheme with the other existing counterparts we have made some graphical displays, in the form of ARL curves. Three selective graphs of different charts/schemes are given in Figures 3.1 – 3.3. In these figures RR CUSUM (EWMA) stands for the runs rules based CUSUM (EWMA) schemes and the other terms/symbols used are self-explanatory.

Figure 3.1: ARL curves for the proposed scheme, the Classical CUSUM, the FIR CUSUM and Runs Rules based CUSUMs at $ARL_0 = 168$

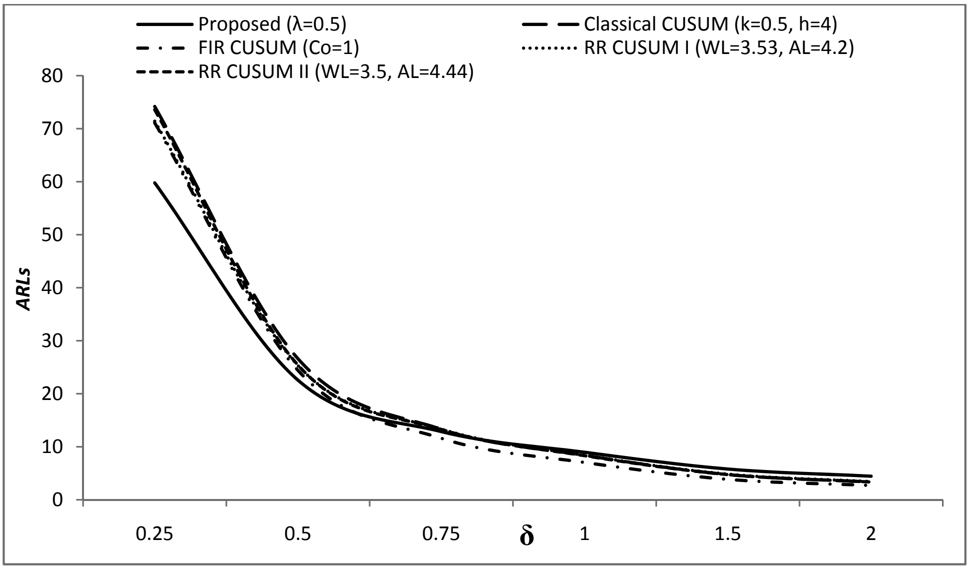

Figure 3.2: ARL **curves for the proposed scheme and adaptive CUSUM at** $ARL_0 = 400$

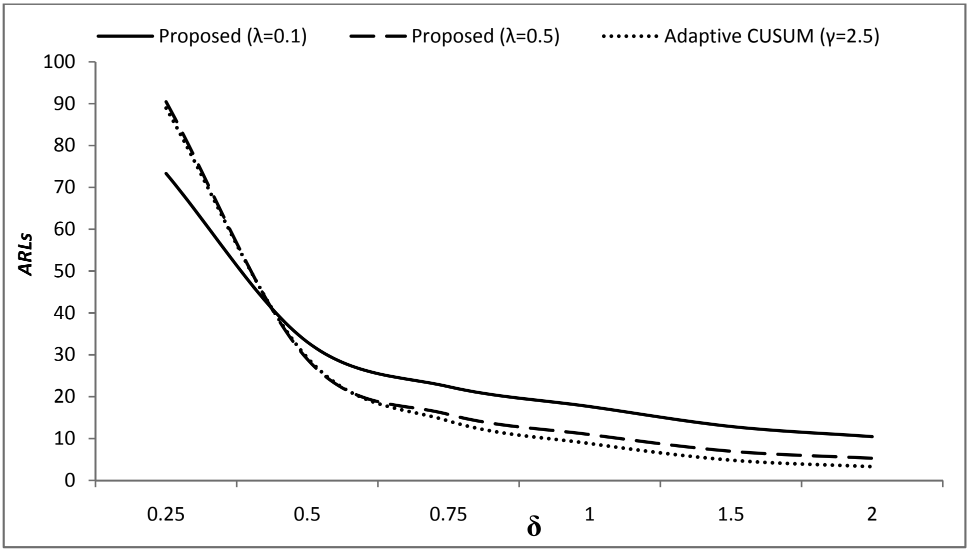

Figure 3.3: ARL **curves for the proposed scheme, the classical EWMA, the FIR EWMA, the runs rules based EWMA and the weighted CUSUM at** $ARL_0 = 500$

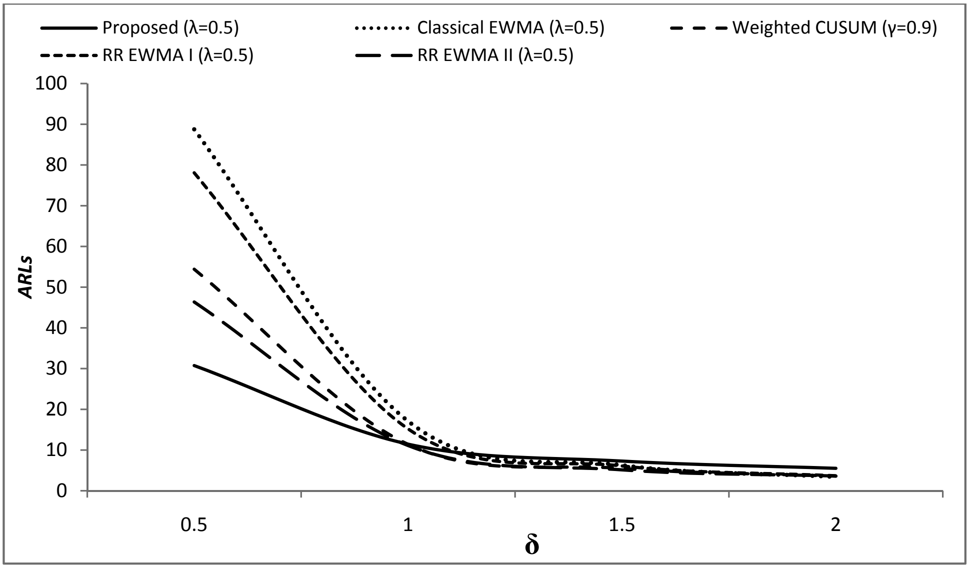

By examining the graphs of ARL curves of different schemes under study we see that the ARL curve of the proposed schemes are on the lower side which shows evidence for the dominance of the proposed scheme over the other schemes. For small values of δ, the difference between the ARL of the proposed scheme and the other schemes is larger whereas for the moderate values of δ this difference almost disappears. For large values of δ, the ARL curve of the proposed chart seems above the ARL curves of some other charts showing the poor performance of the proposed chart for large shifts.

To sum up, we may infer that in general the proposed chart is superior for small and moderate shifts while for larger shifts its performance is inferior to some of the other schemes under investigation.

3.1.3 Illustrative example

Besides exploring the statistical properties of a method it is always good to provide its application on some data for illustration purposes. Here we present an illustrative example to show how the proposed scheme can be applied in the real situation. For this purpose a dataset is generated containing 40 observations. The first 20 observations are generated from the in control situation (i.e. $N(0,1)$ so that the target mean is 0) and the remaining 20 observations are generated from an out of control situation with a small shift introduced in the process (i.e. $N(0.5,1)$). The classical CUSUM, the classical EWMA and the proposed scheme are applied to this dataset and the parameters are selected to be $k = 0.5$ and $h = 5.07$ for the classical CUSUM scheme, $\lambda = 0.25$ and $L = 3$ for the classical EWMA scheme, $\lambda_q = 0.25$, $k_q = 0.5$ and $h_q = 20.18$ for the proposed scheme to guarantee that $ARL_0 = 500$.

Figure 3.4: The classical CUSUM chart for the simulated dataset using $k = 0.5$ and $h = 5.09$ at $ARL_0 = 500$

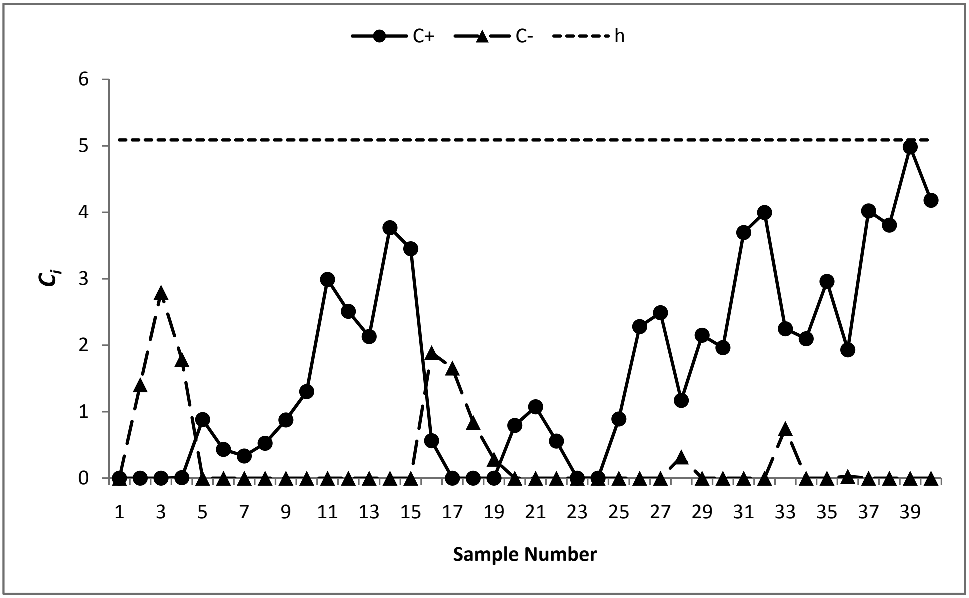

Figure 3.5: The classical EWMA chart for the simulated dataset using $\lambda = 0.25$ and $L = 3$ at $ARL_0 = 500$

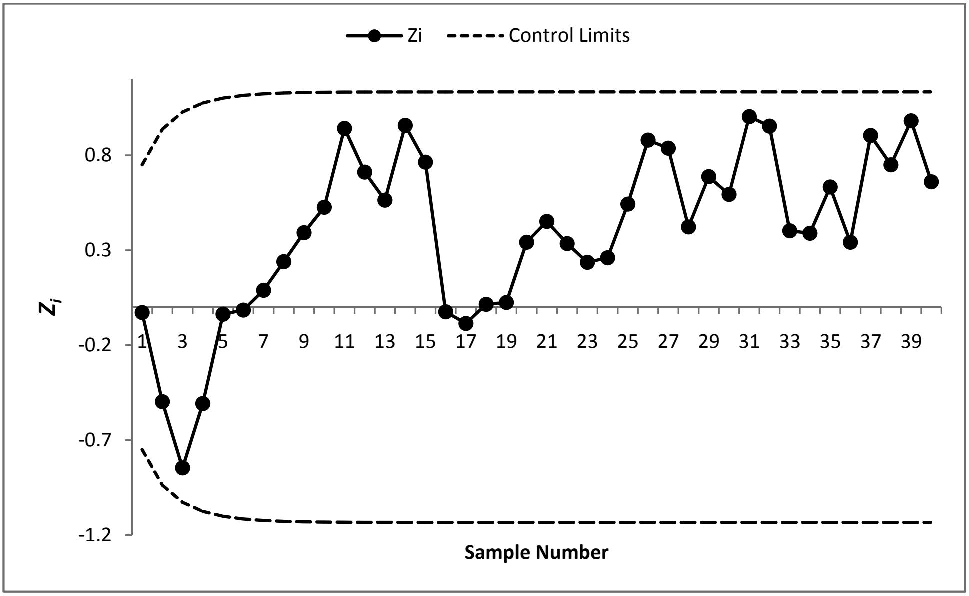

Figure 3.6: The proposed scheme for the simulated dataset using $\lambda_q = 0.25$, $k_q = 0.5$ and $h_q = 20.18$ at $ARL_0 = 500$

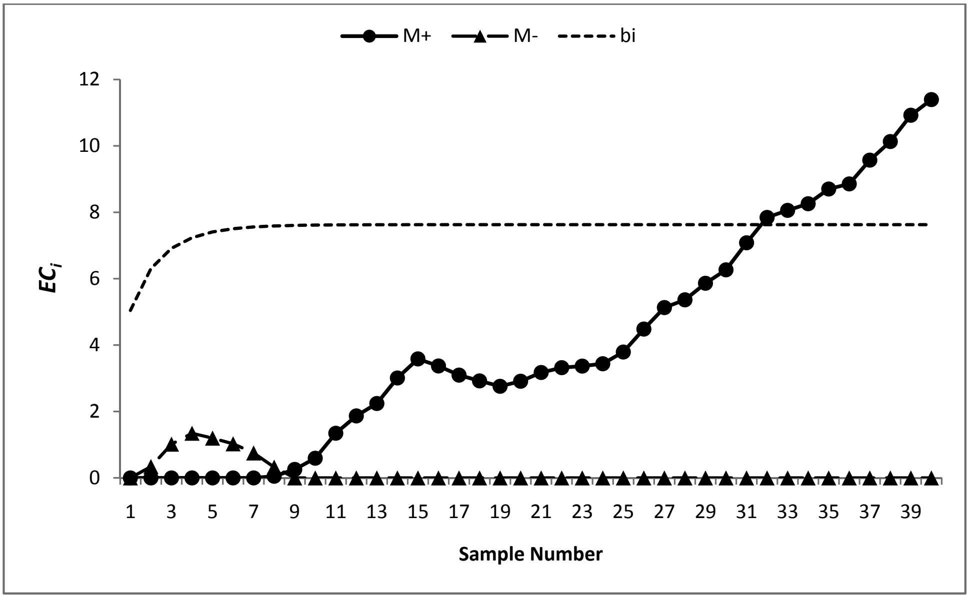

The calculations for the proposed scheme are given in Table 3.6 and the graphical display of all three control structures are provided in Figures 3.4 – 3.6 with the statistics C_i^+ and C_i^- plotted against the control limit H for the classical CUSUM scheme; Z_i plotted against the control limits given in (1.4) for the classical EWMA scheme; and M_i^+ and M_i^- plotted against the control limit H_q for the proposed scheme.

From Table 3.6 and Figure 3.6 it is obvious that out of control signals are received at samples # 32, 33, 34, 35, 36, 37, 38, 39 and 40 by the proposed scheme (giving 8 out of control signals). Figures 3.4 – 3.5 show that the separate applications of the classical CUSUM and EWMA schemes fail to detect any out of control situation for the given dataset. This clearly indicates superiority of the proposed scheme over the classical CUSUM and EWMA schemes and it is exactly in accordance with the findings of subsection 3.1.1.

TABLE 3.6: Application example of the proposed scheme using $\lambda_q = 0.25$, $a^* = 0.5$ and $b^* = 20.18$ at $ARL_0 = 500$

Sample No.	$X_i = Y_i$	Q_i	K'_q	M_i^+	M_i^-	H'_q	Sample No.	$X_i = Y_i$	Q_i	K'_q	M_i^+	M_i^-	H'_q
1	-0.113	-0.028	0.125	0	0	5.045	21	0.781	0.452	0.189	3.175	0	7.627
2	-1.906	-0.498	0.156	0	0.341	6.306	22	-0.016	0.335	0.189	3.321	0	7.627
3	-1.891	-0.846	0.171	0	1.016	6.915	23	-0.061	0.236	0.189	3.368	0	7.627
4	0.508	-0.508	0.179	0	1.344	7.235	24	0.332	0.26	0.189	3.439	0	7.627
5	1.374	-0.037	0.184	0	1.198	7.409	25	1.391	0.543	0.189	3.793	0	7.627
6	0.05	-0.015	0.186	0	1.027	7.506	26	1.89	0.879	0.189	4.483	0	7.627
7	0.401	0.089	0.187	0	0.751	7.559	27	0.709	0.837	0.189	5.131	0	7.627
8	0.692	0.239	0.188	0.051	0.323	7.589	28	-0.82	0.423	0.189	5.364	0	7.627
9	0.851	0.392	0.188	0.255	0	7.606	29	1.481	0.687	0.189	5.863	0	7.627
10	0.927	0.526	0.189	0.593	0	7.615	30	0.314	0.594	0.189	6.268	0	7.627
11	2.187	0.941	0.189	1.346	0	7.621	31	2.231	1.003	0.189	7.082	0	7.627
12	0.02	0.711	0.189	1.868	0	7.623	32	0.802	0.953	0.189	7.846*	0	7.627
13	0.12	0.563	0.189	2.242	0	7.625	33	-1.25	0.402	0.189	8.059*	0	7.627
14	2.138	0.957	0.189	3.01	0	7.626	34	0.351	0.389	0.189	8.260*	0	7.627
15	0.183	0.764	0.189	3.585	0	7.627	35	1.362	0.632	0.189	8.703*	0	7.627
16	-2.389	-0.024	0.189	3.371	0	7.627	36	-0.529	0.342	0.189	8.856*	0	7.627
17	-0.269	-0.086	0.189	3.097	0	7.627	37	2.59	0.904	0.189	9.571*	0	7.627
18	0.317	0.015	0.189	2.923	0	7.627	38	0.287	0.75	0.189	10.132*	0	7.627
19	0.055	0.025	0.189	2.759	0	7.627	39	1.676	0.981	0.189	10.924*	0	7.627
20	1.293	0.342	0.189	2.912	0	7.627	40	-0.303	0.66	0.189	11.395*	0	7.627

* indicates proposed scheme giving out of control signal

3.2 Mixed EWMA-CUSUM chart for dispersion

Page (1963) introduced the CUSUM chart for monitoring the increase in process dispersion using sample ranges. Following him, Tuprah and Ncube (1987), Chang and Gan (1995) and Acosta-Mejia et al. (1999) proposed several improved versions of the CUSUM chart for process dispersion. On the other hand, Wortham and Ringer (1971) suggested an EWMA control chart for monitoring the process dispersion. Ng and Case (1989) and Crowder and Hamilton (1992) proposed improved versions of the EWMA chart for monitoring process variance. Castagliola (2005) and Castagliola et al. (2009) proposed EWMA respectively CUSUM control charts for monitoring the process variance based on a logarithmic transformation of the sample variance. This article proposes a new memory-type control chart based on the same transformation, named as CS-EWMA chart, for monitoring the process dispersion by mixing the effects of EWMA and CUSUM charts.

After presenting the basic structures of the EWMA and CUSUM charts for monitoring the process dispersion in the next subsection, we present the details of our proposed CS-EWMA chart for process standard deviation in the subsequent subsection.

3.2.1 S^2-EWMA control chart

Castagliola (2005) proposed an S^2-EWMA control chart for monitoring the process dispersion. This control structure is based on a three parameter logarithmic transformation which is given as:

$$T_i = a_T + b_T \ln(S_i^2 + c_T) \tag{3.5}$$

where S_i^2 is the sample variance for i^{th} sample defined as $S_i^2 = \frac{\sum_{j=1}^{n}(X_{ij}-\bar{X}_i)^2}{n-1}$, X_{ij} represents the j^{th} observation from the i^{th} sample of size n from a normal distribution with mean μ, standard deviation σ_0 and $\bar{X}_i$ is the average of the i^{th} sample. The constants a_T, b_T and c_T are defined as $b_T = B_T(n)$, $c_T = C_T(n)\sigma_0^2$ and $a_T = A_T(n) - 2B_T(n)\ln(\sigma_0)$ as in Castagliola (2005). He derived the distribution of T_i and showed that if the constants a_T, b_T and c_T are judiciously selected, then the distribution of variable T_i becomes very close to the normal distribution with mean $\mu_T(n)$ and variance $\sigma_T^2(n)$, i.e. $T_i \approx N\left(\mu_T(n), \sigma_T^2(n)\right)$ (cf. Appendix A in Castagliola (2005)). Table 3.7 reproduces the values of $A_T(n)$, $B_T(n)$, $C_T(n)$, $\mu_T(n)$ and $\sigma_T(n)$ for $n = 3,4,5, \dots ,15$ from Table I in Castagliola (2005).

Now using the approximately normally distributed variable T_i from Castagliola (2005), the plotting statistic for the S^2-EWMA chart is defined as:

$$Z_i = \lambda T_i + (1-\lambda)Z_{i-1} \tag{3.6}$$

where λ is the sensitivity parameter chosen as $0 < \lambda \leq 1$ and the initial value of Z_i is taken as $Z_0 = A_T(n) + B_T(n)\ln\big(1 + C_T(n)\big)$. The control limits for the statistic given in (3.6) are given as:

$$LCL = \mu_T(n) - L\sqrt{\tfrac{\lambda}{2-\lambda}}\sigma_T(n), \quad CL = \mu_T(n), \quad UCL = \mu_T(n) + L\sqrt{\tfrac{\lambda}{2-\lambda}}\sigma_T(n) \tag{3.7}$$

where L is the control limit coefficient that determines the distance between LCL and UCL.

Table 3.7: Values of $\mu_T(n)$, $\sigma_T(n)$, $A_T(n)$, $B_T(n)$ and $C_T(n)$

n	$A_T(n)$	$B_T(n)$	$C_T(n)$	$\mu_T(n)$	$\sigma_T(n)$
3	-0.6627	1.8136	0.6777	0.02472	0.9165
4	-0.7882	2.1089	0.6261	0.01266	0.9502
5	-0.8969	2.3647	0.5979	0.00748	0.9670
6	-0.9940	2.5941	0.5801	0.00485	0.9765
7	-1.0827	2.8042	0.5678	0.00335	0.9825
8	-1.1647	2.9992	0.5588	0.00243	0.9864
9	-1.2413	3.1820	0.5519	0.00182	0.9892
10	-1.3135	3.3548	0.5465	0.00141	0.9912
11	-1.3820	3.5189	0.5421	0.00112	0.9927
12	-1.4473	3.6757	0.5384	0.00090	0.9938
13	-1.5097	3.8260	0.5354	0.00074	0.9947
14	-1.5697	3.9705	0.5327	0.00062	0.9955
15	-1.6275	4.1100	0.5305	0.00052	0.9960

The ARL values of S^2-EWMA are given in Table 3.8 for different values of λ, where τ represents the amount of shift in the standard deviation (i.e. $\tau = {}^{\sigma_1}/_{\sigma_0}$ with σ_1 representing the shifted standard deviation) and the in control ARL is fixed at 200, as is done in earlier work on this subject. The $ARLs$ in this section are evaluated through simulation procedures by running 10^5 replications. The program is developed in R language.

Table 3.8: ARL values for the S^2-EWMA chart with $n = 5$ and $ARL_0 = 200$

τ	$\lambda = 0.05$ $L = 2.269$	$\lambda = 0.1$ $L = 2.452$	$\lambda = 0.2$ $L = 2.592$	$\lambda = 0.3$ $L = 2.634$	$\lambda = 0.4$ $L = 2.643$	$\lambda = 0.5$ $L = 2.639$
0.5	9.257	6.866	5.616	5.448	5.928	7.606
0.6	11.679	8.931	7.856	8.481	10.735	16.909
0.7	16.101	13.03	13.064	16.699	25.58	48.763
0.8	26.108	23.679	29.961	46.058	80.157	166.467
0.9	63.459	70.501	107.839	169.543	274.071	474.331
0.95	133.554	153.817	204.856	264.011	327.699	392.103
1	199.781	200.702	200.756	200.262	200.59	199.224
1.05	78.77	92.938	98.675	98.004	97.342	96.541
1.1	32.542	41.746	47.688	49.736	50.94	51.373
1.2	11.986	15.382	17.449	18.537	19.274	20.022
1.3	7.064	8.766	9.571	9.909	10.226	10.527
1.4	5.054	6.09	6.419	6.517	6.6	6.753
1.5	3.983	4.722	4.835	4.801	4.787	4.82
2	2.133	2.418	2.343	2.225	2.148	2.098
3	1.338	1.456	1.395	1.336	1.294	1.267

Note that the results from Table 3.8 coincide with the results of Table III of Castagliola (2005).

3.2.2 CUSUM-S^2 control chart

Taking inspiration from the S^2-EWMA chart, Castagliola et al. (2009) proposed a CUSUM-S^2 chart for monitoring the process dispersion which is based on the statistic T_i given in (3.5). The CUSUM-S^2 chart uses two plotting statistics, named as C^+ and C^-, and given as:

$$\left.\begin{aligned} C_i^+ &= \max\left[0, \left(T_i - \mu_T(n)\right) - K + C_{i-1}^+\right] \\ C_i^- &= \max\left[0, -\left(T_i - \mu_T(n)\right) - K + C_{i-1}^-\right] \end{aligned}\right\} \qquad (3.8)$$

where K is the reference value and the sensitivity parameter of the CUSUM-S^2 chart. The initial values for the plotting statistics given in (3.8) are taken equal to zero, i.e. $C_0^+ = C_0^- =$

0. These plotting statistics are plotted against a control limit H and an out of control signal is received if either of the two statistics (i.e. C^+ and C^-) is plotted above H. K and H are jointly the two parameters of CUSUM-S^2 chart and their standard forms are given as:

$$K = k\sigma_T(n), \qquad H = h\sigma_T(n) \tag{3.9}$$

where k and h are constants which determine the properties of the chart. The ARL values for the CUSUM-S^2 chart for different choices of its parameters are given in Table 3.9 with ARL_0 fixed at 200.

Table 3.9: ARL values for the CUSUM-S^2 chart with $n = 5$ and $ARL_0 = 200$

τ	$K = 0.1$ $H = 10.53$	$K = 0.25$ $H = 6.476$	$K = 0.5$ $H = 3.855$	$K = 0.75$ $H = 2.62$	$K = 1$ $H = 1.906$
0.5	9.059	6.516	5.199	5.071	6.121
0.6	11.382	8.452	7.303	8.264	13.223
0.7	15.489	12.169	12.295	18.314	43.032
0.8	24.394	21.619	29.699	60.662	170.474
0.9	54.649	63.997	116.766	226.253	475.443
0.95	114.332	143.17	213.662	294.554	379.161
1	199.846	199.241	199.841	200.769	199.625
1.05	102.864	104.01	104.806	102.974	100.707
1.1	52.641	50.675	53.502	54.227	54.99
1.2	25.057	20.867	20.373	20.777	21.353
1.3	16.451	12.763	11.255	11.092	11.18
1.4	12.434	9.256	7.654	7.2	7.115
1.5	10.068	7.341	5.832	5.26	5.126
2	5.509	3.885	2.873	2.41	2.197
3	3.347	2.379	1.686	1.404	1.3

3.2.3 Design structure of the proposed chart

In this subsection we propose a memory-type control chart which is based on mixing the effects of EWMA and CUSUM charts into a single control chart structure. For the location parameter this idea was explored in Section 3.1. Again let X_{ij} (i.e. the j^{th}

observation of i^{th} sample with $j = 1,2, \ldots \ldots, n$ and $i = 1,2, \ldots \ldots$) be distributed normally with mean μ_0 and variance σ_0^2 under an in control situation. Then the two plotting statistics (named as M_i^+ and M_i^-) for the proposed CS-EWMA chart are given as:

$$\left.\begin{aligned} M_i^+ &= \max\left[0, \left(Q_i - \mu_T(n)\right) - K_q' + M_{i-1}^+\right] \\ M_i^- &= \max\left[0, -\left(Q_i - \mu_T(n)\right) - K_q' + M_{i-1}^-\right] \end{aligned}\right\} \tag{3.10}$$

where K_q' is the reference value for the proposed chart, like K in (3.8). The initial value for both plotting statistics is taken equal to zero, i.e. $M_0^+ = M_0^+ = 0$. Q_i is the EWMA statistic which is defined as:

$$Q_i = \lambda_q T_i + \left(1 - \lambda_q\right) Q_{i-1} \tag{3.11}$$

where λ_q is the smoothing constant like λ in (3.6) and is chosen as $0 < \lambda_q \leq 1$. T_i is the statistic defined in (3.5). The initial value for the statistic Q_i is taken as $Q_0 = A_T(n) + B_T(n) \ln\left(1 + C_T(n)\right)$. The statistics M_i^+ and M_i^- are now plotted against the control limit H_q' and an out of control signal is received if either of the two plotting statistics given in (3.10) is plotted above H_q'. If M_i^+ is plotted above H_q' that would indicate a positive shift in the process standard deviation and if the value of M_i^- gets larger than H_q' then it would be declared that the process standard deviation has shifted downwards. The standard forms of K_q' and H_q' depending upon the variance of Q_i (i.e. $\text{variance}(Q_i) = \sigma_T^2(n)\left(\frac{\lambda_q}{2-\lambda_q}\right)$, cf. (3.7)) are given as:

$$\left.\begin{aligned} K_q' &= k_q\left(\sigma_T(n)\sqrt{\frac{\lambda_q}{2-\lambda_q}}\right) = K_q\sqrt{\frac{\lambda_q}{2-\lambda_q}} \\ H_q' &= h_q\left(\sigma_T(n)\sqrt{\frac{\lambda_q}{2-\lambda_q}}\right) = H_q\sqrt{\frac{\lambda_q}{2-\lambda_q}} \end{aligned}\right\} \tag{3.12}$$

where $K_q = k_q \sigma_T(n)$ and $H_q = h_q \sigma_T(n)$. Here in (3.12), we have used the asymptotic standard deviation of the statistic Q but the practitioner may use the exact standard deviation as discussed by Steiner (1999). Note that the CUSUM-S^2 is a special case of the proposed

CS-EWMA chart with $\lambda_q = 1$. Finally, a detailed study on the ARL performance of the proposed CS-EWMA chart is given in Tables 3.10 – 3.15, where the ARL_0 is fixed at 200 and n = 5. The algorithm developed in R language for computing the $ARLs$ is given in Appendix 3.2.

Values of H_q for sample sizes other than 5 can be found by the relation $H_{q(n\neq5)} = H_{q(n=5)}\left(\frac{\sigma_T(n\neq5)}{\sigma_T(n=5)}\right)$ for a fixed $ARL_0 = 200$. From Tables 3.10 – 3.15, we can conclude that:

i. for fixed values of n, K_q and ARL_0, the value of H_q decreases with an increase in the value of λ_q and vice versa;

ii. for fixed values of n, λ_q and ARL_0, large values of K_q are giving small ARL_1 values for detecting a positive shift in the process dispersion;

Table 3.10: ARL values for the CS-EWMA chart with $\lambda_q = 0.05$, $n = 5$ and $ARL_0 = 200$

τ	$K_q = 0.1$ $H_q = 62.6$	$K_q = 0.25$ $H_q = 47.06$	$K_q = 0.5$ $H_q = 29.5$	$K_q = 0.75$ $H_q = 18.15$	$K_q = 1$ $H_q = 10.62$
0.5	23.156	20.626	17.482	15.133	13.289
0.6	26.652	23.825	20.32	17.749	15.758
0.7	32.317	28.983	24.993	22.144	19.969
0.8	43.072	38.98	34.238	31.092	28.876
0.9	73.716	68.713	63.844	61.61	61.053
0.95	127.175	123.052	120.583	121.6	123.108
1	199.718	200.262	200.951	200.69	199.752
1.05	94.196	88.525	84.496	82.271	81.696
1.1	52.536	47.005	41.056	37.801	35.939
1.2	31.726	27.331	22.219	18.725	16.32
1.3	24.789	21.241	16.942	13.848	11.534
1.4	21.141	18.078	14.341	11.569	9.429
1.5	18.774	16.091	12.706	10.183	8.233
2	13.481	11.562	9.112	7.224	5.712
3	10.16	8.729	6.877	5.442	4.271

Table 3.11: ARL values for the CS-EWMA chart with $\lambda_q = 0.1, n = 5$ and $ARL_0 = 200$

τ	$K_q = 0.1$ $H_q = 48.1$	$K_q = 0.25$ $H_q = 35.5$	$K_q = 0.5$ $H_q = 22.27$	$K_q = 0.75$ $H_q = 14.1$	$K_q = 1$ $H_q = 8.81$
0.5	17.682	15.366	12.769	10.995	9.717
0.6	20.542	17.895	14.96	13.009	11.626
0.7	25.299	22.109	18.707	16.487	15.072
0.8	34.747	30.731	26.633	24.372	23.188
0.9	63.816	58.764	55.477	55.787	57.655
0.95	115.831	113.49	115.278	120.601	126.425
1	199.304	199.885	200.85	199.751	200.113
1.05	102.296	96.919	95.415	95.943	96.935
1.1	55.637	50.376	45.925	44.641	44.409
1.2	30.526	26.334	22.075	19.62	18.345
1.3	22.596	19.244	15.62	13.331	11.874
1.4	18.601	15.786	12.672	10.624	9.178
1.5	16.218	13.729	10.956	9.064	7.73
2	11.075	9.385	7.424	6.039	4.997
3	8.098	6.881	5.438	4.395	3.559

Table 3.12: ARL values for the CS-EWMA chart with $\lambda_q = 0.2, n = 5$ and $ARL_0 = 200$

τ	$K_q = 0.1$ $H_q = 35.2$	$K_q = 0.25$ $H_q = 24.96$	$K_q = 0.5$ $H_q = 15.47$	$K_q = 0.75$ $H_q = 10.03$	$K_q = 1$ $H_q = 6.53$
0.5	14.017	11.652	9.421	8.106	7.222
0.6	16.572	13.807	11.243	9.796	8.858
0.7	20.988	17.597	14.579	12.978	12.141
0.8	30.235	25.828	22.383	21.258	21.411
0.9	59.291	54.54	54.423	59.188	65.493
0.95	112.046	111.302	120.099	132.689	145.693
1	200.201	199.572	200.733	200.695	200.392
1.05	104.94	100.801	100.762	103.131	104.378
1.1	56.775	51.104	48.576	48.77	49.734
1.2	29.533	24.981	21.284	19.8	19.186
1.3	20.761	17.182	13.998	12.367	11.485
1.4	16.545	13.588	10.88	9.367	8.401
1.5	14.048	11.505	9.131	7.731	6.791
2	9.041	7.414	5.805	4.797	4.078
3	6.369	5.252	4.117	3.372	2.797

Table 3.13: ARL values for the CS-EWMA chart with $\lambda_q = 0.3, n = 5$ and $ARL_0 = 200$

τ	$K_q = 0.1$ $H_q = 28.13$	$K_q = 0.25$ $H_q = 19.37$	$K_q = 0.5$ $H_q = 11.87$	$K_q = 0.75$ $H_q = 7.78$	$K_q = 1$ $H_q = 5.16$
0.5	12.39	9.956	7.911	6.822	6.134
0.6	14.876	11.99	9.621	8.444	7.772
0.7	19.235	15.661	12.875	11.729	11.362
0.8	28.467	23.896	21.086	21.167	22.79
0.9	57.66	53.647	56.972	66.231	78.395
0.95	111.3	112.994	128.065	147.259	164.091
1	200.262	199.154	199.005	200.568	199.814
1.05	105.433	101.759	102.912	105.905	106.502
1.1	56.456	50.968	49.573	51.114	52.289
1.2	28.726	23.988	20.749	19.841	19.724
1.3	19.793	16.096	13.122	11.908	11.206
1.4	15.467	12.395	9.873	8.664	7.917
1.5	12.948	10.325	8.125	6.969	6.265
2	7.991	6.376	4.933	4.108	3.535
3	5.473	4.409	3.412	2.789	2.366

Table 3.14: ARL values for the CS-EWMA chart with $\lambda_q = 0.4, n = 5$ and $ARL_0 = 200$

τ	$K_q = 0.1$ $H_q = 23.43$	$K_q = 0.25$ $H_q = 15.83$	$K_q = 0.5$ $H_q = 9.62$	$K_q = 0.75$ $H_q = 6.308$	$K_q = 1$ $H_q = 4.24$
0.5	11.425	8.956	7.014	6.056	5.526
0.6	13.878	10.937	8.707	7.703	7.26
0.7	18.23	14.579	12.041	11.259	11.47
0.8	27.332	22.911	20.802	22.072	25.63
0.9	56.545	53.599	61.015	76.068	94.607
0.95	110.015	115.617	138.526	161.045	184.439
1	199.007	200.336	200.485	199.411	199.888
1.05	104.542	102.206	105.385	106.762	107.729
1.1	55.908	50.87	50.536	52.258	53.902
1.2	28.069	23.363	20.537	19.92	20.051
1.3	19.113	15.296	12.611	11.57	11.075
1.4	14.786	11.625	9.3	8.193	7.625
1.5	12.235	9.581	7.494	6.484	5.892
2	7.32	5.716	4.373	3.647	3.158
3	4.884	3.852	2.965	2.414	2.134

Table 3.15: ARL values for the CS-EWMA chart with $\lambda_q = 0.5, n = 5$ and $ARL_0 = 200$

τ	$K_q = 0.1$ $H_q = 20.1$	$K_q = 0.25$ $H_q = 13.25$	$K_q = 0.5$ $H_q = 7.99$	$K_q = 0.75$ $H_q = 5.27$	$K_q = 1$ $H_q = 3.57$
0.5	10.819	8.244	6.394	5.563	5.16
0.6	13.25	10.215	8.096	7.292	7.082
0.7	17.575	13.835	11.575	11.222	12.113
0.8	26.704	22.207	21.05	23.96	30.154
0.9	56.118	53.989	65.611	86.907	113.788
0.95	111.12	118.942	146.808	177.365	205.588
1	200.775	199.405	199.3062	199.499	200.476
1.05	104.617	102.52	105.77	107.044	106.577
1.1	55.436	50.59	51.073	53.56	54.65
1.2	27.554	22.734	20.376	20.218	20.334
1.3	18.626	14.656	12.186	11.379	11.054
1.4	14.272	11.049	8.842	7.888	7.449
1.5	11.76	9.015	7.041	6.138	5.654
2	6.863	5.226	3.98	3.31	2.91
3	4.487	3.464	2.601	2.22	1.87

iii. for fixed values of n, λ_q and ARL_0, negative shifts of small magnitude are detected efficiently using moderate values of K_q like $0.25 \leq K_q \leq 0.5$, whereas for large shifts in the negative direction, large values of K_q are recommended;

iv. for fixed values of n, K_q and ARL_0, large values of λ_q are recommended for detecting large positive shifts and vice versa while for negative shifts, varied behavior is seen;

v. for fixed values of n, λ_q and ARL_0, the value of H_q decreases with an increase in the value of K_q and vice versa;

In this section we have used the statistic T_i to design the control structure of our proposed chart. Many other transformations of S_i^2, that result into a statistic which is distributed approximately normal, can be used. Acosta-Mejia et al. (1999) proposed two such transformations named as P_σ and χ. Castagliola et al. (2010) proposed a four parameter Johnston transformation and named the resulting variable as U_i. Huwang et al. (2010)

proposed a logarithmic transformation and showed that $Y_i = \ln\left({S_i^2}/{\sigma_0^2} \right)$ follows approximately a normal distribution which can be used to design a memory control chart to monitor the process dispersion. In the next subsection we compare the control charts based on these transformations with our proposal.

3.2.4 Comparisons

This subsection contains the comparison of the proposed CS-EWMA chart with the S^2-EWMA, CUSUM-S^2 and some other recently proposed CUSUM and EWMA charts for monitoring the process dispersion.

CS-EWMA versus S^2-EWMA: The ARL values for the S^2-EWMA chart (discussed in Section 2.1) are given in Table 3.8. Comparison reveals that the performance of the proposed chart with $K_q = 1$ is almost the same as compared to the S^2-EWMA for the positive shifts, but for negative shifts, the performance of the CS-EWMA chart is far more superior than the S^2-EWMA. Moreover, the performance of S^2-EWMA becomes very poor for moderate and large values of λ, even the ARL_1 values become larger than the prefixed ARL_0 for negative shifts. This is not the case with the proposed CS-EWMA chart, as for large values of λ_q, the CUSUM factor in the proposed chart still makes it remain better in terms of $ARLs$ (cf. Table 3.8 vs. Tables 3.10 – 3.15).

CS-EWMA versus CUSUM-S^2: Table 3.9 contains the ARL values for the CUSUM-S^2 chart proposed by Castagliola et al. (2009). This CUSUM-S^2 chart is a special form of our proposed CS-EWMA chart with $\lambda_q = 1$. The performance of the proposed chart is better than CUSUM-S^2 chart, especially for small values of smoothing constant λ_q. The additional parameter (i.e. λ_q) in CS-EWMA chart makes sure that the performance of the proposed chart is not deflated for large values of K_q like it occurs with the CUSUM-S^2 chart for large values of K (cf. Table 3.9 vs. Tables 3.10 – 3.15).

CS-EWMA versus some other EWMA and CUSUM charts: Acosta-Mejia et al. (1999) proposed some CUSUM-type charts (named as χ CUSUM, P_σ CUSUM and CP CUSUM) for monitoring process dispersion and compared the performance of their proposed charts with the CUSUM R chart by Page (1963), CUSUM S chart by Tuprah and Ncube (1987) and CUSUM $\ln S^2$ chart by Chang and Gan (1995). They showed through comparison that their proposed CP CUSUM is performing better (in terms of ARL values) than the other charts discussed. Similarly, Huwang et al. (2010) proposed two new EWMA type charts (named as $HHW1$ CUSUM and $HHW2$ CUSUM) for monitoring the standard deviation of a process. They also compared the performance of their proposed chart with some other competitors, like the CH EWMA chart by Crowder and Hamilton (1992) and the SJ EWMA chart by Shu and Jiang (2008), and showed that their proposed charts are more sensitive (in detecting shifts) than the other competitors. The ARL values of the charts discussed by Acosta-Mejia et al. (1999) are given in Table 3.16, while Table 3.17 contains the $ARLs$ of the charts discussed by Huwang et al. (2010).

Table 3.16: ARL values for some one-sided CUSUM-type charts for detecting variance increases with $n = 5$ and $ARL_0 = 200$

τ	CUSUM $\ln S^2$ $K = 0.068$ $H = 2.66$	CUSUM R $K = 2.56$ $H = 4.88$	χ CUSUM $K = 0.38$ $H = 4.28$	P_σ CUSUM $K = 0.38$ $H = 4.28$	CUSUM S $K = 1.1034$ $H = 1.90$	CP CUSUM $K = 1.193$ $H = 18.45$
1	199.93	201.80	200.70	201.10	200.60	200.76
1.1	42.94	40.40	41.04	41.04	38.80	34.60
1.2	18.07	17.60	17.17	17.15	16.85	14.14
1.3	10.75	10.82	10.23	10.21	10.36	8.42
1.4	7.63	7.81	7.26	7.24	7.50	5.93
1.5	5.98	6.13	5.66	5.65	5.85	4.58
2	3.18	3.13	2.90	2.98	3.01	2.20

Table 3.17: ARL values for some one-sided EWMA-type charts for detecting variance increases with $n = 5$ and $ARL_0 = 200$

τ	$\lambda = 0.05$				$\lambda = 0.1$			
	CH-EWMA ($L = 1.055$)	SJ-EWMA ($L = 1.568$)	HHW1-EWMA ($L = 1.828$)	HHW2-EWMA ($L = 1.872$)	CH-EWMA ($L = 1.303$)	SJ-EWMA ($L = 1.943$)	HHW1-EWMA ($L = 2.079$)	HHW2-EWMA ($L = 2.139$)
1	200.33	200.75	200.92	199.57	200.02	200.36	199.51	200.35
1.1	43.24	32.26	28.89	27.28	44.26	35.15	34.32	32.05
1.2	18.09	14.43	11.69	10.78	18.23	14.96	14.1	12.69
1.3	10.77	9.17	6.85	6.2	10.56	9.09	8.2	7.21
1.4	7.63	6.73	4.75	4.24	7.35	6.53	5.65	4.89
1.5	5.98	5.38	3.62	3.22	5.68	5.13	4.28	3.68
2	3.18	2.93	1.8	1.62	2.95	2.72	2.03	1.76
τ	$\lambda = 0.2$				$\lambda = 0.3$			
	CH-EWMA ($L = 1.513$)	SJ-EWMA ($L = 2.270$)	HHW1-EWMA ($L = 2.253$)	HHW2-EWMA ($L = 2.355$)	CH-EWMA ($L = 1.598$)	SJ-EWMA ($L = 2.433$)	HHW1-EWMA ($L = 2.302$)	HHW2-EWMA ($L = 2.477$)
1	200.64	199.48	199.43	200.65	199.4	199.67	200.22	199.45
1.1	46.63	39.73	41.18	37.87	48.48	43.45	46.14	41.79
1.2	18.79	16.05	16.66	14.7	19.52	17.25	18.65	16.2
1.3	10.54	9.21	9.45	8.16	10.67	9.56	10.35	8.82
1.4	7.16	6.4	6.45	5.49	7.09	6.43	6.9	5.81
1.5	5.41	4.89	4.83	4.07	5.24	4.8	5.11	4.26
2	2.67	2.45	2.24	1.88	2.47	2.3	2.32	1.93

Table 3.18: ARL values for one-sided CS-EWMA chart with $K_q = 1, n = 5$ and $ARL_0 = 200$

τ	$\lambda_q = 0.05$ $H_q = 5.39$	$\lambda_q = 0.1$ $H_q = 5.13$	$\lambda_q = 0.2$ $H_q = 4.54$	$\lambda_q = 0.3$ $H_q = 3.928$	$\lambda_q = 0.4$ $H_q = 3.42$	$\lambda_q = 0.5$ $H_q = 3.01$
1	200.4035	200.9845	200.7247	200.1826	200.621	199.6103
1.1	23.963	31.478	36.48	39.44	41.226	43.263
1.2	11.261	13.798	15.39	16.031	16.599	17.147
1.3	8.006	9.1	9.485	9.553	9.635	9.684
1.4	6.53	7.041	7.012	6.837	6.721	6.641
1.5	5.685	5.941	5.689	5.432	5.224	5.112
2	3.975	3.834	3.423	3.08	2.858	2.673
3	3.04	2.732	2.347	2.143	1.894	1.674

All charts presented in Tables 3.16 – 3.17 are one-sided, i.e. designed to detect just positive shift in the process dispersion. For a valid comparison of the proposed chart with these charts, we have evaluated the ARL values of the proposed chart with the one-sided structure for monitoring an increase in process standard deviation. These $ARLs$ are given in Table 3.18 with $K_q = 1$ and $ARL_0 = 200$.

It can be noticed through the comparison that the proposed chart is outperforming all its competitors in the form of EWMA and CUSUM type charts (cf. Tables 3.16 – 3.17 vs. Table 3.18).

Finally, before concluding this subsection, we provide the ARL curves of the different charts discussed above. Figure 3.7 contains the ARL curves of the two-sided charts containing: CS-EWMA chart with $\lambda_q = 0.2$, $K_q = 0.25$ and $H_q = 24.96$; S^2-EWMA chart with $\lambda = 0.2$ and $L = 2.592$; CUSUM-S^2 chart with $K = 0.25$ and $H = 6.476$. Figure 3.8 shows the ARL curves of the one-sided charts for positive shifts containing: CS-EWMA chart with $\lambda_q = 0.05$, $K_q = 1$ and $H_q = 5.39$; CP CUSUM chart with $K = 1.193$ and $H = 18.45$; CUSUM S chart with $K = 1.1034$ and $H = 1.90$; CH EWMA chart with $\lambda = 0.05$ and $L = 1.055$; SJ EWMA chart with $\lambda = 0.05$ and $L = 1.568$; and $HHW2$ EWMA chart with $\lambda = 0.05$ and $L = 1.872$.

Figure 3.7: ARL curves for two-sided structures of CS-EWMA, S^2-EWMA and CUSUM-S^2 charts with $ARL_0 = 200$

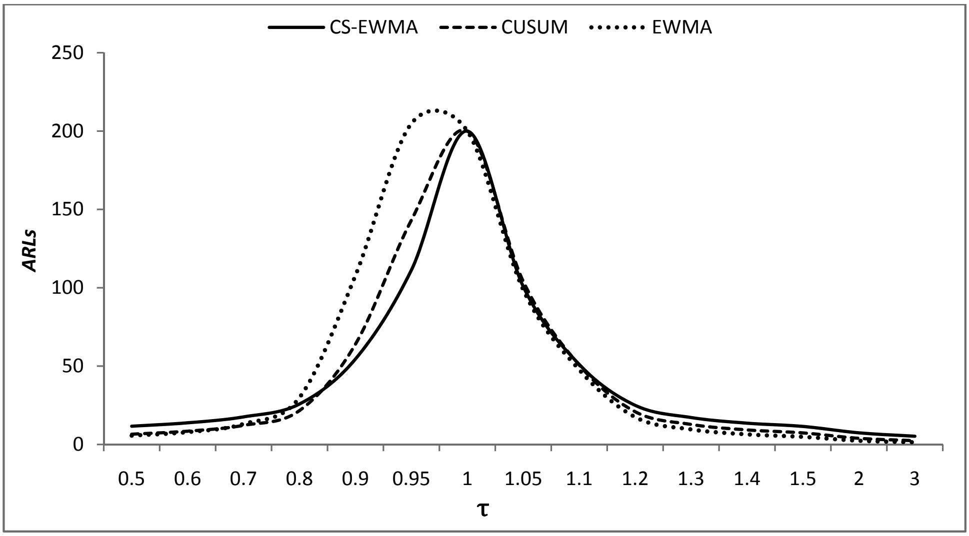

Figure 3.8: ARL curves for one-sided structures of CS-EWMA, CP CUSUM, CUSUM S, SJ EWMA, CH EWMA and $HHW2$ EWMA charts with $ARL_0 = 200$

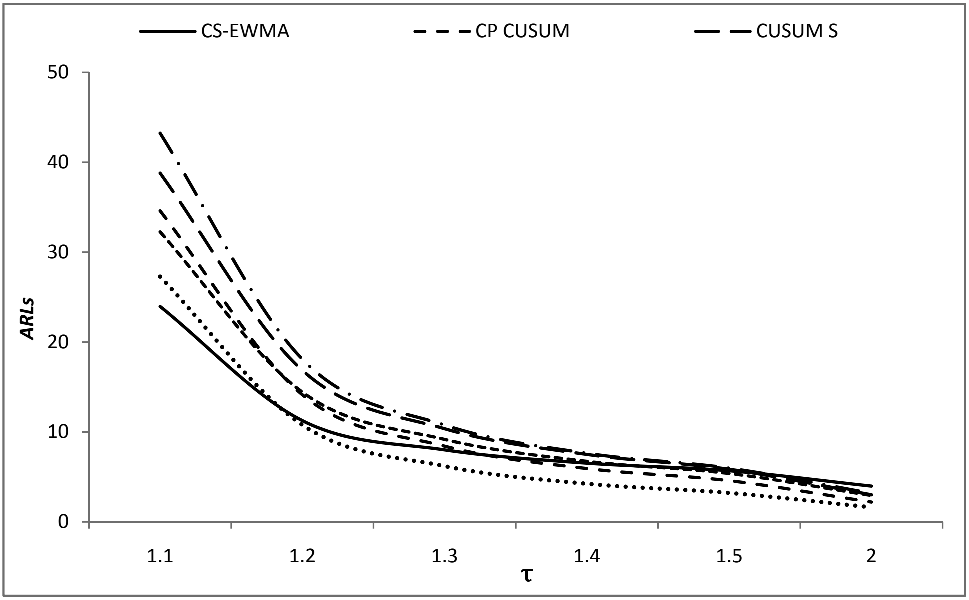

Figure 3.7 shows that the performance of all three charts is almost the same for positive shifts but for negative shifts, the proposed chart is giving a better ARL performance. Similarly, in Figure 3.8, the ARL curve of the proposed chart seems lower than all other curves for small values of τ and thus showing a better performance for small positive shifts.

3.2.5 Illustrative example

An application of CS-EWMA chart on a simulated dataset is provided in this subsection to show the implementation of the proposal. For this purpose, two datasets are generated having 40 samples of size $n = 5$ for both the samples. First 20 samples are generated from $N(10,4)$ referring to an in control situation with $\mu = 10$ and $\sigma_0^2 = 4$. For dataset 3.1, the remaining 20 observations are generated from $N(10,5)$ showing a positive shift in the process standard deviation with $\tau = \sqrt{5}/\sqrt{4} = 1.118$. Similarly, for dataset 3.2, the remaining 20 observations are generated from $N(10,3)$ showing a negative shift in dispersion with $\tau = 0.866$. Now the S^2-EWMA chart, CUSUM-S^2 chart and their mixture named as CS-EWMA chart are applied to the given datasets. The chart output of the S^2-EWMA chart with $\lambda = 0.2$ and $L = 2.592$ is shown in Figure 3.9. Figure 3.10 shows the graphical display of the CUSUM-S^2 with $K = 0.5$ and $H = 3.855$. The calculation details for the proposed chart with $\lambda_q = 0.2$, $K_q = 0.5 \Rightarrow K'_q = 0.167$ and $H_q = 15.47 \Rightarrow H'_q = 5.157$ are given in Table 3.19, whereas the chart output is given in Figure 3.11.

Figure 3.9: Graphical display of the S^2-EWMA chart with $\lambda = 0.2$ and $L = 2.592$

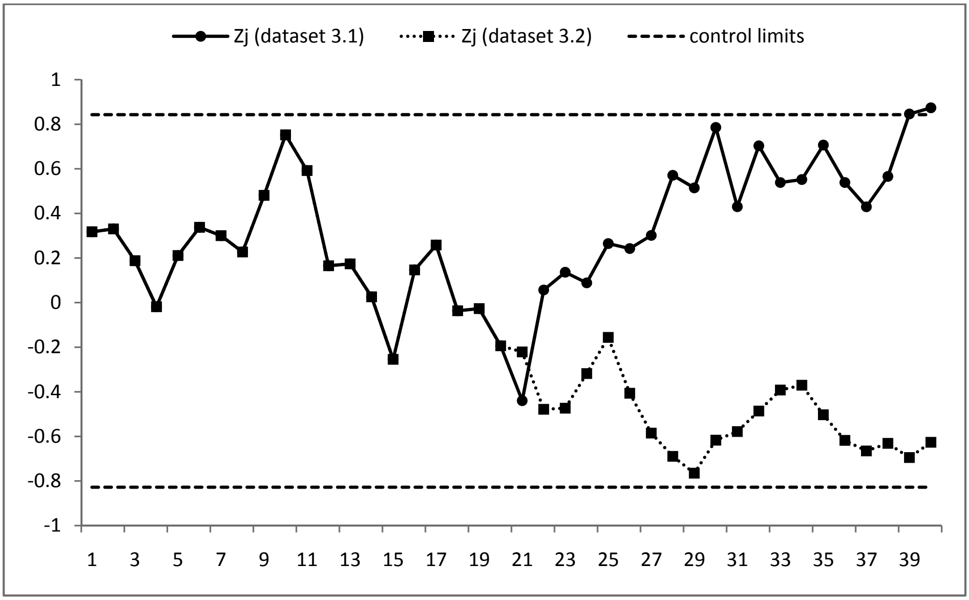

Figures 3.9 – 3.11 clearly indicate that all three charts are giving out of control signals at samples 39 and 40 for dataset 3.1 (i.e. positive shift in the process dispersion). Moreover, the proposed CS-EWMA chart detected a negative shift for dataset 3.2 at samples 37, 38, 39 and

40 but the other two charts did not signal the downward shift in the process standard deviation.

Figure 3.10: Graphical display of the CUSUM S^2 chart with $K = 0.5$ and $H = 3.855$

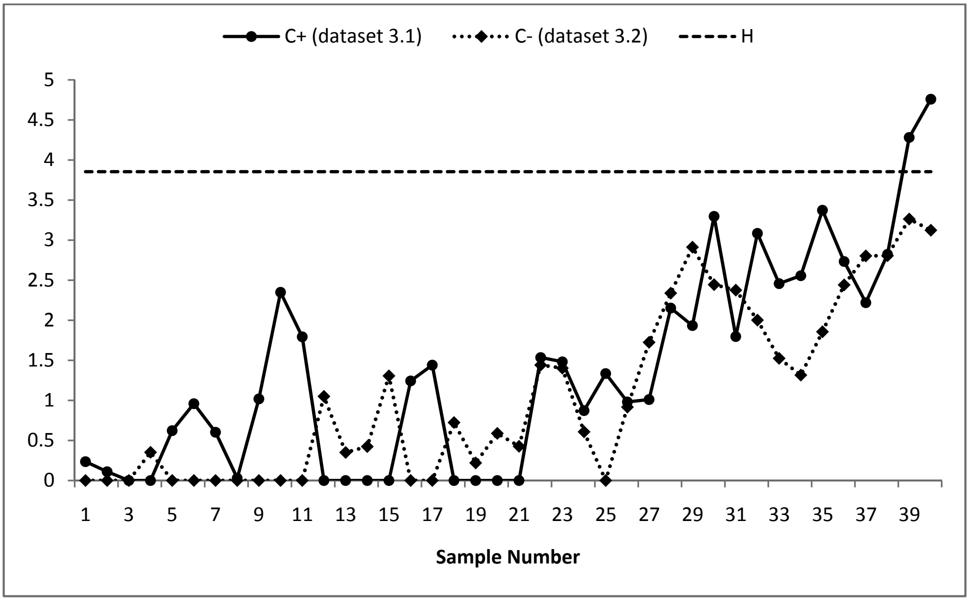

Figure 3.11: Graphical display of the CS-EWMA chart with $\lambda_q = 0.2$, $K_q = 0.5$ and $H_q = 15.47$

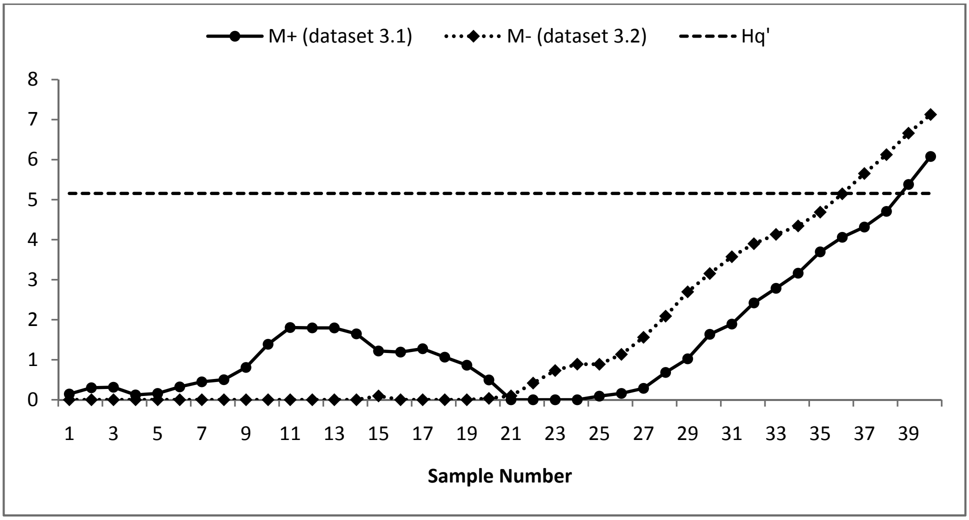

Table 3.19: Calculation details of the proposed CS-EWMA chart for dataset 3.1

Sample No.	S_i^2	T_i	Q_i	M_i^+	M_i^-	Sample No.	S_i^2	T_i	Q_i	M_i^+	M_i^-
1	5.61	0.74	0.32	0.14	0	21	0.81	-1.42	-0.44	0	0.32
2	4.48	0.38	0.33	0.3	0	22	11.47	2.04	0.06	0	0.1
3	2.58	-0.38	0.19	0.31	0	23	4.69	0.45	0.14	0	0
4	1.7	-0.84	-0.02	0.12	0	24	3.21	-0.1	0.09	0	0
5	7.04	1.13	0.21	0.16	0	25	6.42	0.97	0.26	0.09	0
6	5.96	0.84	0.34	0.32	0	26	3.84	0.15	0.24	0.16	0
7	3.84	0.15	0.3	0.45	0	27	4.94	0.54	0.3	0.29	0
8	3.29	-0.07	0.23	0.5	0	28	9.35	1.65	0.57	0.68	0
9	8.62	1.5	0.48	0.81	0	29	4.21	0.29	0.51	1.02	0
10	10.33	1.84	0.75	1.39	0	30	10.5	1.87	0.79	1.64	0
11	3.33	-0.05	0.59	1.81	0	31	1.45	-0.99	0.43	1.89	0
12	0.65	-1.54	0.17	1.8	0	32	10.1	1.8	0.7	2.42	0
13	3.99	0.21	0.17	1.8	0	33	3.16	-0.12	0.54	2.79	0
14	2.21	-0.57	0.03	1.65	0	34	5.16	0.61	0.55	3.16	0
15	0.88	-1.38	-0.25	1.22	0.1	35	7.84	1.32	0.71	3.7	0
16	9.86	1.75	0.15	1.19	0	36	3.14	-0.13	0.54	4.06	0
17	5.48	0.71	0.26	1.28	0	37	3.44	-0.01	0.43	4.32	0
18	1.1	-1.22	-0.04	1.07	0	38	6.96	1.11	0.57	4.71	0
19	3.48	0.01	-0.03	0.86	0	39	11.04	1.97	0.85	5.38*	0
20	1.67	-0.86	-0.19	0.5	0.03	40	6.47	0.98	0.87	6.08*	0

* indicates an out of control signal by CS-EWMA chart

3.3 Concluding remarks

CUSUM control charts and EWMA control charts are the two most commonly used memory control charts in the literature. These control schemes do not only use the current observation but also accumulate the information from the past to give a quick signal if the process is slightly off-target. In this chapter we have combined the CUSUM and EWMA control schemes into a single control structure and proposed a mixed EWMA-CUSUM control scheme for monitoring the process location. Performance of the proposed scheme is compared with other CUSUM and EWMA type control charts which are meant to detect small and moderate shifts in the process. The comparisons revealed that the proposed scheme is really good at detecting the smaller shifts in the process as compared to the other schemes under study.

Following our proposal for location, this chapter also proposes a new memory-type control chart, named as the CS-EWMA chart, for monitoring the process standard deviation. The design of the proposed chart is based on mixing the effects of EWMA and CUSUM control charts into a single control structure. The performance of the proposed CS-EWMA chart is evaluated using ARL as indicator. In terms of ARL values, the proposed chart is compared with existing CUSUM and EWMA control charts and it is noticed that the proposed chart has better performance for both positive as well as negative shifts in the process dispersion. Finally, an illustrative example is provided to show the application of the proposed chart.

Appendix 3.1

```
x=c(); Q=c(); sdp=c(); K=c(); H=c(); Mp=c(); Mn=c(); rl=c(); k=0.5;
h=37.42; ld=0.1
mu=0; sig=1
for(j in 1:50000)
{
      for(i in 1:1000000)
      {
            x[i]=rnorm(1,mu,sig)
            if(i==1)
                  {Q[i]=ld*x[i]+(1-ld)*mu;}
                  else{Q[i]=ld*x[i]+(1-ld)*Q[i-1];}
            sdp[i]=sqrt((ld/(2-ld))*(1-(1-ld)^(2*i)))
            K[i]=k*sdp[i]
            H[i]=h*sdp[i]
            if(i==1)
                  {Mp[i]=max(0,Q[i]-K[i]);}
                  else{Mp[i]=max(0,Q[i]-K[i]+Mp[i-1]);}
            if(i==1)
                  {Mn[i]=max(0,-Q[i]-K[i]);}
                  else{Mn[i]=max(0,-Q[i]-K[i]+Mn[i-1]);}
            if(Mp[i]>H[i] | Mn[i]>H[i])
                  {rl[j]=i; break;}
                  else{rl[j]=0;}
      }
}
mean(rl)
```

Appendix 3.2

```
Q=c(); Mp=c(); Mn=c(); rl=c(); Tk=c()
n=5; a=-0.8969; b=2.3647; c=0.5979; ETi=0.00748; STi=0.9670
Z0=a+b*log(1+c,exp(1))
ld=0.05; K=0.1*sqrt(ld/(2-ld)); H=62.6*sqrt(ld/(2-ld))
for(j in 1:50000)
{
      for(i in 1:1000000)
      {
            x=rnorm(n,0,1)
            T[i]=a+b*log(var(x)+c,exp(1))
            if(i==1)
                  {Q[i]=ld*T[i]+(1-ld)*Z0;}
                  else{Q[i]=ld*T[i]+(1-ld)*Q[i-1];}
            if(i==1)
```

```
                {Mp[i]=max(0,Q[i]-ETi-K);}
                else{Mp[i]=max(0,Q[i]-ETi-K+Mp[i-1]);}
          if(i==1)
                {Mn[i]=max(0,-Q[i]+ETi-K);}
                else{Mn[i]=max(0,-Q[i]+ETi-K+Mn[i-1]);}
          if(Mp[i] > H | Mn[i] > H)
                {rl[j]=i;break;}
                else{rl[j]=0;}
     }
}
mean(rl)
```

Chapter 4

Auxiliary information based CUSUM and EWMA control charts

Two popular categories of control charts are CUSUM and EWMA charts, which are good at quickly detecting the presence of small and moderate disturbances. Targeting on small and moderate shifts in the process mean, this chapter proposes EWMA- and CUSUM-type control charts which utilize the information of auxiliary variable(s). The regression estimation technique for the mean is used in defining the control structure of the proposed charts. It is shown that the proposed charts are performing better than their competitors which are also designed for detecting small shifts. This chapter is based on an article by Abbas, Riaz and Does (2012c), consisting of the EWMA-type control charts based on auxiliary information.

4.1 Control charts using auxiliary information

Information accessible at the stage of estimation other than that in the sample is called auxiliary information. The concept of using auxiliary information is frequently used in the field of survey sampling and estimation techniques. Auxiliary information can be used at either or both the design and estimation stage. Sampling techniques like probability sampling (cf. Fuller (2009)) and rank set sampling (cf. McIntyre (1952)) are examples of the utilization of auxiliary information at the sample selection stage. Ratio, product and regression-type estimators are examples of utilization of auxiliary information at the estimation stage (cf. Cochran (1977) and Fuller (2002)). These estimators are designed in such a way that they not only utilize the sample information but also make use of the information available other than that. This makes these estimators more efficient than the conventional ones.

This auxiliary information is also used in control charting techniques in order to enhance their performance. Examples are the regression control chart proposed by Mandel (1969) and cause-selecting control charts proposed by Zhang (1985). The control structure of these control charts is based on regressing the study variable on the auxiliary variable. The residuals obtained from that regression are used for monitoring the process (see also Wade and Woodall (1993)). Riaz (2008a) introduced the concept of using auxiliary information at the time of estimating the plotting statistic of a control chart. He proposed a control chart which uses a regression-type estimator as the plotting statistic to monitor the variability of the process and showed the dominance (in terms of power) of his proposed control chart over the well-known Shewhart-type control charts for the same purpose (i.e. R, S and S^2 charts). Riaz (2008b) proposed a regression-type estimator to monitor the location of the process. He not only showed the superiority of his proposal over the Shewhart's $\bar{X}$ −chart but also over the regression charts (cf. Mandel (1969)) and the cause-selecting charts (cf. Zhang (1985)). Later Riaz and Does (2009) proposed another variability chart based on a ratio-type estimator and proved the dominance of their proposed chart over the one based on regression-type estimator. Following these authors, this chapter proposes the use of auxiliary information with the control structure of EWMA and CUSUM charts. The regression estimation technique is used to exploit the information from the auxiliary variable and without loss of generality the case of individual observations have been considered.

4.2 EWMA control charts using auxiliary information

Let an auxiliary variable X_i be correlated with the variable of interest Y_i and let us denote the correlation between these two variables by ρ_{YX}. The observations of Y and X are obtained in the paired form for each sample and the population mean and variance of X (i.e. μ_X and σ_X^2 respectively) are assumed to be known. Also we assume bivariate normality of Y and X, i.e.

$$\binom{Y}{X} \sim N_2\left(\binom{\mu_Y}{\mu_X}, \begin{pmatrix} \sigma_Y^2 & \rho_{YX}\sigma_Y\sigma_X \\ \rho_{YX}\sigma_Y\sigma_X & \sigma_X^2 \end{pmatrix}\right) \tag{4.1}$$

where N_2 represents the bivariate normal distribution. The regression estimate of the population mean μ_Y (cf. Cochran (1977)) is given as:

$$M_{X_i} = Y_i + \beta_{YX}(\mu_X - X_i) \tag{4.2}$$

where β_{YX} is the change in Y due to one unit change in X and is $\beta_{YX} = \rho_{YX}\left(\frac{\sigma_Y}{\sigma_X}\right)$. The mean and variance of the statistic M_X in (4.2) are given as:

$$E(M_X) = \mu_Y,\ V(M_X) = \sigma_M^2 = \sigma_Y^2(1-\rho_{YX}^2) \tag{4.3}$$

Equation (4.3) implies that M_X is also an unbiased estimator of μ_Y and $\sigma_M^2 < \sigma_Y^2$ as long as $\rho_{YX}^2 > 0$. Based on the regression estimator in (4.2), the plotting statistic for the proposed EWMA chart based on a single auxiliary variable (named as M_XEWMA chart) is defined as:

$$Z_i' = \lambda' M_{X_i} + (1-\lambda')Z_{i-1}' \tag{4.4}$$

where λ' is the smoothing constant for the proposed statistic and M_{X_i} is the value of statistic M_X for the i^{th} sample. Z_{i-1}' represents the past information (like Z_{i-1}) and its initial value (i.e. Z'_0) is also taken equal to the target mean μ_0, i.e. the in control mean of Y. Now based on (4.3) the time varying control limits for the proposed chart are:

$$\left.\begin{aligned} LCL &= \mu_0 - L'\sigma_M\sqrt{\tfrac{\lambda'}{2-\lambda'}\left(1-(1-\lambda')^{2i}\right)} \\ CL &= \mu_0 \\ UCL &= \mu_0 + L'\sigma_M\sqrt{\tfrac{\lambda'}{2-\lambda'}\left(1-(1-\lambda')^{2i}\right)} \end{aligned}\right\} \tag{4.5}$$

where L' determines the width of the control limits for the proposed M$_X$EWMA chart. The ARL values for the proposed M$_X$EWMA chart with time varying limits are given in Tables 4.1 – 4.5 for some selective choices of ρ_{YX} in which δ represents the amount of shift in the study variable, i.e. $\delta = \frac{|\mu_1-\mu_0|}{\sigma_Y}$ where μ_1 is the out of control mean of Y. The program (developed in R language) for evaluating the $ARLs$ is given in Appendix 4.1 which is replicated 50,000 for each simulated value. Note that μ_X remains constant.

Table 4.1: ARL values for the proposed M$_X$EWMA chart with time varying limits, $\rho_{YX} = 0.05$ and $ARL_0 = 500$

δ	$\lambda' = 0.03$ $L' = 2.483$	$\lambda' = 0.05$ $L' = 2.639$	$\lambda' = 0.1$ $L' = 2.824$	$\lambda' = 0.25$ $L' = 3$	$\lambda' = 0.5$ $L' = 3.072$	$\lambda' = 0.75$ $L' = 3.088$
0	500.3011	500.8313	499.7023	499.6045	500.9026	499.9704
0.25	66.3103	77.5273	103.1312	168.8081	254.324	321.6227
0.5	21.2101	23.6211	28.7434	47.2173	88.1445	139.8713
0.75	10.7125	11.8433	13.592	19.2345	35.401	62.2502
1	6.632	7.2905	8.2072	10.3617	17.1148	30.3995
1.5	3.4443	3.7573	4.1644	4.7647	6.2628	9.7633
2	2.244	2.4205	2.6563	2.9313	3.3701	4.4521
2.5	1.6555	1.7719	1.9147	2.0831	2.2565	2.6079
3	1.3401	1.4104	1.5112	1.6109	1.6904	1.8151
4	1.0642	1.0882	1.1224	1.1609	1.184	1.1946
5	1.0049	1.0085	1.0131	1.0221	1.0265	1.0281

Table 4.2: ARL values for the proposed M_XEWMA chart with time varying limits, $\rho_{YX} = 0.25$ and $ARL_0 = 500$

δ	$\lambda' = 0.03$ $L' = 2.483$	$\lambda' = 0.05$ $L' = 2.639$	$\lambda' = 0.1$ $L' = 2.824$	$\lambda' = 0.25$ $L' = 3$	$\lambda' = 0.5$ $L' = 3.072$	$\lambda' = 0.75$ $L' = 3.088$
0	500.0592	500.5358	499.1371	499.8049	499.951	500.5678
0.25	63.1554	73.8038	97.5858	161.9697	245.9632	313.2722
0.5	20.1268	22.4316	27.1393	44.1797	83.0098	132.8202
0.75	10.1982	11.2488	12.8277	18.0008	32.9028	57.9059
1	6.3049	6.9254	7.7548	9.7748	15.8281	28.0123
1.5	3.2871	3.5816	3.9532	4.5005	5.832	8.9444
2	2.1384	2.3119	2.5261	2.7962	3.1754	4.0979
2.5	1.5945	1.6997	1.8406	1.9877	2.1497	2.4354
3	1.2952	1.363	1.4519	1.5523	1.6178	1.7158
4	1.0495	1.0687	1.0955	1.132	1.1476	1.1565
5	1.0044	1.0067	1.0108	1.0149	1.0178	1.0183

Table 4.3: ARL values for the proposed M_XEWMA chart with time varying limits, $\rho_{YX} = 0.5$ and $ARL_0 = 500$

δ	$\lambda' = 0.03$ $L' = 2.483$	$\lambda' = 0.05$ $L' = 2.639$	$\lambda' = 0.1$ $L' = 2.824$	$\lambda' = 0.25$ $L' = 3$	$\lambda' = 0.5$ $L' = 3.072$	$\lambda' = 0.75$ $L' = 3.088$
0	500.7792	499.5635	499.8114	499.692	500.7859	500.9686
0.25	52.6523	61.1011	80.6591	135.7683	216.0974	285.4555
0.5	16.6817	18.5391	22.044	34.5785	65.3989	108.1412
0.75	8.4242	9.3261	10.5432	14.1099	24.7989	44.3004
1	5.2477	5.7592	6.4306	7.8001	11.9099	20.6193
1.5	2.7663	3.0129	3.3183	3.7182	4.5573	6.5619
2	1.8392	1.9673	2.1455	2.3486	2.5852	3.136
2.5	1.3979	1.48	1.5834	1.7044	1.7964	1.9476
3	1.17	1.2168	1.2786	1.3501	1.3947	1.4325
4	1.0155	1.0253	1.038	1.0513	1.0606	1.064
5	1.0007	1.0012	1.0019	1.002	1.0028	1.0056

Table 4.4: ARL values for the proposed M_XEWMA chart with time varying limits, $\rho_{YX} = 0.75$ and $ARL_0 = 500$

δ	$\lambda' = 0.03$ $L' = 2.483$	$\lambda' = 0.05$ $L' = 2.639$	$\lambda' = 0.1$ $L' = 2.824$	$\lambda' = 0.25$ $L' = 3$	$\lambda' = 0.5$ $L' = 3.072$	$\lambda' = 0.75$ $L' = 3.088$
0	500.0659	499.5868	500.7509	500.4051	499.2859	499.7069
0.25	33.8532	38.4587	48.8401	84.1265	146.8905	211.6496
0.5	10.6126	11.7078	13.4213	18.9673	34.9019	61.2737
0.75	5.398	5.9343	6.6291	8.0816	12.4585	21.7022
1	3.4068	3.7177	4.1045	4.7175	6.1522	9.5862
1.5	1.8835	2.0268	2.2095	2.4126	2.6787	3.2731
2	1.3299	1.4043	1.4969	1.5949	1.6784	1.7904
2.5	1.1006	1.1309	1.1772	1.2269	1.2577	1.2721
3	1.0199	1.0296	1.0429	1.0608	1.0733	1.0742
4	1.0001	1.0004	1.0006	1.0011	1.0014	1.0017
5	1	1	1	1	1	1

Table 4.5: ARL values for the proposed M_XEWMA chart with time varying limits, $\rho_{YX} = 0.95$ and $ARL_0 = 500$

δ	$\lambda' = 0.03$ $L' = 2.483$	$\lambda' = 0.05$ $L' = 2.639$	$\lambda' = 0.1$ $L' = 2.824$	$\lambda' = 0.25$ $L' = 3$	$\lambda' = 0.5$ $L' = 3.072$	$\lambda' = 0.75$ $L' = 3.088$
0	500.1483	499.3424	500.5895	500.2327	500.0067	500.7743
0.25	9.6039	10.6139	12.1289	16.7024	30.2287	53.736
0.5	3.1274	3.4017	3.7577	4.2576	5.389	8.1474
0.75	1.75	1.8739	2.0315	2.2142	2.4181	2.8603
1	1.2547	1.3136	1.3951	1.4846	1.5468	1.622
1.5	1.0102	1.0162	1.0216	1.034	1.0418	1.0432
2	1	1.0003	1.003	1.0005	1.0006	1.0013
2.5	1	1	1	1	1	1
3	1	1	1	1	1	1
4	1	1	1	1	1	1
5	1	1	1	1	1	1

The ARL_0 in Tables 4.1 – 4.5 is fixed at 500 which will enable us to make comparison of the proposed control chart with some other charts/schemes. Tables 4.1 – 4.5 refer to a situation where the information about the population correlation coefficient is assumed to be known, because the information about the population correlation coefficient ρ_{YX} is known in many practical situations (cf. Garcia and Cebrian (1996)). However, this may not be the case in every situation. Then we have to estimate the value of ρ_{YX} from preliminary samples (m). The estimators used to estimate ρ_{YX} and β_{YX} are:

$$\hat{\rho}_{YX} = \frac{\sum_{i=1}^{m}(Y_i-\bar{Y})(X_i-\bar{X})}{\sqrt{\sum_{i=1}^{m}(Y_i-\bar{Y})^2\sum_{i=1}^{m}(X_i-\bar{X})^2}}, \qquad \hat{\beta}_{YX} = \frac{\sum_{i=1}^{m}(Y_i-\bar{Y})(X_i-\bar{X})}{\sum_{i=1}^{m}(X_i-\bar{X})^2} \tag{4.6}$$

From Tables 4.1 – 4.5, the main findings about our proposed M_XEWMA control chart for monitoring the location of a process are given as:

i. the use of auxiliary information in the form of a regression estimator boosts the performance of EWMA control chart, especially for large values of ρ_{YX};
ii. for fixed values of ρ_{YX} and δ, the performance of the proposed chart with time varying limits is better for small values of λ';
iii. for fixed values of λ', L' and δ, the performance of the proposed chart is better for the large values of ρ_{YX};
iv. for all choices of λ', L' and ρ_{YX} the proposed chart is ARL unbiased, i.e. ARL_1 never exceeds ARL_0 for any value of δ;
v. for small values of ρ_{YX}, the ARL for the proposed scheme decreases gradually with an increase in the value of δ but for the large values of ρ_{YX}, the ARL for the proposed scheme decreases rapidly with an increase in the value of δ.

Note that if we apply the same set up with samples sizes $n > 1$ instead of $n = 1$, the results will be the same with the obvious adjustments in the control limits in (4.2) and (4.3).

4.2.1 Comparisons

In this subsection we provide a broad comparison of our proposed M_XEWMA chart with the classical CUSUM, the classical EWMA and some of their recent modifications. Below, we present the one by one comparison of the proposed scheme with its counterparts:

M_XEWMA versus classical EWMA: $ARLs$ for the classical EWMA chart with time varying are given in Table 2.2. Comparing the M_XEWMA chart (with $\lambda' = 0.25$) with the classical EWMA chart we can see that for all the values of ρ_{YX} the ARL performance of the M_XEWMA chart is better than the classical EWMA for a fixed value of δ (cf. Table 2.2 vs. Tables 4.1 – 4.5). Moreover, an important point here is that the classical EWMA is a special case of the M_XEWMA chart, i.e. applying M_XEWMA chart to a process where $\rho_{YX} = 0$ is equivalent to applying the classical EWMA. From Table 4.1 we see that for $\rho_{YX} = 0.05$ the results almost coincides with the results of Table 2.2 as was to be expected.

It is to be noted here that the results of proposed M_XEWMA chart with time varying limits are on the same pattern as compared to the classical EWMA with time varying limits while the proposed chart with asymptotic limits (computational results are not provided here) is mainly following the pattern of classical EWMA with asymptotic limits.

M_XEWMA versus classical CUSUM: The classical CUSUM proposed by Page (1954) is discussed briefly in Section 1.2. A comprehensive study on the CUSUM charts is given by Hawkins and Olwell (1998). The $ARLs$ for the CUSUM chart are given in Table 4.6 with ARL_0 fixed at 500.

Comparing the M_XEWMA chart with the classical CUSUM chart we observe that the newly proposed chart is outperforming the classical CUSUM even for small values of ρ_{YX} (cf. Table 4.6 vs. Tables 4.1 – 4.5).

TABLE 4.6: *ARL* values for the classical CUSUM scheme

k	h	δ										
		0	0.25	0.5	0.75	1	1.5	2	2.5	3	4	5
0.25	8.585	500	94.8	31.08	17.54	12.17	7.58	5.55	4.41	3.69	2.84	2.26
0.5	5.071	500	145.5	38.87	17.32	10.52	5.82	4.06	3.15	2.6	2.03	1.72
0.75	3.539	500	200.7	57.07	22.13	11.6	5.45	3.55	2.67	2.18	1.63	1.24
1	2.665	500	249.5	81.44	30.9	14.67	5.75	3.41	2.45	1.94	1.38	1.09

M_XEWMA versus runs rules based CUSUM and EWMA: The $ARLs$ for the runs rules based CUSUM are provided in Tables 2.7 – 2.8 and for runs rules based EWMA these are given in Tables 2.15 – 2.16. Comparing the M_XEWMA chart with runs rules based CUSUM and EWMA we can see that the proposed chart is uniformly surpassing both the CUSUM schemes I & II and the EWMA simple $2/2$ scheme. The EWMA modified $2/3$ scheme is performing better than the proposed chart as long as $\rho_{YX} < 0.5$, but once we have $\rho_{YX} \geq 0.5$, the proposed chart outperforms the EWMA modified $2/3$ scheme as well (cf. Tables 2.7 – 2.8 & 2.15 – 2.16 vs. Tables 4.1 – 4.5).

M_XEWMA versus MEWMA: Lowry et al. (1992) introduced a multivariate extension of the EWMA chart named as MEWMA chart. For the bivariate case, the MEWMA statistic is

$$\begin{pmatrix} Z1_i \\ Z2_i \end{pmatrix} = r\begin{pmatrix} Y_i \\ X_i \end{pmatrix} + (1-r)\begin{pmatrix} Z1_{i-1} \\ Z2_{i-1} \end{pmatrix}$$

and the chart gives an out of control signal if $T_i^2 = C_1(Z1_i \quad Z2_i)\begin{pmatrix} \sigma_X^2 & -\sigma_{YX} \\ -\sigma_{YX} & \sigma_Y^2 \end{pmatrix}\begin{pmatrix} Z1_i \\ Z2_i \end{pmatrix} > h_4$. Here $C_1 = \frac{2-r}{r(1-(1-r)^{2i})\sigma_Y^2\sigma_X^2(1-\rho_{YX}^2)}$. Lowry et al. (1992) assumed, that the mean of both the variables are equal (i.e. $\mu_Y = \mu_X = \mu$). According to this assumption the ARL values of MEWMA only depend upon the shift parameter $\delta = \sqrt{\frac{2}{1+\rho_{YX}}}\mu$. We have evaluated the ARL values of this bivariate EWMA chart through Monte Carlo simulation by running 10^5

replications. To validate our simulation code, we have replicated Table 1 of Lowry et al. (1992) article and found the same results.

Now using our simulation code, we find the ARL values of the bivariate EWMA with the mean of X fixed and defining the shift in the mean of Y as we have defined in Tables 4.1 – 4.5. These $ARLs$ are given in Table 4.7 where $r = 0.1$ and $h_4 = 10.833$ with $ARL_0 = 500$.

TABLE 4.7: ARL values for MEWMA charts with $r = 0.1$ and $h_4 = 10.833$ at $ARL_0 = 500$

δ	$\rho_{YX} = 0.05$	$\rho_{YX} = 0.25$	$\rho_{YX} = 0.5$	$\rho_{YX} = 0.75$	$\rho_{YX} = 0.95$
0	500.57	501.6147	501.0223	498.4386	500.4125
0.5	36.81699	34.50276	27.63295	16.425	4.41316
1	9.8781	9.31899	7.66392	4.85723	1.55707
1.5	4.91344	4.65957	3.88276	2.54956	1.05029
2	3.08706	2.94745	2.47956	1.6849	1.00066
2.5	2.19454	2.10018	1.79616	1.27854	1.00001
3	1.6936	1.6269	1.41069	1.08457	1

Comparing the performance of the bivariate EWMA with the proposed chart, it can be noticed that the proposed chart has smaller ARL_1 values as compared to the bivariate EWMA chart for all the corresponding values of ρ_{YX} (cf. Table 4.7 vs. Tables 4.1 – 4.5).

4.2.2 The case of two auxiliary variables

Let us consider three variables, named as Y, X and W, following a trivariate normal distribution (N_3) out of which Y is the study variable, while X and W are two auxiliary variables, i.e.

$$\begin{pmatrix} Y \\ X \\ W \end{pmatrix} \sim N_3\left(\begin{pmatrix} \mu_Y \\ \mu_X \\ \mu_W \end{pmatrix}, \begin{pmatrix} \sigma_Y^2 & \sigma_{YX} & \sigma_{YW} \\ \sigma_{XY} & \sigma_X^2 & \sigma_{XW} \\ \sigma_{WY} & \sigma_{XW} & \sigma_W^2 \end{pmatrix}\right) \tag{4.7}$$

Based on the above trivariate normal distribution, Kadilar and Cingi (2005) provided a regression estimator for estimating the population mean of the study variable Y which are given as:

$$M_{T_i} = Y_i + \beta_{YX}(\mu_X - X_i) + \beta_{YW}(\mu_W - W_i) \tag{4.8}$$

where $\beta_{YX} = \frac{\sigma_{YX}}{\sigma_X^2}$ and $\beta_{YW} = \frac{\sigma_{YW}}{\sigma_W^2}$. The mean and variance of M_T is given as:

$$E(M_T) = \mu_Y,\ V(M_T) = \sigma_T^2 = \sigma_Y^2(1 - \rho_{YX}^2 - \rho_{YW}^2 + 2\rho_{YX}\rho_{YW}\rho_{XW}) \tag{4.9}$$

where ρ_{YX} is the Pearson's correlation coefficient between Y and X, and similarly ρ_{YW} and ρ_{XW} are defined. Now the plotting statistic and the control limits of the EWMA chart based on two auxiliary variables is given as:

$$Z_i^{"} = \lambda^{"} M_{T_i} + (1 - \lambda^{"})Z_{i-1}^{"} \tag{4.10}$$

$$\left.\begin{aligned} LCL &= \mu_0 - L^{"}\sigma_M\sqrt{\frac{\lambda^{"}}{2-\lambda^{"}}(1-(1-\lambda^{"})^{2i})} \\ CL &= \mu_0 \\ UCL &= \mu_0 + L^{"}\sigma_M\sqrt{\frac{\lambda^{"}}{2-\lambda^{"}}(1-(1-\lambda^{"})^{2i})} \end{aligned}\right\} \tag{4.11}$$

where $\lambda^{"}$ is the smoothing constant for the proposed statistic. $Z_{i-1}^{"}$ represents the past information and its initial value (i.e. $Z_0^{"}$) is also taken equal to the target mean μ_0 i.e. the in control mean of Y. $L^{"}$ determines the width of the control limits for the proposed EWMA chart based on two auxiliary variables.

Finally, after a simulation study like we have done with one auxiliary variable, the key conclusions about the EWMA chart based on two auxiliary variables are:

i. ARL_1 values for the proposed chart decrease with an increase in values of either or both ρ_{YX} and ρ_{YW} but they increase as the value of ρ_{XW} increases;

ii. the combinations of ρ_{YX} , ρ_{YW} and ρ_{XW} (e.g. $(\rho_{YX}, \rho_{YW}, \rho_{XW}) = (0.5, 0.75, 0)$ and $(\rho_{YX}, \rho_{YW}, \rho_{XW}) = (0.75, 0.5, 0)$) for which the values of plotting statistic M_T and its variance σ_T^2 are the same, yield the same $ARLs$;

iii. for fixed values of $\lambda^{''}$ and ARL_0, the value of $L^{''}$ remains the same for any possible combination of ρ_{YX} , ρ_{YW} and ρ_{XW};

iv. the performance of the proposed chart is usually better for the smaller values of $\lambda^{''}$;

v. auxiliary information really improves the performance (which is not a surprise!).

4.2.3 Illustrative example

In this subsection, we give an illustrative example for which we generate a dataset (named as dataset 4.1) containing 30 observations in total. The first 20 observations are generated from a trivariate normal distribution given as:

$$\begin{pmatrix} Y \\ X \\ W \end{pmatrix} \sim N_3 \left(\begin{pmatrix} 10 \\ 5 \\ 5 \end{pmatrix}, \begin{pmatrix} 1 & 0.5 & 0.5 \\ 0.5 & 1 & 0 \\ 0.5 & 0 & 1 \end{pmatrix} \right)$$

Hence the in control mean of the study variable Y equals 10. The remaining 10 observations are generated from an out of control situation with a shift of one sigma in the mean of the study variable Y (i.e. $\delta = 1$) given as:

$$\begin{pmatrix} Y \\ X \\ W \end{pmatrix} \sim N_3 \left(\begin{pmatrix} 11 \\ 5 \\ 5 \end{pmatrix}, \begin{pmatrix} 1 & 0.5 & 0.5 \\ 0.5 & 1 & 0 \\ 0.5 & 0 & 1 \end{pmatrix} \right)$$

Now the variable Y is used to setup the classical EWMA control chart (with plotting statistic represented by Z_i and parameters $\lambda = 0.25$ and $L = 3$), variables Y and X are used to setup the M$_X$EWMA control chart (with plotting statistic represented by Z_i' and parameters $\lambda' = 0.25$ and $L' = 3$) and variables Y, X and W are used to setup the M$_T$EWMA control chart (with plotting statistic represented by $Z_i^{''}$ and parameters $\lambda^{''} = 0.25$ and $L^{''} = 3$). The calculation steps for applying the M_XEWMA chart are given in Table 4.7, whereas the graphical display of the three charts is given in Figure 4.1.

Table 4.8: Simulated dataset 4.1 and calculation steps of M_XEWMA chart

Sample No.	Y_i	X_i	W_i	M_X	Z_i'	UCL	Sample No.	Y_i	X_i	W_i	M_X	Z_i'	UCL
1	10.07	5.22	4.34	9.97	9.99	10.65	16	11.06	5.86	6.67	10.63	10.12	10.98
2	11.21	7.15	4.15	10.13	10.03	10.81	17	10.15	5.48	3.77	9.92	10.07	10.98
3	8.32	4.91	4.46	8.37	9.61	10.89	18	9.12	5.18	4.58	9.03	9.81	10.98
4	9.63	2.95	4.32	10.65	9.87	10.93	19	10.5	4.97	6.67	10.51	9.99	10.98
5	7.4	4.08	4.26	7.86	9.37	10.95	20	8.67	5.5	3.55	8.42	9.59	10.98
6	10.56	4.16	5.86	10.98	9.77	10.97	21	10.41	5.29	4.05	10.26	9.76	10.98
7	9.52	4.55	4.69	9.74	9.76	10.97	22	10.11	3.33	3.91	10.95	10.06	10.98
8	8.85	5.23	4.02	8.74	9.51	10.98	23	12.59	5.2	7.1	12.49	10.67	10.98
9	9.58	5.45	4.62	9.36	9.47	10.98	24	11.59	4.98	4.65	11.6	10.9	10.98
10	10.98	5.04	4.48	10.96	9.84	10.98	25	11.24	6.42	4.27	10.53	10.81	10.98
11	10.11	5.52	5.68	9.85	9.84	10.98	26	10.65	4.81	4.66	10.74	10.79	10.98
12	9.6	4.06	4.76	10.07	9.9	10.98	27	11.09	5.29	3.56	10.94	10.83	10.98
13	10.7	5.25	6.63	10.57	10.07	10.98	28	10.48	5.25	4.36	10.36	10.71	10.98
14	8.35	4.33	4.24	8.68	9.72	10.98	29	11.92	5.04	4.14	11.9	11.01	10.98
15	11.09	5.88	5.02	10.65	9.95	10.98	30	11.17	4.32	5.53	11.51	11.13	10.98

Figure 4.1: Graphical display of M_TEWMA, M_XEWMA and classical EWMA charts for the simulated dataset 4.1

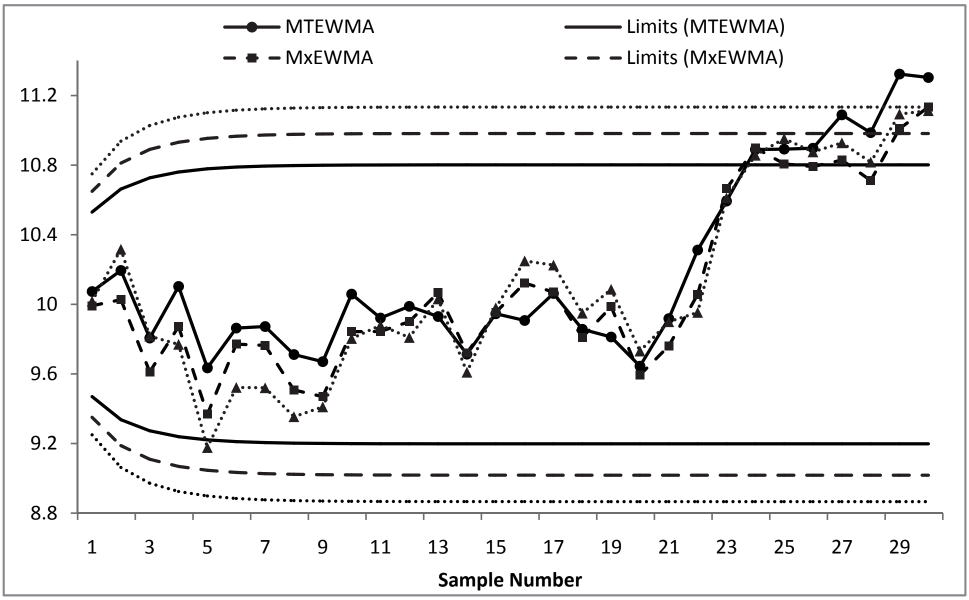

Figure 4.1 indicates that the classical EWMA control chart failed to detect any shift in the mean of the study variable Y. M_XEWMA detected the shift at samples # 29 and 30 (cf. Table 4.8), whereas M_TEWMA detected the shift at samples # 24, 25, 26, 27, 28, 29 and 30.

4.3 CUSUM control charts using auxiliary information

In this section we utilize the efficiency of regression estimator to design a CUSUM-type structure and try to study the effect of this efficient estimator on the ARL performance of CUSUM chart. Now the plotting statistics for the proposed M_XCUSUM chart (which is based on the estimator given in (4.2)) is given as:

$$N_i^+ = \max\left[0, \left(M_{X_i} - \mu_0\right) - K' + N_{i-1}^+\right], \quad N_i^- = \max\left[0, -\left(M_{X_i} - \mu_0\right) - K' + N_{i-1}^-\right] \quad (4.12)$$

Initial values for the statistics given in (4.12) are taken equal to zero i.e. $N_0^+ = N_0^- = 0$. The decision rule for the proposed chart is given as: the statistics N_i^+ and N_i^- are plotted against the control limit H'. For any value of i, if the value of N_i^+ exceeds the value of H' than the process mean is declared to be shifted upwards and if the value of N_i^- exceeds the value of H' than the process mean is said to be moved downwards. K' and H' are defined as:

$$K' = k'\sigma_M, \quad H' = h'\sigma_M \quad (4.13)$$

The values of k' and h' need to be selected carefully because the ARL properties of M_XCUSUM chart mainly depend on these two constants (along with the value of ρ_{YX}). The specifications of M_XCUSUM chart makes it the generalized form of the classical CUSUM chart given in Section 1.2, i.e. for $\rho_{YX} = 0$, the proposed M_XCUSUM chart becomes equivalent to the classical CUSUM in terms of plotting statistic as well ARL performance. For the proposed chart Tables 4.9 – 4.11 contain the $ARLs$ with ARL_0 fixed at 500.

Table 4.9: ARL values for the proposed M_XCUSUM chart with $k' = 0.25$ and $h' = 8.585$ at $ARL_0 = 500$

δ	ρ_{YX}				
	0.05	0.25	0.5	0.75	0.95
0	499.3466	499.1864	499.2012	500.9817	500.6632
0.25	94.6109	89.987	74.984	48.1801	16.1035
0.5	31.0236	29.6155	25.1541	17.3604	7.0516
0.75	17.5129	16.8127	14.5609	10.4637	4.5919
1	12.1546	11.7041	10.2408	7.5157	3.4645
1.5	7.5715	7.3144	6.4712	4.8689	2.3575
2	5.5412	5.3636	4.7791	3.6584	1.9967
2.5	4.4047	4.2701	3.8258	2.9861	1.7963
3	3.6817	3.5743	3.2238	2.5107	1.2199

Table 4.10: ARL values for the proposed M_XCUSUM chart with $k' = 0.5$ and $h' = 5.071$ at $ARL_0 = 500$

δ	ρ_{YX}				
	0.05	0.25	0.5	0.75	0.95
0	499.015	500.0021	500.8843	499.0574	500.1008
0.25	145.2716	138.2263	114.5163	68.9901	15.3663
0.5	38.777	36.3617	28.9044	17.0683	5.3405
0.75	17.2793	16.3181	13.3748	8.6464	3.2904
1	10.4965	9.9897	8.4132	5.7578	2.4388
1.5	5.8086	5.5756	4.8327	3.5082	1.7847
2	4.0503	3.9052	3.4373	2.5806	1.2021
2.5	3.1451	3.0414	2.7049	2.1126	1.0074
3	2.5978	2.5187	2.2684	1.8667	1

The algorithm used for calculating the $ARLs$ in Tables 4.9 – 4.11 is given in Appendix 4.2 where 50,000 simulations are used.

Table 4.11: ARL values for the proposed M_XCUSUM chart with $k' = 1$ and $h' = 2.665$ at $ARL_0 = 500$

δ	ρ_{YX}				
	0.05	0.25	0.5	0.75	0.95
0	499.0466	499.1701	500.5972	499.4241	500.9488
0.25	249.1542	240.639	209.9628	139.8514	26.0941
0.5	81.2212	75.9419	58.9892	30.2808	5.0512
0.75	30.8019	28.4313	21.2702	10.7289	2.5918
1	14.6235	13.5187	10.2682	5.6554	1.795
1.5	5.7314	5.3872	4.3635	2.814	1.1276
2	3.4063	3.2422	2.7406	1.9231	1.0031
2.5	2.4483	2.3484	2.0355	1.4745	1
3	1.9387	1.8674	1.6356	1.1929	1

Before concluding this section, we present the main findings about our proposed M_XCUSUM control chart.

i. the use of an auxiliary variable with the control structure of CUSUM chart is really advantageous in terms of the ARL_1 values if the value of ρ_{YX} is reasonably large (cf. Tables 4.9 – 4.11);

ii. to attain a fixed value of ARL_0, the value of h' has to remain fixed for all the value of ρ_{YX} (cf. Tables 4.9 – 4.11);

iii. to attain a fixed value of ARL_0, the value of h' decrease with an increase in the value of k' and vice versa (cf. Tables 4.9 – 4.11);

iv. for a fixed value of ARL_0, the ARL_1 values decrease rapidly with a decrease in the values of either or both ρ_{YX} and δ (cf. Tables 4.9 – 4.11).

Like M_XCUSUM, a CUSUM chart based on the information of two auxiliary variables (named as M_TCUSUM) can also be easily designed by following the procedure given in subsection 4.2.2.

4.3.1 Comparisons

Now we provide a comparison of M_XCUSUM chart with some of the revisions and extensions of CUSUM and EWMA-type control charts.

M_XCUSUM versus the classical CUSUM: $ARLs$ for two-sided CUSUM chart for different values of k with ARL_0 fixed at 500 are given in Table 4.6. Collectively Tables 4.9 – 4.11 and Table 4.6 validate that the classical CUSUM is a special case of the proposed M_XCUSUM chart. The ARL performance of the proposed chart with $\rho_{YX} = 0.05$ (i.e. close to zero) is almost same as compared to the ARL performance of classical CUSUM. As we increase the value of ρ_{YX} for the proposed chart, its ARL_1 values decrease.

M_XCUSUM versus the classical EWMA: Table 2.2 contains the $ARLs$ of classical EWMA where λ and L are the parameters of EWMA control chart. The comparison of M_XCUSUM chart with the classical EWMA show that the proposed chart is performing better in general for $\rho_{YX} \geq 0.25$ (cf. Table 2.2 vs. Tables 4.9 – 4.11). For large values of ρ_{YX} (like $\rho_{YX} \geq 0.75$) the proposed chart (with any value of k') outperfoms the classical EWMA (with any value of λ).

M_XCUSUM versus M_XEWMA: Comparing the performance of M_XCUSUM chart with M_XEWMA chart for a specific value of ρ_{YX} (e.g. $\rho_{YX} = 0.5$) it can be observed that M_XEWMA (with $\lambda' = 0.1$) has a slightly better ARL performance as compared to the proposed chart but once λ' is greater than 0.1 for the M_XEWMA chart, the proposed chart becomes better than M_XEWMA (cf. Table 4.1 – 4.5 vs. Tables 4.9 – 4.11).

The M_TCUSUM control chart, which is based on two auxiliary variables, has even better properties as was to be expected (results not given here).

4.3.2 Illustrative example

An example to illustrate the application of the proposed chart with a real dataset is provided in this subsection. The three CUSUM-type control charts are applied to the simulated dataset 4.1 with $k = 0.5$ and $h = 5.071$ for the classical CUSUM; $k' = 0.5$ and $h' = 5.071$ for the M_XCUSUM; and $k'' = 0.5$ and $h'' = 5.071$ for M_TCUSUM chart with ARL_0 fixed at 500 for all three charts. The chart output for all three charts is given in Figure 4.2.

Figure 4.2: Graphical display of M_TCUSUM, M_XCUSUM and classical CUSUM charts for simulated dataset 4.1

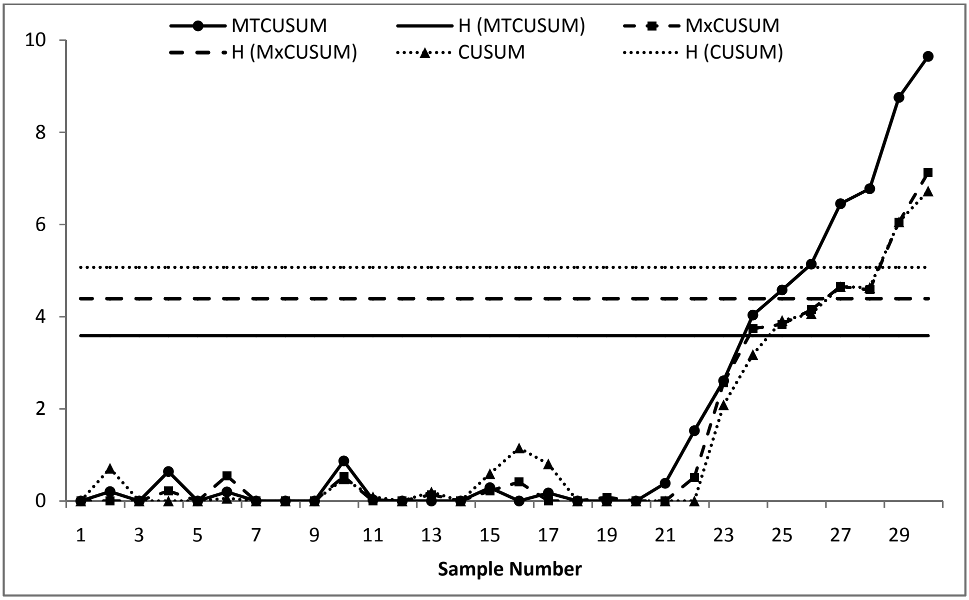

Figure 4.2 shows that M_TCUSUM chart is detecting the positive shift at the 24th sample and onwards, whereas the classical CUSUM and M_XCUSUM are detecting the shift at the 27th and the 29th sample, respectively. This verifies the observations in subsection 4.3.1.

4.4 Concluding remarks

This chapter proposes the use of auxiliary information with the control structures of the EWMA and CUSUM charts. The regression estimation technique is used to exploit the auxiliary information. Note that the proposed M_XEWMA and M_XCUSUM charts are the extended forms of the classical EWMA and CUSUM charts respectively, i.e. the proposed charts are equal to the classical ones when the correlation between the study variable and auxiliary variable(s) is equal to 0. The performance of the proposed charts is evaluated in terms of ARL for different values of the correlation between the study variable and the auxiliary variable(s). A comparison of the proposed charts with the classical CUSUM, the classical EWMA and some of their recent modifications is also made. The comparisons showed that the proposed charts are good at detecting small to moderate shifts in the process location, while their ability to detect large shifts is not bad either. Finally, results are also supported by the illustrative examples.

Appendix 4.1

```
library(MASS)
Mx=c(); Zp=c(); ucl=c(); lcl=c(); rl=c()
muy=0; mux=0; sigyy=1; sigxx=1; sigyx=0.5
betayx=sigyx/sigxx; rho=sigyx/sqrt(sigyy*sigxx)
meanv=c(muy,mux)
sigmam=matrix(c(sigyy,sigyx,sigyx,sigxx),2,2)
muM=muy; sigM=sqrt(sigyy*(1-rho^2))
ld=0.25; L=3
for(j in 1:10000)
{
      for(i in 1:1000000)
      {
            w=mvrnorm(1,meanv,sigmam)
            y=w[1]; x=w[2]
            Mx[i]=y-betayx*x
            if(i==1)
                  {Zp[i]=ld*Mx[i]+ (1-ld)*muM;}
                  else{Zp[i]=ld*Mx[i]+(1-ld)*Zp[i-1];}
            ucl[i]=muM+L*sigM*sqrt((ld/(2-ld))*(1-(1-ld)^(2*i)))
            lcl[i]=muM-L*sigM*sqrt((ld/(2-ld))*(1-(1-ld)^(2*i)))
            if(Zp[i]>ucl[i]|Zp[i]<lcl[i])
                  {rl[j]=i;break;}
                  else{rl[j]=0;}
      }
}
mean(rl)
```

Appendix 4.2

```
library(MASS)
Mx=c(); Np=c(); Nn=c(); rl=c()
muy=0; mux=0; sigyy=1; sigxx=1; sigyx=0.5;
betayx=sigyx/sigxx; rho=sigyx/sqrt(sigyy*sigxx)
meanv=c(muy,mux)
sigmam=matrix(c(sigyy,sigyx,sigyx,sigxx),2,2)
muM=muy; sigM=sqrt(sigyy*(1-rho^2))
K=0.5*sigM; H=5.071*sigM
for(j in 1:100000)
{
      for(i in 1:1000000)
      {
            w=mvrnorm(1,meanv,sigmam)
```

```
            y=w[1]; x=w[2]
            Mx[i]=y-betayx*x
            if(i==1)
                  {Np[i]=max(0,(Mx[i]-muM)-K);}
                  else{Np[i]=max(0,(Mx[i]-muM)-K+Np[i-1]);}
            if(i==1)
                  {Nn[i]=max(0,-(Mx[i]-muM)-K);}
                  else{Nn[i]=max(0,-(Mx[i]-muM)-K+Nn[i-1]);}
            if(Np[i]>H|Nn[i]>H)
                  {rl[j]=i;break;}
                  else{rl[j]=0;}
      }
}
mean(rl)
```

Chapter 5

Progressive control charting

This chapter proposes a control chart for monitoring the process location, named as Progressive Mean (PM) control chart, in which a progressive mean is used as a plotting statistic. Taking the inspiration from the PM chart, two new memory control charts for monitoring the process dispersion, named as floating $T - S^2$ and floating $U - S^2$ control charts, are also proposed. The proposed charts are designed such that they utilize not only the current information but also the past information. Therefore, the proposed charts are natural competitors for the classical CUSUM, the classical EWMA and some recent modifications of these two charts.

This chapter is based on two papers; one for monitoring the location parameter (cf. Abbas, Zafar, Riaz and Does (2012)) and the other for monitoring the dispersion parameter (cf. Abbas, Riaz and Does (2012d)).

5.1 The proposed progressive mean control chart

Let Y be a quality characteristic of which the mean will be monitored. It is assumed that we use individual observations from a normal distribution. If Y_i, $i = 1, 2, 3 \ldots \ldots$ is the sequence of independent and identically distributed observations from the process under investigation, then progressive mean PM is defined as the cumulative average over time. Mathematically, we may define the PM statistic as:

$$PM_i = \frac{\sum_{j=1}^{i} Y_j}{i} \tag{5.1}$$

PM_i is an unbiased estimator of population mean μ_0 and its variance is given by $\frac{\sigma_0^2}{i}$. According to the typical three sigma control limits, the control charting structure based on the PM statistic and its variance may be defined as:

$$LCL_i = \mu_0 - 3\frac{\sigma_0}{\sqrt{i}}, \qquad CL = \mu_0, \qquad UCL_i = \mu_0 + 3\frac{\sigma_0}{\sqrt{i}} \tag{5.2}$$

where all the parameters used in (5.2) are as explained earlier. It is obvious that the control limits given in (5.2) are time varying and exploit the past and present information using equal weights. Note that the design structure of the proposed chart is relative simple and easy to execute compared with the CUSUM and EWMA control charts.

A problem with the control structure in (5.2) is that the control limits remain too wide for the large values of i (wide relative to the plotting statistic). It turns out that it is almost impossible for the plotting statistic in (5.1) to cross the control limits in (5.2), in case of shifted mean. We have solved this issue by imposing a penalty on the control limits such that the control limits are a bit narrower for large values of i. We choose this penalty function equal to $f(i) = i^p$. Hence, the penalized limits for the proposed PM chart are given by:

$$LCL_i = \mu_0 - C'\frac{\sigma_0}{i^{0.5+p}}, \qquad CL = \mu_0, \qquad UCL_i = \mu_0 + C'\frac{\sigma_0}{i^{0.5+p}} \tag{5.3}$$

where C' is a constant that is used to control the run lengths.

In (5.3) we have used different possibilities of p and we have searched for a suitable constant C' for each possibility to fix the in control process properties in terms of ARL_0 and optimum out of control RL properties in terms of ARL_1. We identified $p = 0.2$ as the most suitable choice in terms of optimizing the RL properties. For this optimum choice of $f(i)$ (i.e. $i^{0.2}$) we have worked out the values of constants C' by fixing ARL_0. These constants for some commonly used ARL_0 values are provided in Table 5.1. For these constants and ARL_0 values given in Table 5.1 we have carried out a RL study and the resulting properties in terms of ARL_0 and ARL_1 are provided in Table 5.2. Appendix 5.1 contains the details regarding the algorithm, that is made in R language, used for the computation of $ARLs$. The standard errors for the results of Tables 5.1 – 5.2 remain less than 1.3%.

TABLE 5.1: Values of the control limit constant C' for different choices of ARL_0 for the proposed PM control chart

ARL_0	168	200	370	400	500
C'	3	3.129	3.568	3.639	3.846

TABLE 5.2: ARL values for the proposed chart with different shifts

Pre-fixed ARL_0	δ									
	0	0.25	0.5	0.75	1	1.5	2	3	4	5
500	498.14	47.2353	19.032	11.1564	7.5504	4.5204	3.1455	1.9803	1.4248	1.1186
400	400.938	44.474	17.872	10.313	7.200	4.261	2.985	1.877	1.360	1.0847
370	369.00	17.452	10.166	10.166	7.0941	4.184	2.931	1.721	1,236	1.043
200	200.82	34.7366	14.6914	8.6191	5.9814	3.5996	2.5415	1.6124	1.1981	1.0338
168	170.33	33.0695	12.1479	8.1779	5.659	3.4086	2.4437	1.5555	1.1598	1.0263

We conclude from Tables 5.1 – 5.2:

i. The proposed PM control chart is really good in detecting small and moderate shifts and is still good in detecting large shifts (cf. Table 5.2);

ii. ARL_1 decreases fastly with an increase in δ (cf. Tables 5.1 and 5.2);

iii. The control structure of the proposed chart is very easy compared to the CUSUM and EWMA charts.

Note that if we apply the same set up with samples sizes $n > 1$ instead of $n = 1$, the results will be the same with the obvious adjustments in the control limits in (5.3).

5.1.1 Comparisons

To detect small and moderate shifts, EWMA and CUSUM charts and some of their modifications are available. We have introduced in this chapter a rather simple alternative to these charts, namely the PM control chart, and in this section we compare the performance of our proposed chart with some of its counterparts in terms of ARL. We compare the performance of the proposed chart with the classical EWMA, the classical CUSUM, the fast initial response (FIR) CUSUM, the FIR EWMA, the runs rules based CUSUM, the runs rules based EWMA and the adaptive EWMA. We use for the ARL_0 the values 168, 200, 370, 400 and 500, so that valid comparisons with each chart can be made. Below, we present one by one the comparison of the proposed chart with its competitor.

Proposed versus the classical CUSUM: ARL values for the classical CUSUM are given by in Table 2.1. Comparison of the classical CUSUM with the proposed PM chart clearly shows that the proposed chart almost outperforms the classical CUSUM for all the values of δ (cf. Table 2.1 vs. Table 5.2).

Proposed versus the classical EWMA: Table 2.2 contains the ARL values for the classical EWMA chart. Comparison of Table 2.2 with Table 5.2 shows the uniform superiority of the proposed PM chart over the classical EWMA chart.

Proposed versus FIR CUSUM and FIR EWMA: ARL values for the FIR CUSUM presented by Lucas and Crosier (1982) and FIR EWMA by Lucas and Saccucci (1990) are given in Table 2.10 and Table 2.17, respectively. The comparison of FIR CUSUM and the proposed PM chart indicates that the performance of proposed control chart is better for small and moderate shifts even when the ARL_0 for the FIR CUSUM is not fixed at 168 (cf. Table 2.10 vs. Table 5.2). We may conclude that the proposed chart performs really well for small shifts. The same is the case for the FIR EWMA, i.e. for a 25% head start the performance of the proposed chart is superior to the FIR EWMA for every choice of λ, but as we increase the head start to 50%, the performance of the FIR EWMA becomes better than the proposed chart for the larger shifts with $\lambda = 0.1$ (cf. Table 2.17 vs. Table 5.2).

Proposed versus runs rules based CUSUM and EWMA: In chapter 2 we introduced the runs rules based CUSUM and the runs rules based EWMA, respectively. The $ARLs$ for the runs rules based CUSUM are provided in Tables 2.7 – 2.8 and for runs rules based EWMA these are given in Tables 2.15 – 2.16. The comparison of the runs rules based CUSUM with the proposed chart shows that the proposed chart performs better than the runs rules based CUSUM uniformly for both schemes (cf. Tables 2.7 – 2.8 vs. Table 5.2). Similarly, the comparison of the runs rules based EWMA with the proposed chart also reveals that the proposed chart is superior to the runs rules based EWMA for most of the values of δ (cf. Tables 2.15 – 2.16 vs. Table 5.2).

Proposed versus adaptive EWMA: The adaptive EWMA of Capizzi and Masarotto (2003) is designed so that it performs better for small and large shifts at the same time by giving weights to past information using a suitable function of the current error. Three functions of error represented by $\phi_{hu}(.)$, $\phi_{bs}(.)$ and $\phi_{cub}(.)$ are used in their article. ARL values for the adaptive EWMA with these 3 functions of errors are given in Table 5.3, where the value of δ is targeted between $0.25 - 4$.

TABLE 5.3: ARL values for the adaptive EWMA at $ARL_0 = 500$

Error function	δ							
	0.25	0.5	0.75	1	1.5	2	3	4
$\phi_{hu}(.)$	98.51	40.94	25.04	17.59	10.11	6.08	2.29	1.26
$\phi_{bs}(.)$	135.01	42.72	21.99	13.91	7.12	4.25	2.01	1.28
$\phi_{cub}(.)$	97.03	41.54	25.68	18.16	10.52	6.36	2.35	1.27

The comparison of the proposed chart with the adaptive EWMA shows that the proposed chart also outperforms the adaptive EWMA for all the values of δ (cf. Table 5.3 vs. Table 5.2).

Proposed versus adaptive CUSUM: Jiang et al. (2008) proposed the use of an adaptive CUSUM with EWMA based shift estimator. $ARLs$ for the adaptive CUSUM with $\delta_{min}^{+} = 0.5$ and $\lambda = 0.3$ are given in Table 3.5. Comparison of Table 5.2 and Table 3.5 shows that the proposed PM chart is uniformly superior compared to the adaptive CUSUM with EWMA based shift estimator.

To summarize the results, we have made some ARL curves of the proposed PM chart against its existing counterparts. These are given in Figures 5.1 – 5.3. ARL curves for the proposed chart, the classical EWMA (with $\lambda = 0.1$), the adaptive EWMA (with error function $\phi_{hu}(.)$), the runs rules based CUSUM scheme II (with $WL = 4.8$ and $AL = 5.11$) and the runs rules based EWMA modified $2/3$ scheme (with $\lambda = 0.1$) are presented in Figure 5.1.

FIGURE 5.1: ARL Curves for proposed chart, classical EWMA, adaptive EWMA, runs rules based CUSUM and runs rules based EWMA at $ARL_0 = 500$

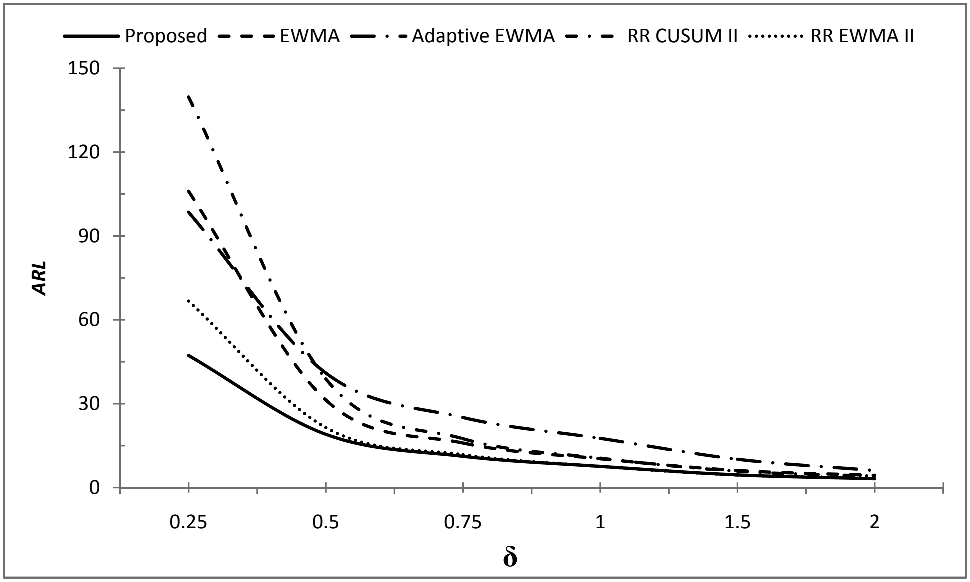

FIGURE 5.2: $\boldsymbol{ARL}$ **curves for proposed chart and adaptive CUSUM at** $\boldsymbol{ARL_0 = 400}$

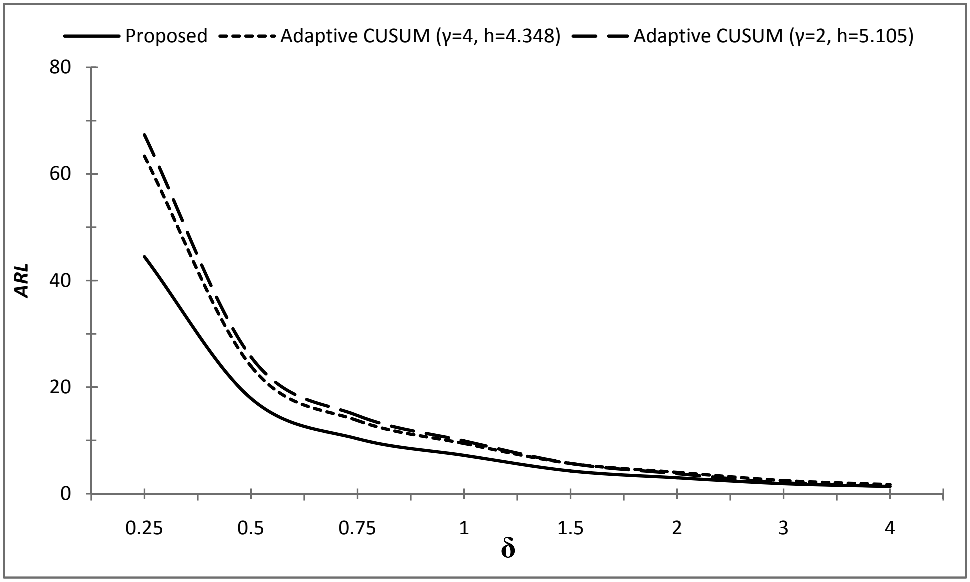

FIGURE 5.3: $\boldsymbol{ARL}$ **curves for proposed chart, classical CUSUM and FIR CUSUM at** $\boldsymbol{ARL_0 = 168}$

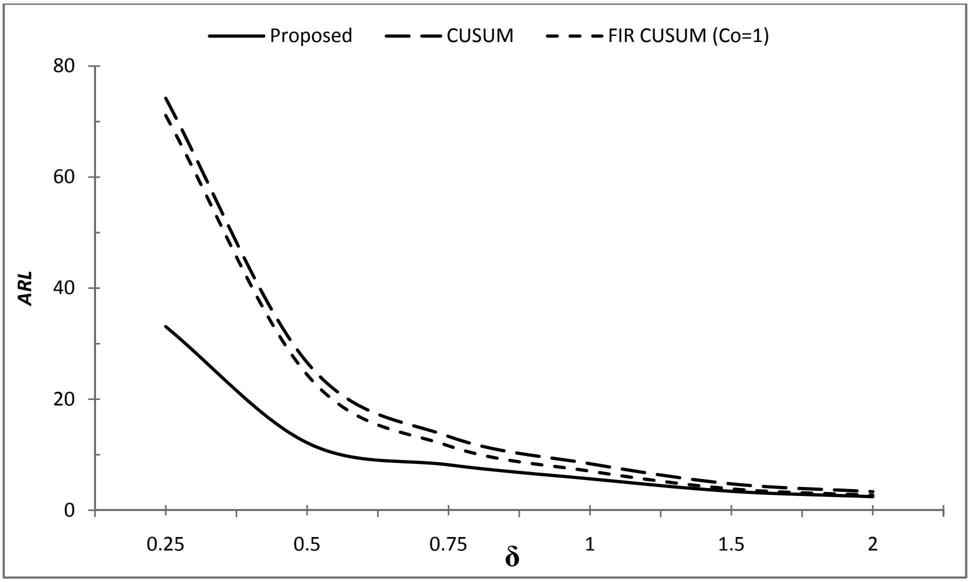

In Figure 5.2 comparison of the proposed chart and the adaptive CUSUM are provided, whereas Figure 5.3 contains the ARL curves for the proposed chart, the classical CUSUM and the FIR CUSUM (with head start $C_0 = 1$). Figures 5.1 – 5.3 clearly show the best performance of the proposed chart against the other methods.

5.1.2 Illustrative example

In this section we demonstrate the application of the proposed PM chart. Also the classical EWMA and the classical CUSUM charts are included in the example to validate the superiority of the proposal. For this purpose we have generated two datasets of 40 and 30 observations, respectively, such that in dataset 5.1 the first 20 observations are generated from $N(0,1)$ (i.e. the in control situation) and the second set of the 20 observations from $N(0.5,1)$ (i.e. the out of control situation having a shift of 0.5σ (small shift)). Similarly, in dataset 5.2 the first 20 observations are generated from $N(0,1)$ and the second set of 10 observations from $N(1.5,1)$ (i.e. an out of control situation having a shift of 1.5σ (moderate shift)). The PM statistic for the proposed chart, the EWMA statistic with $\lambda = 0.25$ and the CUSUM statistic with $k = 0.5$ are calculated. To fix the ARL_0 at 500 we have used $C' = 1.267$ for the PM chart, $L = 3$ for the classical EWMA and $h = 5.07$ for the classical CUSUM. The graphical displays of the proposed PM, EWMA and CUSUM charts are presented in the Figures 5.4, 5.5 and 5.6 for dataset 5.1 and in Figures 5.7, 5.8 and 5.9 for dataset 5.2, respectively.

From Figure 5.4 we can see that the proposed chart gives out of control signals at samples # 35, 36, 37, 38, 39 and 40, thus giving a total of 6 out of control signals. Figure 5.5 shows that the classical EWMA control chart gives one out of control signal at sample # 38 and Figure 5.6 depicts that the classical CUSUM control chart gives out of control signals at samples # 38, 39 and 40, thus giving 3 signals. An upward shift occurred after sample # 20, which is detected by the proposed chart more quickly than the EWMA and the CUSUM. It illustrates the ability of the proposed chart to quickly detect small shifts in the process.

FIGURE 5.4: Graphical display of the proposed *PM* chart for dataset 5.1

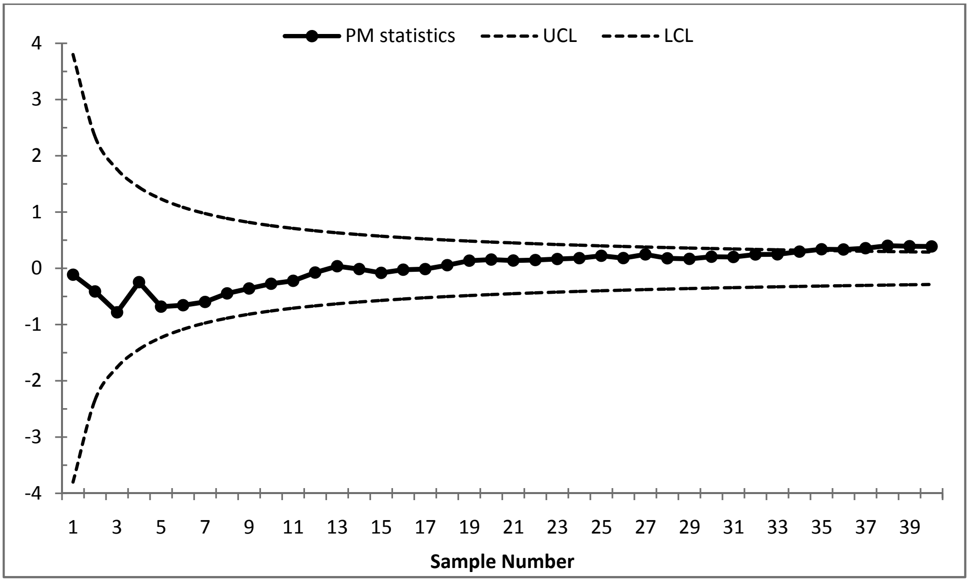

FIGURE 5.5: Graphical display of the classical EWMA chart for dataset 5.1

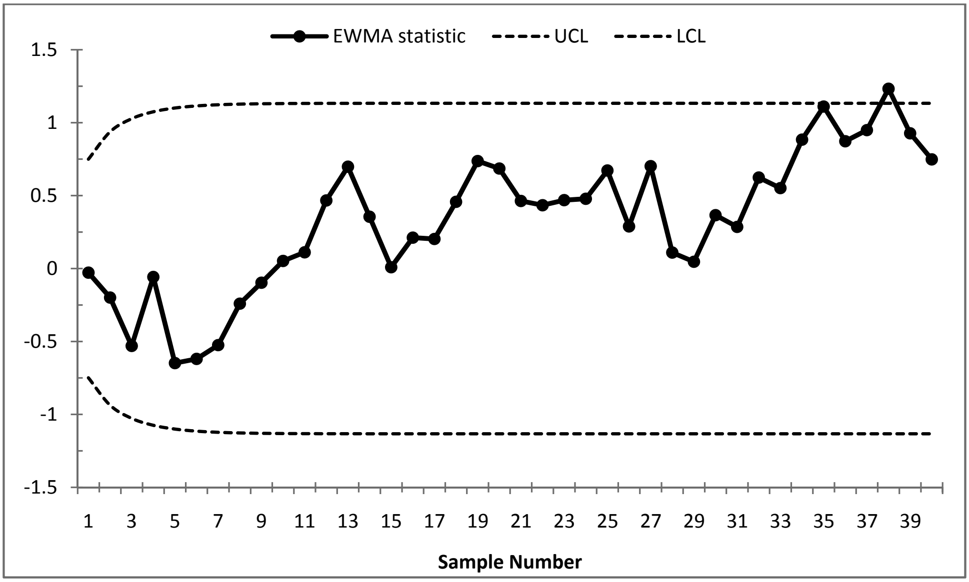

FIGURE 5.6: Graphical display of the classical CUSUM for dataset 5.1

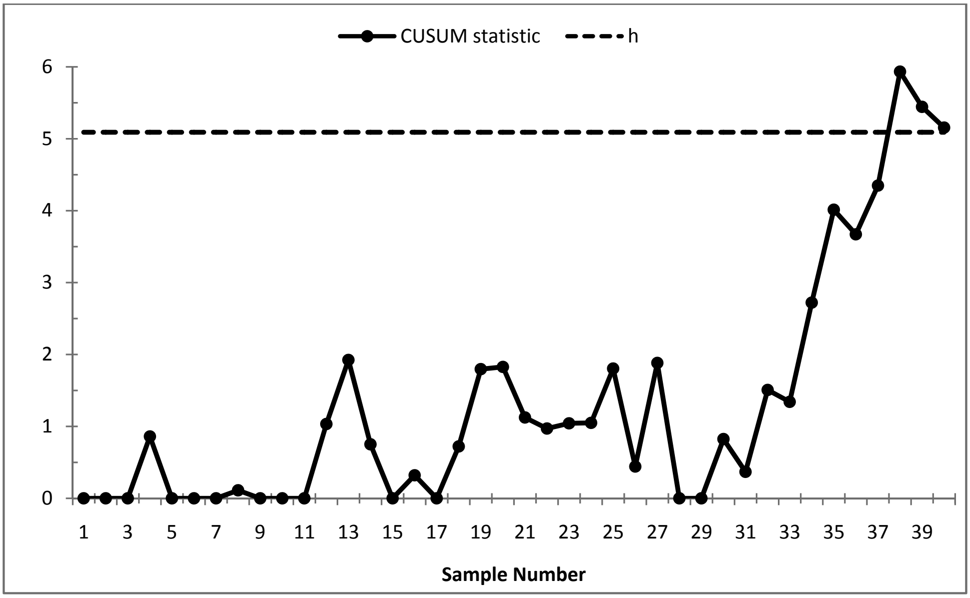

FIGURE 5.7: Graphical display of the proposed *PM* chart for dataset 5.2

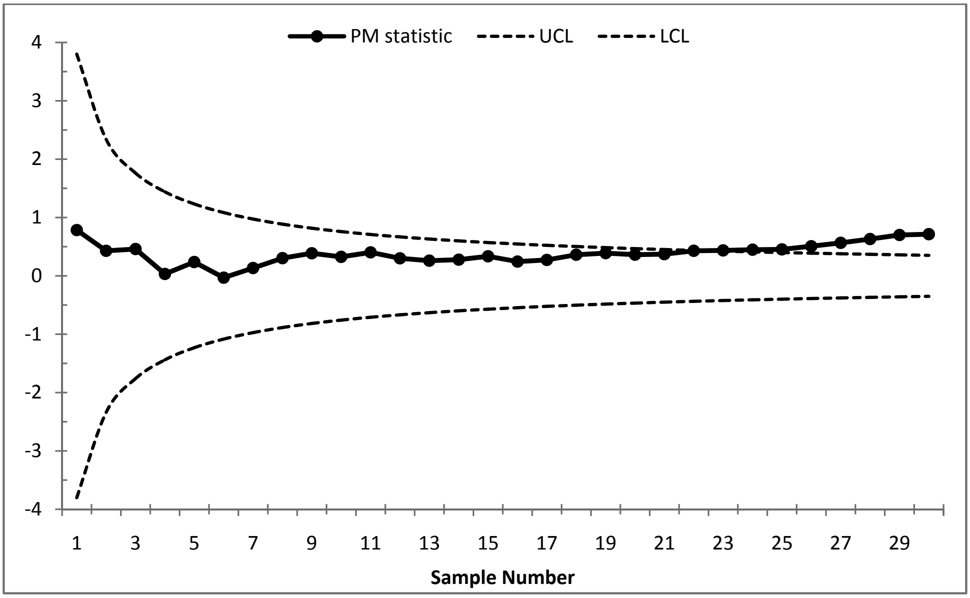

The situation is not much different in dataset 5.2, where the PM chart detects the shift at samples # 23, 24, 25, 26, 27, 28, 29 and 30 (cf. Figure 5.7). The classical EWMA and the CUSUM detect the shift at samples # 27, 28, 29 and 30 (cf. Figures 5.8 and 5.9).

FIGURE 5.8: Graphical display of the classical EWMA chart for dataset 5.2

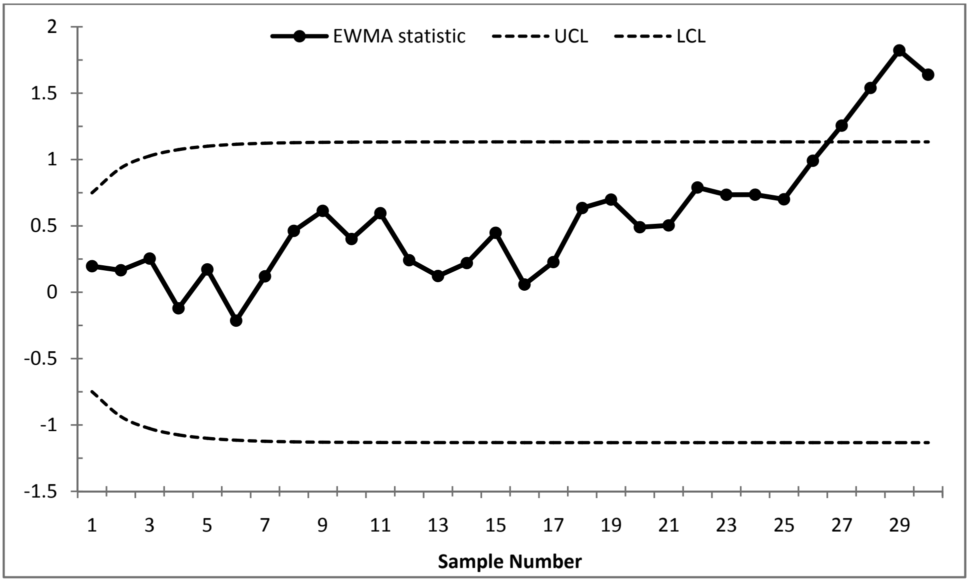

FIGURE 5.9: Graphical display of the classical CUSUM for dataset 5.2

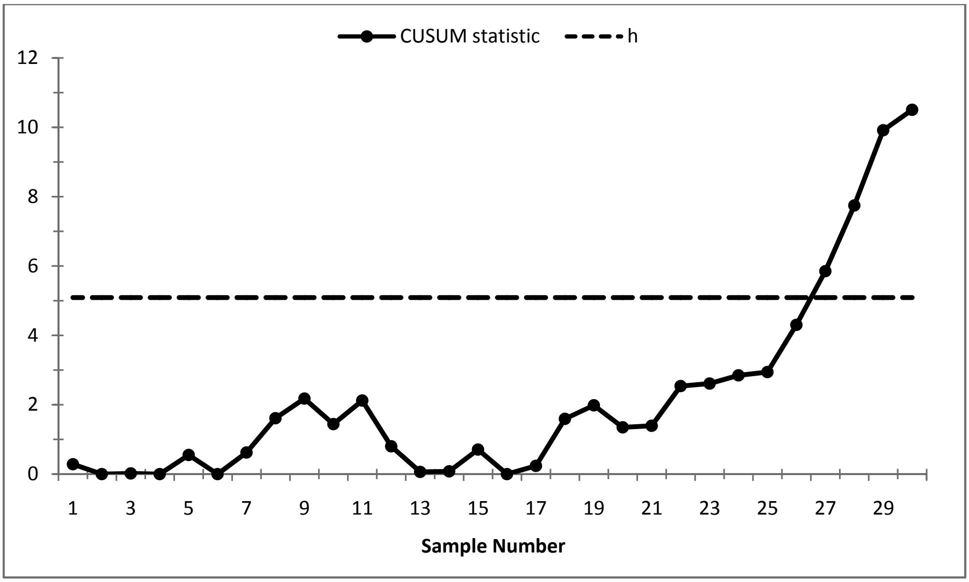

In both small and moderate shifts we see that the proposed chart detect the shift more quickly than the others. The number of signals given by the proposed chart is also greater than the classic ones. These outcomes are exactly in accordance with the findings of subsection 5.1.2.

5.2 Floating control charts for process dispersion

There is a lot of literature available on CUSUM and EWMA-type control charts for monitoring the process dispersion, e.g. see Page (1963), Hawkins (1981), Acosta-Mejia et al. (1999) and Chang and Gan (1995) for CUSUM-type charts and Ng and Case (1989), Crowder and Hamilton (1992) and Huwang et al. (2010) for EWMA-type charts. Additionally, Wu and Tian (2005) and Zhang and Chang (2008) also provided the CUSUM and EWMA charts, respectively, for monitoring the process mean and variance simultaneously.

Most of these charts are based on transforming the sample variance such that the new transformed form may be closely approximated by a normally distributed variable and hence applying the usual CUSUM and EWMA structures (recommended by Page (1954) and Roberts (1959), respectively) on it. In a similar direction, Castagliola (2005) proposed a new S^2 EWMA chart for monitoring the process dispersion. He used a logarithmic three parameter transformation to obtain a normal approximation for sample variance. A similar transformation is used by Castagliola et al. (2009) to setup a CUSUM S^2 chart for monitoring process dispersion. The details regarding the EWMA and CUSUM charts based on the logarithmic transformation are given in Section 3.2.

Castagliola et al. (2010) proposed another similar type of transformation based on a four parameter Johnson S_B transformation. They claimed that this four parameter transformation gives a better approximation to the normal distribution as compared to the three parameter logarithmic transformation. With the notation of Castagliola et al. (2010), it follows that

$$U_i = a_U + b_U \ln\left(\frac{S_i^2 - c_U}{d_U + c_U - S_i^2}\right) \tag{5.4}$$

where $a_U = A_U(n)$, $b_U = B_U(n)$, $c_U = C_U(n)\sigma_0^2$ and $d_U = D_U(n)\sigma_0^2$. Variable U_i in (5.4) follows approximately a normal distribution with mean $\mu_U(n)$ and variance $\sigma_U^2(n)$ where the values of $\mu_U(n)$, $\sigma_U^2(n)$, $A_U(n)$, $B_U(n)$, $C_U(n)$ and $D_U(n)$ for all $n = 3, 4, 5, \ldots, 15$ are given in Table 5.4.

Table 5.4: Values of $\mu_U(n)$, $\sigma_U(n)$, $A_U(n)$, $B_U(n)$ and $C_U(n)$

n	$\mu_U(n)$	$\sigma_U(n)$	$A_U(n)$	$B_U(n)$	$C_U(n)$	$D_U(n)$
3	0.0184	0.9475	3.1936	1.1952	-0.2588	15.077
4	0.0078	0.9739	3.3657	1.3983	-0.2438	12.591
5	0.0039	0.9852	3.5402	1.5727	-0.2352	11.312
6	0.0022	0.9908	3.7111	1.7281	-0.2295	10.530
7	0.0014	0.994	3.8768	1.8698	-0.2254	10.000
8	0.0009	0.9958	4.0369	2.0010	-0.2224	9.618
9	0.0006	0.9970	4.1918	2.1238	-0.2200	9.328
10	0.0004	0.9978	4.3417	2.2396	-0.2181	9.100
11	0.0003	0.9983	4.4869	2.3495	-0.2166	8.917
12	0.0002	0.9987	4.6279	2.4544	-0.2152	8.766
13	0.0002	0.9989	4.7648	2.5549	-0.2141	8.640
14	0.0001	0.9991	4.8981	2.6515	-0.2132	8.532
15	0.0001	0.9993	5.0279	2.7446	-0.2123	8.440

Note that in case of $d_U + c_U - S_i^2 \leq 0$, the transformation given in (5.4) is not possible, but Castagliola et al. (2010) showed that the probability of occurrence of this event is so close to zero that it can be neglected. From the values of c_U and d_U it can be noticed that $d_U + c_U - S_i^2 \leq 0$ implies a very large value of S_i^2 as compared to the value of σ_0^2 so it can be taken as an out of control situation with a large positive shift. Details about the distributional properties of U_i can be found in Castagliola et al. (2010).

Furthermore, it should be noted that any change in the process standard deviation will change the mean of the normalized variables given in (3.5) and (5.4). So based on the these two (approximately) normalized statistics, we are now able to define our new control structures, named as floating $T-S^2$ and floating $U-S^2$ charts, respectively. These charts monitor basically the mean of the transformed statistics in (3.5) and (5.4) and hence control the process dispersion.

5.2.1 Floating $T-S^2$ control chart

The first proposed chart, named as floating $T-S^2$ chart, is based on the three parameter logarithmic transformation given in (3.5). The plotting statistic is given as:

$$FT_i = \frac{\sum_{k=1}^{i} T_k}{i} \tag{5.5}$$

The statistic in (5.5) is a cumulative average of the three parameter logarithmic transformation given in (3.5). According to the probability distribution theory we have that, if T_i follows (approximately) a normal distribution with mean $\mu_T(n)$ and variance $\sigma_T^2(n)$ that $FT_i = \sum_{k=1}^{i} T_k/i$ will have mean $\mu_T(n)$ and variance $\frac{\sigma_T^2(n)}{i}$. This implies that the control limits (including the upper control limit (UCL), center line (CL) and lower control limit (LCL)) for the floating statistic given in (5.5) can be defined as:

$$LCL = \mu_T(n) - K_T\frac{\sigma_T(n)}{\sqrt{i}}, \qquad CL = \mu_T(n), \quad LCL = \mu_T(n) + K_T\frac{\sigma_T(n)}{\sqrt{i}} \tag{5.6}$$

where the width of the control limits is determined by K_T. The ARL_0 can be controlled by adjusting this constant (K_T) as the $ARLs$ for a control chart with wider limits are larger and vice versa. The same problem (like the control limits in (5.2)) also persists with the control structure in (5.6), i.e. the control limits remain too wide for the larger values of i (wide relative to the plotting statistic). Therefore, following (5.3), the penalized control limits for the proposed floating $T - S^2$ chart are given as:

$$LCL_T = \mu_T(n) - K'_T \frac{\sigma_T(n)}{j^{p+0.5}}, \quad CL_T = \mu_T(n), UCL_T = \mu_T(n) + K'_T \frac{\sigma_T(n)}{j^{p+0.5}} \tag{5.7}$$

where K'_T is the adjusted control limit coefficient.

Table 5.5: ARL values for the floating $T - S^2$ chart with $K'_T = 3.129$ and $ARL_0 = 200$

δ	$n = 3$	$n = 5$	$n = 7$	$n = 9$
0.5	6.041	3.779	2.890	2.417
0.6	8.069	5.003	3.810	3.164
0.7	11.874	7.316	5.546	4.585
0.8	20.468	12.625	9.533	7.835
0.9	49.392	31.652	23.918	19.851
0.95	98.625	70.337	56.347	47.163
1.05	92.869	67.545	54.129	46.352
1.1	47.906	31.469	24.452	20.236
1.2	21.249	13.379	10.268	8.496
1.3	12.892	8.130	6.259	5.213
1.4	9.113	5.778	4.461	3.740
1.5	7.040	4.482	3.485	2.941
2	3.316	2.205	1.774	1.527
3	1.834	1.323	1.148	1.067

Table 5.6: ARL values for the floating $T - S^2$ chart with $K'_T = 3.568$ and $ARL_0 = 370$

δ	$n = 3$	$n = 5$	$n = 7$	$n = 9$
0.5	7.157	4.425	3.391	2.807
0.6	9.629	5.892	4.478	3.696
0.7	14.123	8.674	6.542	5.371
0.8	24.638	15.057	11.310	9.280
0.9	61.342	38.450	28.858	23.761
0.95	135.241	91.241	71.136	59.045
1.05	128.999	89.714	69.639	58.704
1.1	60.472	38.941	29.562	24.367
1.2	25.692	16.054	12.208	10.039
1.3	15.356	9.646	7.356	6.110
1.4	10.757	6.792	5.220	4.333
1.5	8.234	5.229	4.049	3.377
2	3.813	2.506	2.001	1.703
3	2.030	1.434	1.206	1.103

Table 5.7: ARL values for the floating $T - S^2$ chart with $K'_T = 3.846$ and $ARL_0 = 500$

δ	$n = 3$	$n = 5$	$n = 7$	$n = 9$
0.5	7.896	4.870	3.712	3.085
0.6	10.599	6.491	4.912	4.054
0.7	15.639	9.538	7.207	5.913
0.8	27.327	16.588	12.501	10.242
0.9	69.082	42.830	32.216	26.335
0.95	158.678	104.768	80.317	66.427
1.05	153.847	102.791	79.859	66.697
1.1	69.135	43.487	33.006	27.250
1.2	28.649	17.766	13.468	11.097
1.3	17.037	10.578	8.085	6.666
1.4	11.847	7.443	5.696	4.728
1.5	9.008	5.711	4.405	3.684
2	4.133	2.719	2.148	1.838
3	2.179	1.519	1.259	1.133

Note that the control limits given in (5.6) are a special case of the limits in (5.7) with $p = 0$. We have tested several values of p and $p = 0.2$ was found to be optimal, i.e. $p = 0.2$ gives smaller ARL_1 values for a fixed ARL_0. Tables 5.5 – 5.7 contain the ARL values for the proposed floating $T - S^2$ chart. The $ARLs$ for the proposed chart are evaluated by running 10^5 simulations. The simulation program is developed in R language.

5.2.2 Floating $U - S^2$ control chart

The plotting statistic for the second proposed chart (based on a four parameter Johnson S_B transformation) to monitor the process dispersion is given as:

$$FU_i = \frac{\sum_{k=1}^{i} U_k}{i} \tag{5.8}$$

Like FT_i in (5.5), here FU_i also have mean $\mu_U(n)$ and variance $\frac{\sigma_U^2(n)}{i}$. Therefore the control limits for this second proposed chart, named as floating $U - S^2$ chart, are given as:

$$LCL_U = \mu_U(n) - K'_U \frac{\sigma_U(n)}{j^{p+0.5}}, \quad CL_U = \mu_U(n), UCL_U = \mu_U(n) + K'_U \frac{\sigma_U(n)}{j^{p+0.5}} \tag{5.9}$$

where K'_U is the control limit coefficient for this second proposed chart. The ARL values for the floating $U - S^2$ chart are given in Tables 5.8 – 5.10.

Table 5.8: ARL values for the floating $U - S^2$ chart with $K'_U = 3.129$ and $ARL_0 = 200$

δ	$n = 3$	$n = 5$	$n = 7$	$n = 9$
0.5	5.737	3.557	2.737	2.305
0.6	7.877	4.830	3.676	3.056
0.7	11.766	7.201	5.447	4.472
0.8	20.684	12.632	9.476	7.789
0.9	49.990	31.946	24.242	19.811
0.95	101.245	71.182	56.534	47.38
1.05	94.654	67.969	54.991	46.672
1.1	48.593	32.012	24.519	20.390
1.2	21.784	13.621	10.427	8.551
1.3	13.266	8.241	6.315	5.227
1.4	9.410	5.883	4.505	3.737
1.5	7.176	4.549	3.496	2.924
2	3.363	2.206	1.754	1.520
3	1.846	1.316	1.141	1.063

From Tables 5.5 – 5.10 we may conclude that:

i. both floating charts are performing good, not only for positive shifts but also for negative shifts in the process standard deviation;

ii. for a fixed ARL_0, the proposed floating $T - S^2$ chart is performing better for small shifts, like $\delta \geq 0.9$ and $\delta \leq 1.3$, whereas the performance of floating $U - S^2$ chart is better for large shifts, like $\delta \leq 0.8$ and $\delta \geq 1.4$;

iii. for the fixed values of p and ARL_0, the values of the control limit coefficients are the same for both proposed charts;

iv. for large values of n, the ARL values for both charts are more symmetric with respect to δ as the distribution of both T_i and U_i becomes very close to normal as n increases.

Table 5.9: ARL values for the floating $U - S^2$ chart with $K'_U = 3.568$ and $ARL_0 = 370$

δ	$n = 3$	$n = 5$	$n = 7$	$n = 9$
0.5	6.809	4.176	3.183	2.649
0.6	9.339	5.692	4.301	3.562
0.7	14.052	8.522	6.413	5.266
0.8	24.861	14.998	11.250	9.176
0.9	62.300	38.592	29.075	23.830
0.95	138.501	92.615	71.719	59.133
1.05	131.474	89.931	70.533	59.158
1.1	62.083	39.362	29.939	24.634
1.2	26.376	16.284	12.254	10.120
1.3	15.833	9.753	7.411	6.090
1.4	11.044	6.888	5.247	4.337
1.5	8.401	5.280	4.027	3.364
2	3.821	2.473	1.946	1.667
3	2.015	1.402	1.187	1.093

Table 5.10: ARL values for the floating $U - S^2$ chart with $K'_U = 3.846$ and $ARL_0 = 500$

δ	$n = 3$	$n = 5$	$n = 7$	$n = 9$
0.5	7.511	4.583	3.480	2.884
0.6	10.318	6.257	4.716	3.889
0.7	15.587	9.379	7.044	5.769
0.8	27.370	16.606	12.389	10.122
0.9	70.351	43.080	32.349	26.301
0.95	161.226	105.404	80.668	66.694
1.05	155.272	103.961	80.665	66.948
1.1	70.928	44.268	33.470	27.389
1.2	29.405	18.016	13.538	11.106
1.3	17.526	10.787	8.137	6.688
1.4	12.167	7.525	5.735	4.723
1.5	9.239	5.746	4.397	3.652
2	4.125	2.654	2.085	1.771
3	2.119	1.460	1.226	1.110

5.2.3 Comparisons

In this section, we compare the performance of the proposed floating charts with some recently proposed CUSUM and EWMA-type control charts for monitoring the process dispersion. The control charts selected for the comparison purpose include the S^2-EWMA by Castagliola (2005), EWMA $J - S^2$ by Castagliola et al. (2010) and CUSUM $-S^2$ by Castagliola et al. (2009) directly, while we have also compared the performance of our proposed charts with the Shewhart $R-$ chart, a CUSUM chart for process dispersion proposed by Page (1963) and an EWMA chart proposed by Crowder and Hamilton (1992), indirectly.

Proposed versus S^2-EWMA and EWMA $J - S^2$: Castagliola (2005) proposed an EWMA chart for monitoring the process dispersion based on the same logarithmic transformation as in (3.5), named as S^2-EWMA. Following him, Castagliola et al. (2010) proposed another EWMA chart based on the same four parameter Johnson S_B transformation as in (5.4), named as EWMA $J - S^2$ for controlling the process standard deviation. The two parameters of these charts are the smoothing parameter λ and the control limit coefficient K. The ARL values of these two charts for the optimal choices of λ and K are given in Table 5.11. Comparing the performance of proposed charts with these EWMA-type charts, we can notice that both proposed charts have smaller ARL_1 values for a fixed $ARL_0 = 370$. Moreover, the proposed charts are showing more dominance for small shifts as compared to large values of δ (cf. Table 5.11vs. Tables 5.6 & 5.9).

Castagliola (2005) showed in his article that the S^2-EWMA control chart performs better than the Shewhart $R-$ chart for small shifts like $\delta \leq 2$. He also proved the dominance of his proposed chart over the CUSUM chart proposed by Page (1963) and the EWMA charts proposed by Crowder and Hamilton (1992). Therefore, we can state that the performance of our proposed charts is better than these charts too.

Table 5.11: ARL values for the S^2-EWMA and EWMA $J-S^2$ charts with $ARL_0 = 370$

δ	S^2-EWMA				EWMA $J-S^2$			
	$n=3$	$n=5$	$n=7$	$n=9$	$n=3$	$n=5$	$n=7$	$n=9$
0.5	10	5.6	4	3.1	9.4	5.2	3.7	2.9
0.6	13.9	8	5.7	4.5	13.6	7.7	5.5	4.3
0.7	21.3	12.6	9.1	7.1	21.2	12.4	8.9	7
0.8	40.8	23.1	17	13.5	40.8	23	16.8	13.4
0.9	130.3	68.9	48.5	38.2	126.5	68.3	48.4	38.1
0.95	289.7	184.8	137.6	110.3	274.3	179.9	135.8	109.4
1.05	173.2	142.3	115.1	96.8	195.9	148	118.1	98.8
1.1	91.9	59.8	45.2	36.9	97	61.6	46.1	37.5
1.2	36.5	22.8	17	13.8	38.8	23.5	17.4	14
1.3	20.3	12.4	9.3	7.5	21.3	13	9.6	7.7
1.4	13.4	8.1	6.1	4.9	13.8	8.4	6.3	5.1
1.5	9.8	5.8	4.4	3.6	9.8	6	4.5	3.7
2	3.9	2.3	1.8	1.5	3.8	2.3	1.8	1.5

Proposed vs. CUSUM $-S^2$: Castagliola et al. (2009) proposed a CUSUM $-S^2$ chart based on the three parameter logarithmic transformation as in (3.5). The $ARLs$ of the CUSUM $-S^2$ chart with optimal parameter choices are given in Table 5.12.

Table 5.12: ARL values for the CUSUM $-S^2$ chart with $ARL_0 = 370$

n	δ												
	0.5	**0.6**	**0.7**	**0.8**	**0.9**	**0.95**	**1.05**	**1.1**	**1.2**	**1.3**	**1.4**	**1.5**	**2**
3	10.8	15.4	24.1	44	108.9	216.9	183.3	98.6	39.5	21.7	14.1	10.2	3.8
5	5.6	8.3	13.4	25.4	68.4	154.8	145.7	64.6	24.3	13.1	8.3	5.9	2.3
7	3.8	5.7	9.4	18.2	51.1	122.9	117.5	49.2	18	9.6	6.1	4.3	1.8
9	2.9	4.4	7.3	14.3	41.3	103.1	99.5	40.3	14.5	7.7	4.9	3.5	1.5

The performance of this CUSUM $-S^2$ control chart is more or less similar to that of S^2-EWMA and EWMA $J - S^2$ charts. Comparing the performance of our proposed charts with the CUSUM $-S^2$, we may conclude that the proposed charts are performing better than the CUSUM $-S^2$ chart for almost all values of δ (cf. Table 5.12 vs. Tables 5.6 & 5.9).

Apart from the tabular comparison, Figures 5.10 and 5.11 provide the ARL curves of the charts discussed in this subsection for an increase and a decrease, respectively, in the process dispersion. It is clear from Figures 5.10 – 5.11 that the ARL curves of both proposed charts are on the lower side of other curves. This shows that the proposed charts have smaller ARL_1 values for a fixed $ARL_0 = 370$. In addition, both proposed charts are showing almost the same performance as their ARL curves coincide in both figures.

Figure 5.10: ARL curves for floating $T - S^2$, floating $U - S^2$, S^2-EWMA, EWMA $J - S^2$ and CUSUM S^2 charts for increase in the process dispersion

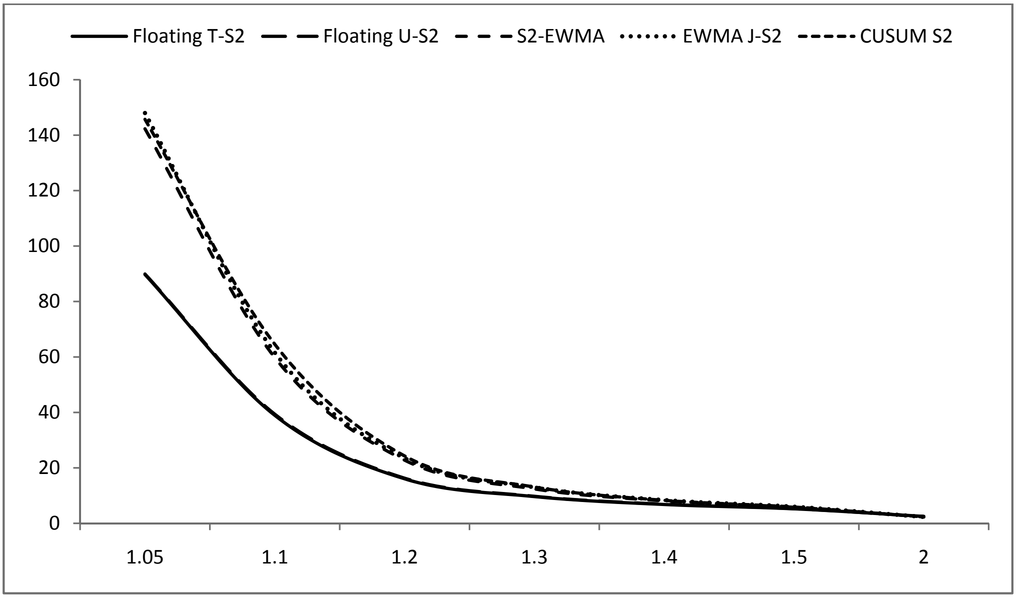

Figure 5.11: ARL curves for floating $T - S^2$, floating $U - S^2$, S^2-EWMA, EWMA $J - S^2$ and CUSUM S^2 charts for decrease in the process dispersion

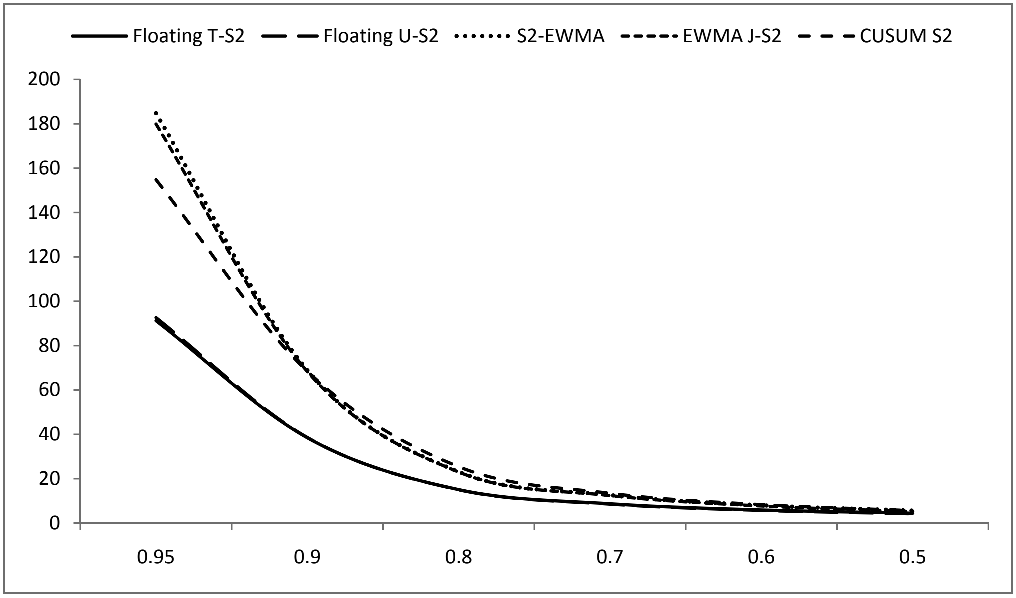

5.2.4 Illustrative example

For illustrating the application of the proposed charts, we generate two datasets (namely dataset 5.3 and dataset 5.4) of 25 subgroups each of size $n = 5$, i.e. one for an increase and the other for a decrease in the process standard deviation. For dataset 5.3, the first 15 subgroups are generated from $N(0,1)$ showing an in control standard deviation while the remaining 10 subgroups are generated from $N(0,1.2)$ referring to an out of control standard deviation with $\delta = 1.2$. Similarly, for dataset 5.4 the first 15 subgroups are the same as for dataset 5.3, whereas the remaining 10 subgroups are taken from $N(0,0.8)$ showing an negative shift in the process dispersion with $\delta = 0.8$. Both proposed charts are applied to the datasets with parameters; $\mu_T(n) = 0.00748$, $\sigma_T(n) = 0.967$, $A_T(n) = -0.8969$, $B_T(n) = 2.3647$, $C_T(n) = 0.5969$, $p = 0.2$ and $K'_T = 3.568$ for the floating $T - S^2$ chart; $\mu_U(n) = 0.0039$, $\sigma_U(n) = 0.9852$, $A_U(n) = 3.5402$, $B_U(n) = 1.5727$, $C_U(n) = -0.2352$, $D_U(n) =$

11.312, $p = 0.2$ and $K_U' = 3.568$ for the floating $U - S^2$ chart. The calculations for both proposed charts with dataset 5.3 are given in Table 5.13. Figure 5.12 shows the chart output of the floating $T - S^2$ chart for both datasets while the chart output of the floating $U - S^2$ chart is given in Figure 5.13.

Table 5.13: Calculation details of the proposed charts for dataset 5.3

Subgroup Number	S_i^2	T_i	FT_i	LCL_T	UCL_T	U_i	FU_i	LCL_U	UCL_U
1	0.815	-0.079	-0.079	-3.443	3.458	-0.045	-0.045	-3.511	3.519
2	0.363	-0.992	-0.536	-2.116	2.131	-0.998	-0.521	-2.16	2.168
3	1.567	0.929	-0.047	-1.592	1.607	0.924	-0.04	-1.625	1.633
4	0.594	-0.482	-0.156	-1.3	1.315	-0.45	-0.142	-1.328	1.336
5	1.565	0.927	0.061	-1.111	1.126	0.922	0.071	-1.135	1.143
6	2.384	1.687	0.332	-0.977	0.992	1.654	0.335	-0.999	1.007
7	0.659	-0.356	0.234	-0.876	0.891	-0.321	0.241	-0.896	0.904
8	0.069	-1.857	-0.028	-0.797	0.812	-2.106	-0.052	-0.816	0.824
9	0.709	-0.264	-0.054	-0.734	0.749	-0.228	-0.072	-0.751	0.759
10	0.564	-0.543	-0.103	-0.681	0.696	-0.513	-0.116	-0.697	0.705
11	0.529	-0.614	-0.149	-0.637	0.651	-0.588	-0.159	-0.652	0.66
12	0.696	-0.287	-0.161	-0.598	0.613	-0.251	-0.167	-0.613	0.621
13	0.875	0.018	-0.147	-0.565	0.58	0.051	-0.15	-0.58	0.588
14	2.485	1.765	-0.01	-0.536	0.551	1.731	-0.015	-0.55	0.558
15	0.431	-0.829	-0.065	-0.511	0.526	-0.818	-0.069	-0.524	0.532
16	2.123	1.47	0.031	-0.488	0.503	1.442	0.025	-0.501	0.509
17	3.219	2.27	0.163	-0.467	0.482	2.247	0.156	-0.48	0.488
18	0.332	-1.068	0.094	-0.449	0.464	-1.085	0.087	-0.461	0.469
19	2.552	1.816	0.185	-0.432	0.447	1.782	0.176	-0.444	0.451
20	0.148	-1.592	0.096	-0.416	0.431	-1.731	0.081	-0.428	0.436
21	3.935	2.677	0.219	-0.402	0.417	2.694	0.205	-0.413	0.421
22	1.592	0.957	0.253	-0.389	0.404	0.95	0.239	-0.4	0.408
23	3.744	2.575	0.354	-0.377	0.392	2.579	0.341	-0.388	0.395
24	1.834	1.205	0.389*	-0.366	0.38	1.187	0.376	-0.376	0.384
25	1.215	0.51	0.394*	-0.355	0.37	0.525	0.382**	-0.365	0.373

* indicates an out of control signal by floating $T - S^2$ chart
** indicates an out of control signal by floating $U - S^2$ chart

It can be seen from Figures 5.12 – 5.13 that the proposed charts are effectively detecting both positive and negative shifts. This can also be confirmed from Table 5.13, where the floating $T - S^2$ chart is signaling at subgroups # 24 and 25, while the floating $U - S^2$ chart is detecting the positive shift at subgroup # 25.

Figure 5.12: Chart output of floating $T - S^2$ chart for datasets 5.3 & 5.4

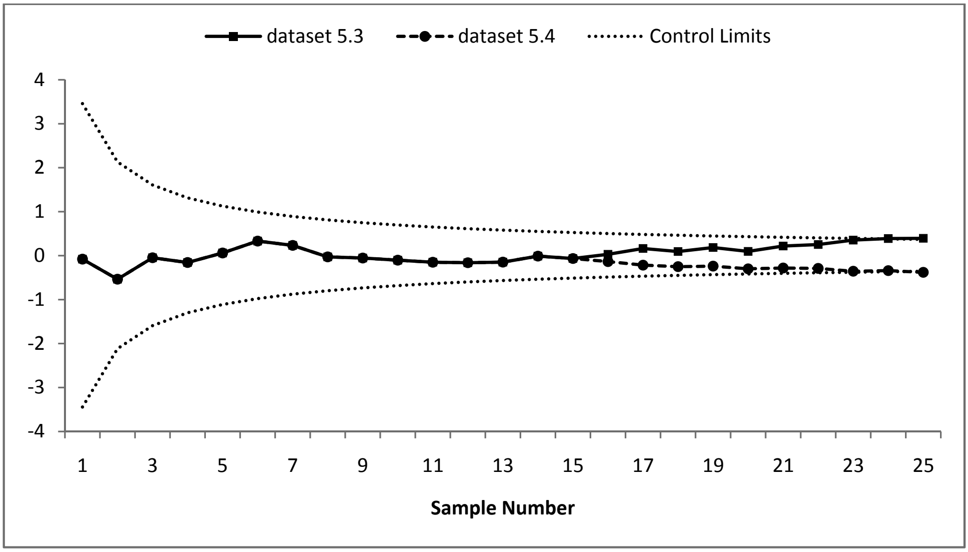

Figure 5.13: Chart output of floating $U - S^2$ chart for datasets 5.3 & 5.4

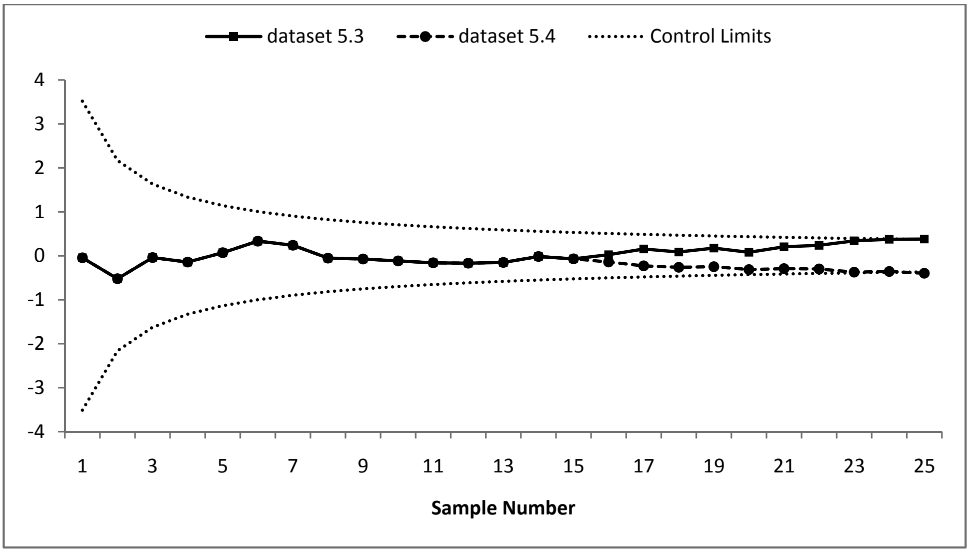

5.3 Concluding remarks

To monitor the location of a process two main types of charts, named as Shewhart-type control charts and memory control charts (like EWMA and CUSUM) are available. Former are recommended for large shifts ($3 \leq \delta \leq 5$) while latter are good at detecting small and moderate shifts (like $0.25 \leq \delta \leq 1.5$). In this chapter, we have proposed another type of memory control chart, the so called PM control chart. The performance of the new chart is evaluated in terms of $ARLs$ and we have compared the performance of proposed control chart with different existing memory control charts. Comparisons revealed that the newly proposed chart performs very good and outperforms its competitors for small and moderate shifts but also shows good performance for large shifts.

Following the PM chart for location, two memory-type control charts for process dispersion, named as the floating $T - S^2$ control chart (based on a three parameter logarithmic transformation) and the floating $U - S^2$ control chart (based on a four parameter Johnson S_B transformation) are proposed. The performance evaluation of the proposed charts is done by calculating the ARL values using simulation procedures. These $ARLs$ are compared with some EWMA- and CUSUM-type control charts for monitoring the process standard deviation. The comparisons show that the proposed charts are dominating the other charts in terms of ARL values. Moreover, an inter-proposed charts comparison shows that the floating $T - S^2$ chart is better for small shifts, whereas the floating $U - S^2$ chart is superior for large shifts in the process dispersion. At the end, an illustrative example is provided which shows the application of the proposed charts on simulated datasets.

Appendix 5.1

```
y=c(); PM=c(); ucl=c(); lcl=c(); rl=c()
mu=0; sig=1
p=0.2; K=3.129
for(j in 1:100000)
{
      for(i in 1:1000000)
      {
            y[i]=rnorm(1,mu,sig)
            PM[i]=mean(y[1:i])
            ucl[i]=mu+K*(sig/i^(0.5+p))
            lcl[i]=mu-K*(sig/i^(0.5+p))
            if(PM[i]>ucl[i]|PM[i]<lcl[i])
                  {rl[j]=i;break;}
                  else{rl[j]=0;}
      }
}
mean(rl)
```

Appendix 5.2

```
rl=c(); Tj=c(); FT=c(); ucl=c(); lcl=c()
n=5; a=-0.8969; b=2.3647; c=0.5979; ETj=0.00748; STj=0.9670
p=0.2; K=3.129
mu=0; sig=1
for(j in 1:100000)
{
      for(i in 1:1000000)
      {
            x=rnorm(n,mu,sig)
            Tj[i]=a+b*log(var(x)+c,exp(1))
            FT[i]=mean(Tj[1:i])
            ucl[i]=ETj+K*(STj/i^(0.5+p))
            lcl[i]=ETj-K*(STj/i^(0.5+p))
            if(FT[i]>ucl[i]|FT[i]<lcl[i])
                  {rl[j]=i; break;}
                  else{rl[j]=0;}
      }
}
mean(rl)
```

References

Abbas, N., Riaz, M. and Does, R.J.M.M. (2011). Enhancing the Performance of EWMA Charts. *Quality and Reliability Engineering International*, 27(6), 821 – 833.

Abbas, N., Riaz, M. and Does, R.J.M.M. (2012a). Mixed Exponentially Weighted Moving Average – Cumulative Sum charts for Process Monitoring. *Quality and Reliability Engineering International*, DOI: 10.1002/qre.1385.

Abbas, N., Riaz, M. and Does, R.J.M.M. (2012b). CS-EWMA Chart for Monitoring Process Dispersion. *Quality and Reliability Engineering International*, DOI: 10.1002/qre.1414.

Abbas, N., Riaz, M. and Does, R.J.M.M. (2012c). An EWMA-type Control Chart for Monitoring the Process Mean Using Auxiliary Information. Accepted for publication in *Communications in Statistics – Theory and Methods*.

Abbas, N., Riaz, M. and Does, R.J.M.M. (2012d). New Memory-type Control Charts for Monitoring the Process Dispersion. Submitted to *International Journal of Production Research*.

Abbas, N., Zafar, R.F., Riaz, M. and Hussain, Z. (2012). Progressive Mean Control Chart for Monitoring Location Parameter. *Quality and Reliability Engineering International*, DOI: 10.1002/qre.1386.

Acosta-Mejia, C., Pigniatiello, J. and Rao, B. (1999). A comparison of Control Charting Procedures for Monitoring Process Dispersion. *IIE Transactions*, 31(6), 569-579.

Antzoulakos, D.L. and Rakitzis, A.C. (2008). The Modified r out of m Control Chart. *Communications in Statistics – Theory and Methods*, 37(2), 396-408.

Bonetti, P.O., Waeckerlin, A., Schuepfer, G. and Frutiger, A. (2000). Improving Time-Sensitive Processes in the Intensive Care Unit: the Example of 'Door-to-Needle Time' in Acute Myocardial Infarction. *International Journal for Quality in Health Care*, 12(4), 311-317.

Brook, D. and Evans, D.A. (1972). An Approach to the Probability Distribution of CUSUM Run Length. *Biometrika*, 59(3), 539 - 549.

Capizzi, G.and Masarotto, G. (2003). An Adaptive Exponentially Weighted Moving Average Control Chart. *Technometrics*, 45(3), 199-207.

Castagliola, P. (2005). A New S^2-EWMA Control Chart for Monitoring Process Variance. *Quality and Reliability Engineering International*, 21(8), 781-794.

Castagliola, P., Celano, G. and Fichera, S. (2009). A New CUSUM-S^2 Control Chart for Monitoring the Process Variance. *Journal of Quality in Maintenance Engineering*, 15(4), 344-357.

Castagliola, P., Celano, G. and Fichera, S. (2010). A Johnson's Type Transformation EWMA-S^2 Control Chart. *International Journal of Quality Engineering and Technology*, 1(3), 253-275.

Chang, T.C. and Gan, F.F. (1995). A Cumulative Sum Control Chart for Monitoring Process Variance. *Journal of Quality Technology*, 27(2), 109-119.

Chatterjee, S. and Qiu, P. (2009). Distribution-Free Cumulative Sum Control Charts Using Bootstrap-Based Control Limits. *Annals of Applied Statistics*, 3(1), 349-369.

Cochran, W.G. (1977). *Sampling Techniques*. 3rd ed. New York: John Wiley and Sons.

Crowder, S.V. and Hamilton, M.D. (1992). An EWMA for Monitoring a Process Standard Deviation. *Journal of Quality Technology*, 24(1), 12-21.

Ewan, W.D. and Kemp, K.W. (1960). Sampling inspection of continuous processes with no autocorrelation between successive results. *Biometrika*, 47(3-4), 363-380.

Fuller, W.A. (2002). Regression Estimation for Survey Samples. *Survey Methodology*, 28(1), 5-23.

Fuller, W.A. (2009). *Sampling Statistics*. John Wiley and Sons Inc., Hoboken, New Jersey.

Garcia, M.R. and Cebrian, A.A. (1996). Repeated Substitution Method: The Ratio Estimator for the Population Variance. *Metrika*, 43(1), 101-105.

Hawkins, D.M. (1981). A CUSUM for a Scale Parameter. *Journal of Quality Technology*, 13(4), 228-231.

Hawkins, D.M. and Olwell, D.H. (1998). *Cumulative Sum Charts and Charting Improvement*. Springer, New York.

Huwang, L., Huang, C. J. and Wang, Y.H.T. (2010). New EWMA Control Charts for Monitoring Process Dispersion. *Computational Statistics and Data Analysis*, 54(10), 2328-2342.

Jiang, W., Shu, L. and Aplet, D.W. (2008). Adaptive CUSUM Procedures with EWMA-Based Shift Estimators. *IIE Transactions*, 40(10), 992-1003.

Kadilar, C. and Cingi, H. (2005). A New Estimator Using Two Auxiliary Variables. *Applied Mathematics and Computation*, 162(2), 901–908.

Khoo, M.B.C. (2004). Design of Runs Rules Schemes. *Quality Engineering*, 16(1), 27–43.

Klein, M. (2000). Two Alternatives to the Shewhart X Control Chart. *Journal of Quality Technology*, 32(4), 427–431.

Koutras, M.V., Bersimis, S. and Maravelakis, P.E. (2007). Statistical Process Control using Shewhart Control Charts with Supplementary Runs Rules. *Methodology and Computing in Applied Probability*, 9(2), 207–224.

Lowry, C.A., Woodall, W.H., Champ, C.W. and Rigdon, S.E. (1992). A Multivariate Exponentially Weighted Moving Average Control Chart. *Technometrics*, 34(1), 46 – 53.

Lucas, J.M. (1982). Combined Shewhart-CUSUM Quality Control Schemes. *Journal of Quality Technology*, 14(2), 51-59.

Lucas, J.M. and Crosier, R.B. (1982). Fast Initial Response for CUSUM Quality-Control Scheme. *Technometrics*, 24(3), 199-205.

Lucas J.M. and Saccucci M.S. (1990). Exponentially Weighted Moving Average Control Schemes: Properties and Enhancements. *Technometrics*, 32(1), 1–12.

Mandel, B.J. (1969). The Regression Control Chart. *Journal of Quality Technology*, 1(1), 1-9.

McIntyre, G.A. (1952). A Method for Unbiased Selective Sampling, Using Ranked Sets. *Australian Journal of Agricultural Research*, 3(4), 385-390.

Montgomery, D.C. (2009). *Introduction to Statistical Quality Control*. 6th ed. New York: John Wiley & Sons.

Nelson, L.S., (1984), The Shewhart Control Chart – Tests for Special Causes, *Journal of Quality Technology*, 16(4), 237-239

Ng, C.H. and Case, K.E. (1989). Development and Evaluation of Control Charts Using Exponentially Weighted Moving Averages. *Journal of Quality Technology*, 21(4), 242-250.

Page, E.S. (1954). Continuous Inspection Schemes. *Biometrika*, 41(1-2), 100-115.

Page, E.S. (1963). Controlling the Standard Deviation and Warning Lines by CUSUM. *Technometrics*, 5(3), 307-309.

Palm, A.C. (1990). Tables of Run Length Percentiles for Determining the Sensitivity of Shewhart Control Charts for Averages with Supplementary Runs Rules. *Journal of Quality Technology*, 22(4), 289–298.

Riaz, M. (2008a). Monitoring Process Variability using Auxiliary Information. *Computational Statistics*, 23(2), 253-276.

Riaz, M. (2008b). Monitoring Process Mean Level using Auxiliary Information. *Statistica Neerlandica*, 62(4), 458-481.

Riaz, M., Abbas, N. and Does, R.J.M.M. (2011). Improving the Performance of CUSUM Charts. *Quality and Reliability Engineering International*, 27(4), 415 – 424.

Riaz, M. and R.J.M.M. Does (2009). A process variability control chart. *Computational Statistics*, 24(2), 345–368.

Roberts, S.W. (1959), Control Chart Tests Based on Geometric Moving Averages, *Technometrics*, 1(3), 239-250.

Shewhart, W.A. (1931). *Economic Control of Quality of Manufactured Product*, New York: 1931. Reprinted by ASQC, Milwaukee, 1980.

Shmueli, G. and Cohen, A. (2003). Run-Length Distribution for Control Charts with Runs and Scans Rules. *Communications in Statistics – Theory and Methods*, 32(2), 475–495.

Shu, L.J. and Jiang, W. (2008). A New EWMA Chart for Monitoring Process Dispersion. *Journal of Quality Technology*, 40(3), 319-331.

Siegmund, D.O. (1985). *Sequential Analysis: Test and Confidence Intervals*. New York: Springer-Verlag.

Steiner, S.H. (1999). EWMA control charts with time varying control limits and fast initial response. *Journal of Quality Technology*, 31(1), 75 – 86.

Tuprah, K. and Ncube, M. (1987). A Comparison of Dispersion Quality Control charts. *Sequential Analysis*, 6(2), 155-163.

Wade, M.R. and Woodall, W.H. (1993). A Review and Analysis of Cause-Selecting Control Charts. *Journal of Quality Technology*, 25(3), 161-169.

Waldmann, K.H. (1995). Design of double CUSUM quality control schemes. *European Journal of Operational Research*, 95(3), 641-648.

Westgard, J.O., Groth, T., Aronsson, T. and De Verdier. C.H. (1977). Combined Shewhart-CUSUM Control Chart for Improved Quality Control in Clinical Chemistry. *Clinical Chemistry*, 23(10), 1881-1887.

Wortham, A.W. and Ringer, L.J. (1971). Control via Exponentially Smoothing. *The Logistics and Transportation Review*, 7(1), 33-39.

Wu, Z. and Tian, Y. (2005). Weighted-loss-Function CUSUM chart for Monitoring Mean and Variance of a Production Process. *International Journal of Production Research*, 43(14), 3027–3044.

Yashchin, E. (1989). Weighted Cumulative Sum Technique. *Technometrics*, 31(1), 321-338.

Zhang, G.X. (1985). Cause-Selecting Control Charts-A New Type of Quality Control Charts. *The QR Journal*, 12, 221-225.

Zhang, G. and Chang, S.I. (2008). Multivariate EWMA Control Charts Using Individual Observations for Process Mean and Variance Monitoring and Diagnosis. *International Journal of Production Research*, 46(24), 6855–6881.

Samenvatting

Het doel van statistische procesbeheersing is om een procesvoering te krijgen die geschoeid is op een kwantitatieve leest. De regelkaart is het belangrijkste gereedschap van statistische procesbeheersing en werd in 1924 door Shewhart geïntroduceerd in het bedrijfsleven. Het is een grafiek van metingen van een kwaliteitskarakteristiek van het proces op de verticale as uitgezet tegen de tijd op de horizontale as. De grafiek wordt aangevuld met regelgrenzen die de procesinherente variatie markeren. Zodra een meting buiten de regelgrenzen valt dan noemen we het proces niet beheerst. In de loop der jaren is hier veel onderzoek naar gedaan.

In begin vijftiger jaren van de vorige eeuw ontwikkelde Page een nieuw type regelkaart: de gecumuleerde som regelkaart, beter bekend geworden als de CUSUM regelkaart. Kort daarna, in 1959, presenteerde Roberts de exponentieel gewogen voortschrijdend gemiddelde regelkaart, die bekend werd onder de naam van EWMA regelkaart. Beide regelkaarten gebruiken naast de laatst gemeten waarneming ook de voorafgaande waarnemingen om te oordelen of het proces beheerst is. In die zin hebben deze regelkaarten een geheugen. In hoofdstuk 1 worden beide regelkaarten geïntroduceerd.

De standaard signaleringsregel is dat als een waarneming buiten de regelgrenzen valt, het proces niet beheerst is. Door vervanging van de regelgrenzen door waarschuwings- en/of actiegrenzen kunnen ook patronen van opeenvolgende waarnemingen als signaleringsregels gebruikt worden. In hoofdstuk 2 worden deze aanpassingen gebruikt om de CUSUM - en EWMA regelkaarten tot snellere signalering te laten komen bij met name kleine verschuivingen in het gemiddelde. Hiervoor wordt als criterium genomen de gemiddelde run lengte, waarbij als definitie van de run lengte gebruikt wordt: het aantal opeenvolgende waarnemingen dat nodig is om tot een signaal te komen. Het blijkt dat de aanpassingen in hoofdstuk 2 tot substantiële verbetering leiden voor het sneller signaleren van kleine verschuivingen in het gemiddelde.

In hoofdstuk 3 worden de CUSUM – en EWMA regelkaarten gecombineerd tot een gemeenschappelijke regelkaart. Deze gecombineerde regelkaart wordt ontwikkeld voor zowel het monitoren van de locatie als van de spreiding. Vergelijkingen op basis van de gemiddelde run lengten worden gemaakt met bestaande regelkaarten. Het blijkt dat de gecombineerde regelkaart tot betere resultaten leidt.

Een betere beheersing van de procesparameters kan ook verkregen worden door gebruik te maken van aanvullende informatie uit de data. Door het benutten van de correlatie tussen de kwaliteitskarakteristiek en de aanvullende kenmerken, zijn nieuwe CUSUM – en EWMA regelkaarten ontwikkeld. In hoofdstuk 4 worden deze nieuwe regelkaarten vergeleken met bestaande regelkaarten die gebruikt worden voor hetzelfde doel. Het blijkt dat aanvullende informatie de prestaties van de regelkaarten substantieel verbetert.

Tot slot wordt in het laatste hoofdstuk een nieuw type regelkaart voorgesteld die wordt gebaseerd op het progressief voortschrijdend gemiddelde. Deze regelkaart wordt zowel voor de locatie parameter als voor de spreidingsparameter ontwikkeld. De prestaties, wederom in termen van de gemiddelde run lengte, blijken in de praktijk uitstekend te zijn.

Curriculum Vitae

Nasir Abbas was born in Rawalpindi (Pakistan) on 21st June, 1987. He completed his schooling in 2003 from F.G. Secondary School, Mehfooz Road, Rawalpindi, Pakistan. He earned his F.Sc. and B.Sc in 2005 and 2007, respectively, from the F.G. Sir Syed College, The Mall, Rawalpindi, Pakistan with the major subjects as Mathematics, Statistics and Physics at F.Sc. level, and Mathematics, Statistics and Economics as B.Sc. level. He got his M.Sc. in Statistics from the Department of Statistics Quaid-i-Azam University Islamabad Pakistan in 2009 where he secured the top position in his department and M.Phil in Statistics from the Department of Statistics Quaid-i-Azam University Islamabad Pakistan in 2011.

Additionally, he is also serving as Assistant Census Commissioner in Pakistan Bureau of Statistics from July 2011-present. His current research interests include Statistical Quality Control particularly control charting based on the classical, Bayesian as well as non-parametric methodologies.